



Laboratory and Field Performance of PGxx-28 and PGxx-34 Binders and New Binder Type Selection Catalog

Technical Report 5-6674-01-R1

Cooperative Research Program

TEXAS A&M TRANSPORTATION INSTITUTE
COLLEGE STATION, TEXAS

sponsored by the
Federal Highway Administration and the
Texas Department of Transportation
<https://tti.tamu.edu/documents/5-6674-01-R1.pdf>

1. Report No. FHWA/TX-25/5-6674-01-R1		2. Government Accession No.		3. Recipient's Catalog No.	
4. Title and Subtitle LABORATORY AND FIELD PERFORMANCE OF PGXX-28 AND PGXX-34 BINDERS AND NEW BINDER TYPE SELECTION CATALOG				5. Report Date Published: February 2025	
				6. Performing Organization Code	
7. Author(s) Sheng Hu and Fujie Zhou				8. Performing Organization Report No. Report 5-6674-01-R1	
9. Performing Organization Name and Address Texas A&M Transportation Institute The Texas A&M University System College Station, Texas 77843-3135				10. Work Unit No. (TRAVIS)	
				11. Contract or Grant No. Project 5-6674-01	
12. Sponsoring Agency Name and Address Texas Department of Transportation Research and Technology Implementation Office 125 E. 11 th Street Austin, Texas 78701-2483				13. Type of Report and Period Covered Technical Report: September 2018–August 2022	
				14. Sponsoring Agency Code	
15. Supplementary Notes Project sponsored by the Texas Department of Transportation and the Federal Highway Administration. Project Title: Statewide Implementation of New Binder Selection Catalog and New Binder Performance Tests URL: https://tti.tamu.edu/documents/5-6674-01-R1.pdf					
16. Abstract Asphalt binder is one of the most expensive and critical materials used in the construction and maintenance of asphalt pavements. A key step toward a long-lasting asphalt pavement is selecting a proper binder performance grade (PG). The Texas Department of Transportation’s current binder PG selection catalog serves its purpose well for new pavement constructions but not for overlays. The most significant difference between new constructions and asphalt overlays is preexisting cracks underlying the asphalt overlays. The preexisting cracks significantly impact asphalt overlay performance in terms of early reflective cracking, which was not considered in the current PG binder selection catalogs. This project evaluated many softer but polymer-modified asphalt binders in laboratory and field performance. These soft, highly modified binders (PGxx-28 or PGxx-34) proved to have better cracking resistance and are recommended to be used in the colder areas of Texas. A new statewide binder selection catalog was developed and validated based on the laboratory test results, field observations, and overlay performance simulations. In addition, an IDEAL cracking test was performed to evaluate binder quality through aging and mix cracking resistance.					
17. Key Words Asphalt Binder, Performance Grade, PG, Selection Catalog, Pure Linear Amplitude Sweep, PLAS, Polymer-Modified, Overlay			18. Distribution Statement No restrictions. This document is available to the public through NTIS: National Technical Information Service Alexandria, Virginia http://www.ntis.gov		
19. Security Classif. (of this report) Unclassified		20. Security Classif. (of this page) Unclassified		21. No. of Pages 114	22. Price

LABORATORY AND FIELD PERFORMANCE OF PGXX-28 AND PGXX-34 BINDERS AND NEW BINDER TYPE SELECTION CATALOG

by

Fujie Zhou
Senior Research Engineer
Texas A&M Transportation Institute

and

Sheng Hu
Associate Research Engineer
Texas A&M Transportation Institute

Report 5-6674-01-R1

Project 5-6674-01

Project Title: Statewide Implementation of New Binder Selection Catalog and New Binder Performance Tests

Sponsored by the
Texas Department of Transportation
and the
Federal Highway Administration

Published: February 2025

TEXAS A&M TRANSPORTATION INSTITUTE
College Station, Texas 77843-3135

DISCLAIMER

This research was sponsored by the Texas Department of Transportation (TxDOT) and the Federal Highway Administration (FHWA). The contents of this report reflect the views of the authors, who are responsible for the facts and the accuracy of the data presented herein. The contents do not necessarily reflect the official view or policies of FHWA or TxDOT. This report does not constitute a standard, specification, or regulation.

This report is not intended for construction, bidding, or permit purposes. The researcher in charge of the project was Fujie Zhou.

The United States Government and the State of Texas do not endorse products or manufacturers. Trade or manufacturers' names appear herein solely because they are considered essential to the object of this report.

ACKNOWLEDGMENTS

This project was sponsored by TxDOT and FHWA. The authors thank the personnel who contributed to the coordination and accomplishment of the work presented here. Special thanks are extended to Ms. Joanne Steele for serving as the project manager. Many people volunteered their time to serve as project advisors, including:

- Enad Mahmoud.
- Gisel Carrasco.
- Pravat Karki.
- Sandeep Pandey.
- Zahra SotoodehNia.
- Mohammad Ilias.

TABLE OF CONTENTS

	Page
List of Figures	ix
List of Tables	xii
Chapter 1. Introduction	1
Background.....	1
Report Organization.....	2
Chapter 2. Laboratory Asphalt Binder and Mixture Tests: PGxx-22, PGxx-28, and PGxx-34	3
Introduction.....	3
Asphalt Binder Selection and MSCR Evaluation	3
Correlation between MSCR Binder Test and Asphalt Mix Rutting Test	4
Materials and Asphalt Mix Rutting Test.....	4
Test Results and Analysis	5
Fatigue Cracking Resistance: LAS Tests and Limitations	7
Effect of Binder Sources and PGs	8
Effect of Aging	9
Effect of Engineering Agents.....	10
New Fatigue Cracking Resistance: PLAS Tests.....	11
Effect of Binder Sources and PGs	14
Effect of Aging	15
Effect of Engineering Agents.....	16
Correlation with Laboratory Mixture Cracking Tests	16
Correlation with Full-Scale Accelerated Pavement Tests	17
Summary and Conclusion	19
Chapter 3. Field Performance of Test Sections with PGxx-22, PGxx-28, and PGxx-34 Binders	21
Introduction.....	21
SH 15 Test Sections in Amarillo District	21
General Description	21
Field Survey	22
US 62 Test Sections in Childress District.....	27
General Description	27
Field Survey	28
Loop 820 Test Sections in Fort Worth District.....	32
General Description	32
Field Survey	33
Fairground Road Test Sections in Odessa District	35
General Description	35
Field Survey	36
FM 468 Test Sections in Laredo District.....	37
General Description	37
Field Survey	38
SH 7 Test Sections in Bryan District	41
General Description	41

Field Survey	44
SH 214 Test Sections in Lubbock District.....	46
General Description	46
Field Survey	50
APT Test Sections in Dallas District	52
General Description	52
APT Test Results	54
FM 2105 Test Sections in San Angelo District	55
General Description	55
Field Survey	58
SH 71 Test Sections in Austin District	59
General Description	59
Field Survey	61
Summary and Conclusions	63
Chapter 4. Revised Statewide Asphalt Binder Selection Catalog.....	67
Introduction.....	67
Statewide PG Binder Selection Catalog Currently Used in Texas	67
Statewide Asphalt Binder Selection Catalog for Overlay.....	69
New Statewide Asphalt Binder Selection Catalog.....	71
Summary and Conclusion	78
Chapter 5. Binder Quality: Aging and Cracking Resistance.....	81
Introduction.....	81
Laboratory Mix and Binder Test Plan	81
Laboratory Test Results and Discussion.....	82
Binder Test Results and Discussion.....	87
Summary and Conclusion	98
Chapter 6. Conclusions and Recommendation	99
Conclusions.....	99
Recommendations.....	100
References	101

LIST OF FIGURES

	Page
Figure 1. MSCR Test Results of Nine Asphalt Binders.	4
Figure 2. Aggregate Gradations of Mixes Used in This Study.....	5
Figure 3. HWTT Results of Gravel Mixes with Five Binders.....	6
Figure 4. HWTT Results of Limestone Mixes with Five Binders.....	6
Figure 5. HWTT Results of Granite Mixes with Five Binders.....	7
Figure 6. LAS Test and Analysis: An Illustration.	8
Figure 7. LAS Test Results: Original Binders.....	9
Figure 8. LAS Test Results: Effect of Chemical Aging.	10
Figure 9. LAS Test Results: Effect of Engineering Agents.....	11
Figure 10. PLAS Test and Analysis: An Illustration.	14
Figure 11. PLAS Test Results: Original Binders.....	15
Figure 12. PLAS Test Results: Effect of Chemical Aging.	15
Figure 13. PLAS Test Results: Effect of Engineered Binders.....	16
Figure 14. PLAS Test Results: Correlation with Mixture Cracking Results.....	17
Figure 15. Three-Dimensional Layout of the FHWA-ALF Test Section (Gibson et al. 2012).	18
Figure 16. PLAS Test Results: Correlation with FHWA-ALF Cracking Test Results.	19
Figure 17. SH 15 Test Sections: Location Map via Google.	22
Figure 18. SH 15 Test Section 1: Survey Pictures.....	23
Figure 19. SH 15 Test Section 2: Survey Pictures.....	24
Figure 20. SH 15 Test Section 3: Survey Pictures.....	25
Figure 21. SH 15 Test Section 4: Survey Pictures.....	26
Figure 22. SH 15 Test Sections: Survey Results.	27
Figure 23. US62 Test Sections: Location Map via Google.	28
Figure 24. US 62 Test Section 1: Survey Pictures.....	29
Figure 25. US 62 Test Section 2: Survey Pictures.....	30
Figure 26. US 62 Test Section 3: Survey Pictures.....	31
Figure 27. US 62 Test Sections: Survey Results.	32
Figure 28. Loop 820 Test Sections: Location Map via Google.....	33
Figure 29. Loop 820 Test Sections 0 to 3: Survey Pictures.....	34
Figure 30. Loop 820 Test Sections: Cracking Conditions.....	35
Figure 31. North Fairground Road Test Sections: Location Map via Google.....	36
Figure 32. North Fairground Road Test Section 1: Survey Pictures.	37
Figure 33. North Fairground Road Test Section 2: Survey Pictures.	37
Figure 34. FM 468 Test Sections: Location Map via Google.....	38
Figure 35. FM 468 Test Section 1: Survey Pictures.	39
Figure 36. FM 468 Test Section 2: Survey Pictures.	40
Figure 37. Location of Project SH 7.	41
Figure 38. Example of SH 7 Pavement Condition after the 2-In. Milling.....	42
Figure 39. Applying Tact Coat.	43
Figure 40. Paving Asphalt Mix.....	43
Figure 41. Compacting the Mat.	44

Figure 42. No Rutting on Both Test Sections on SH 7.....	45
Figure 43. Cracking Observed on Control Section with PG64-22.	45
Figure 44. No Cracking on Test Section with PG64-28.	46
Figure 45. Location of Project SH 214.	47
Figure 46. Pavement Condition of SH 214.	47
Figure 47. Applying Tack Coat.	48
Figure 48. Paving Fiberglass Fabric Interlayer.....	48
Figure 49. Paving Asphalt Mix.....	49
Figure 50. Compacting the Mat.	49
Figure 51. No Rutting on the Test Section with PG64-34 on SH 214.....	50
Figure 52. No Cracking on the Test Section with PG64-34 on SH 214.	51
Figure 53. No Rutting on the Test Section with PG70-28 on SH 214.....	51
Figure 54. No Cracking on the Test Section with PG70-28 on SH 214.	51
Figure 55. Location of Dallas APT Test Sections.	52
Figure 56. Schematic Drawing of the Test Sections.	53
Figure 57. Paving Operation at Dallas Test Sections.	53
Figure 58. Compacting Test Sections at Dallas Test Sections.....	54
Figure 59. Fatigue Cracking on Test Section O with PG70-22 (Left) and Section P with PG64-28 (Right).....	55
Figure 60. Location of FM 2105 Test Sections.	56
Figure 61. Applying Tack Coat on FM 2105.....	56
Figure 62. Paving Operation on FM 2105.	57
Figure 63. Compacting Test Sections on FM 2105.	57
Figure 64. No Rutting on the Test Section with PG70-28 on FM 2105.	58
Figure 65. No Cracking on the Test Section with PG70-28 on FM 2105.	58
Figure 66. No Rutting on the Test Section with PG70-22 on FM 2105.	59
Figure 67. No Cracking on the Test Section with PG70-22 on FM 2105.	59
Figure 68. Location of SH 71 Test Sections.	60
Figure 69. Paving Operation on SH 71.....	60
Figure 70. Compaction Operation on SH 71.	61
Figure 71. No Rutting on the Test Section with PG70-28 on SH 71.....	62
Figure 72. No Cracking on the Test Section with PG70-28 on SH 71.	62
Figure 73. No Rutting on the Test Section with PG70-22 on SH 71.....	63
Figure 74. No Cracking on the Test Section with PG70-22 on SH 71.	63
Figure 75. Asphalt Binder Grade Recommendation: TxDOT Method.....	68
Figure 76. Asphalt Binder Grade Adjustment: TxDOT Method.	69
Figure 77. PG Recommendation for New Construction.....	75
Figure 78. PG Recommendation for Asphalt Overlay over Existing AC.....	76
Figure 79. PG Recommendation for Asphalt Overlay over JPCP.....	77
Figure 80. Asphalt Binder PG Recommendation and Adjustment: New Method.....	78
Figure 81. Cracking Resistance Evolution or Each Mix with Conditioning Time (or Level).	84
Figure 82. Cracking Resistance Evolution or Each Mix with Conditioning Time (or Level).	85
Figure 83. Extracted and Recovered Binders: Shear Modulus versus Phase Angle in Black Space.....	88

Figure 84. Virgin Binders: Shear Modulus versus Phase Angle in Black Space.	91
Figure 85. Comparison between Mix and Binder Property Evolution under Six Conditioning Protocols.	93
Figure 86. Comparison between Binder RTFO, PAV20, PAV40 Aging, and Loose Mix Oven Conditioning.....	95

LIST OF TABLES

	Page
Table 1. Optimum Asphalt Content of Each Mix.....	4
Table 2. Compositions of Asphalt Mixes Used on SH 7.....	42
Table 3. Laboratory Test Results of SH 7 Mixes.....	44
Table 4. Compositions of Asphalt Mixes Used on SH 214.....	47
Table 5. Laboratory Test Results of SH 214 SMA Mixes.....	50
Table 6. Compositions of Asphalt Mixes: 2 and 4.....	53
Table 7. Laboratory Test Results of Dallas APT Mixes.....	54
Table 8. Compositions of Asphalt Mixes Used on FM 2105.....	56
Table 9. Laboratory Test Results of FM 2105 Mixes.....	58
Table 10. Compositions of Asphalt Mixes Used on SH 71.....	60
Table 11. Laboratory Test Results of SH 71 Mixes.....	61
Table 12. Overlay Performance Simulation Factorial.....	70
Table 13. Asphalt Binder Grade Recommendation.....	72
Table 14. Asphalt Binder Grade Recommendation: New Catalog.....	73
Table 15. Thirteen Mixes for Evaluating the Short- and Mid-Term Conditioning Protocols.....	82

CHAPTER 1. INTRODUCTION

BACKGROUND

Asphalt binder, one of the critical components of asphalt mixtures, plays a crucial role in asphalt pavement performance from three aspects:

- Asphalt binder content.
- Binder grade.
- Binder quality.

Asphalt binder content is determined through a mix design process, such as balanced mix design. This study mainly addresses binder grade selection. Binder quality in terms of binder aging and mix cracking resistance is also discussed.

The first step toward a long-lasting asphalt pavement is selecting a proper binder grade. Currently, almost all states in the United States grade asphalt binders using the performance-grade (PG) system. Asphalt binder properties are related to conditions under which the asphalt binder is used. The PG system uses a standard set of tests to measure binder mechanical properties that can be directly related to the field performance of the pavement at extreme temperatures. For example, a binder identified as PG64-22 must meet performance criteria at an average 7-day maximum pavement design temperature of 64°C and a minimum pavement design temperature of -22°C. In general, PG binder selection is a two-phase process:

- Selection of a base binder grade based on project location (or climate) and confidence levels (95 percent versus 98 percent reliability) for both high and low temperatures.
- Possible upgrades for traffic speed and volume, pavement layer, and the use of recycled material.

This process serves its purpose well for new pavement constructions. However, now the Texas Department of Transportation (TxDOT) predominantly works with asphalt overlays. The most significant difference between new constructions and asphalt overlays is preexisting cracks underlying the asphalt overlays. The preexisting cracks significantly impact asphalt overlay performance in terms of early reflective cracking, which was not considered when developing current PG binder selection catalogs. Consequently, current PG asphalt binder selection catalogs such as TxDOT uses have severe limitations when applied to asphalt overlays.

To address this limitation, this project evaluated many softer but polymer-modified asphalt binders (PGxx-28 and PGxx-34) in both the laboratory and field. Based on the laboratory test results and field observations, a revised asphalt binder grade selection catalog was developed and validated. In addition, a series of laboratory experiments was performed to evaluate binder quality through aging and mix cracking resistance. Researchers confirmed that the same PG binders performed significantly differently in cracking resistance.

REPORT ORGANIZATION

This report contains the following chapters:

- Chapter 1 provides background information relative to the project.
- Chapter 2 presents the laboratory binder and mixture test results of asphalt binders commonly used in Texas.
- Chapter 3 describes the field test sections constructed around Texas and their field performance.
- Chapter 4 documents the revised asphalt binder grade selection catalog.
- Chapter 5 discusses the laboratory binder quality evaluation.
- Chapter 6 summarizes the conclusions and recommendations for this project.

CHAPTER 2. LABORATORY ASPHALT BINDER AND MIXTURE TESTS: PGXX-22, PGXX-28, AND PGXX-34

INTRODUCTION

This chapter describes the lab tests performed to evaluate and compare different binders. The multiple stress creep recovery (MSCR) and PG grading tests were performed to evaluate the binder's rutting resistance. The Hamburg wheel tracking test (HWTT) was selected to assess the validity of the MSCR binder test. Five asphalt binders and three aggregates were selected for this evaluation. The five binders are PG64-22, PG64-28, PG64-34, PG70-22, and PG76-22; the three aggregates include limestone, crushed gravels, and granite. A full factorial design with a total of 15 mixes was used for this study.

In addition to asphalt binder rutting resistance, fatigue cracking resistance was evaluated too. The linear amplitude sweep (LAS) test and the pure linear amplitude sweep (PLAS) test were conducted using a dynamic shear rheometer (DSR) instrument. These tests obtained characteristic stiffness versus damage evolution curves, which were then used to estimate the number of cycles required to fail asphalt binders at constant shear strains. The Texas overlay test (OT) (Tex-248-F 2014) and the Illinois flexibility index test (I-FIT) (Al-Qadi et al. 2015) were selected in this study to evaluate the cracking resistance of asphalt mixtures. The rankings of cracking resistance between the binder test and the mixture test results were compared.

To further validate the asphalt binder PLAS test, the field fatigue data from the Federal Highway Administration (FHWA) accelerated loading facility (ALF) testing on polymer-modified asphalt binders were analyzed and compared with the PLAS test results.

ASPHALT BINDER SELECTION AND MSCR EVALUATION

Nine asphalt binders ranging from the softest (PG58-34) to the hardest (PG76-22) were selected for this comparison. The MSCR and PG grading tests were performed at 64°C, the temperature pavements experienced in Texas, based on American Association of State Highway and Transportation Officials (AASHTO) TP 70. Figure 1 shows the test results. It is clear that both J_{nr} and $G^*/\sin \delta$ criteria provide the same overall ranking from the most rutting resistant to the least: PG76-XX, PG70-XX, PG64-XX, and PG58-XX. The advantage of the MSCR test is consideration of the influence of recoverable deformation on rutting resistance. For example, PG64-34 has better rutting performance than PG64-28, followed by PG64-22. Current $G^*/\sin \delta$ -based specification cannot identify the difference among the binders with the same high-temperature PG. Therefore, J_{nr} is overall better than $G^*/\sin \delta$. The MSCR test results also clearly showed the significant benefit of using a softer, highly modified binder to improve asphalt binder rutting resistance. However, it is necessary to evaluate how much the improvement in asphalt binder can be transferred into the rutting resistance of asphalt mixes because it is the asphalt mix (asphalt binder and aggregates) rather than asphalt binder alone that is paved on the road. The following section investigates the rutting resistance of these softer, modified binders in the asphalt mixes and the correlation between J_{nr} and asphalt mix rutting test results.

MSCR@64°C

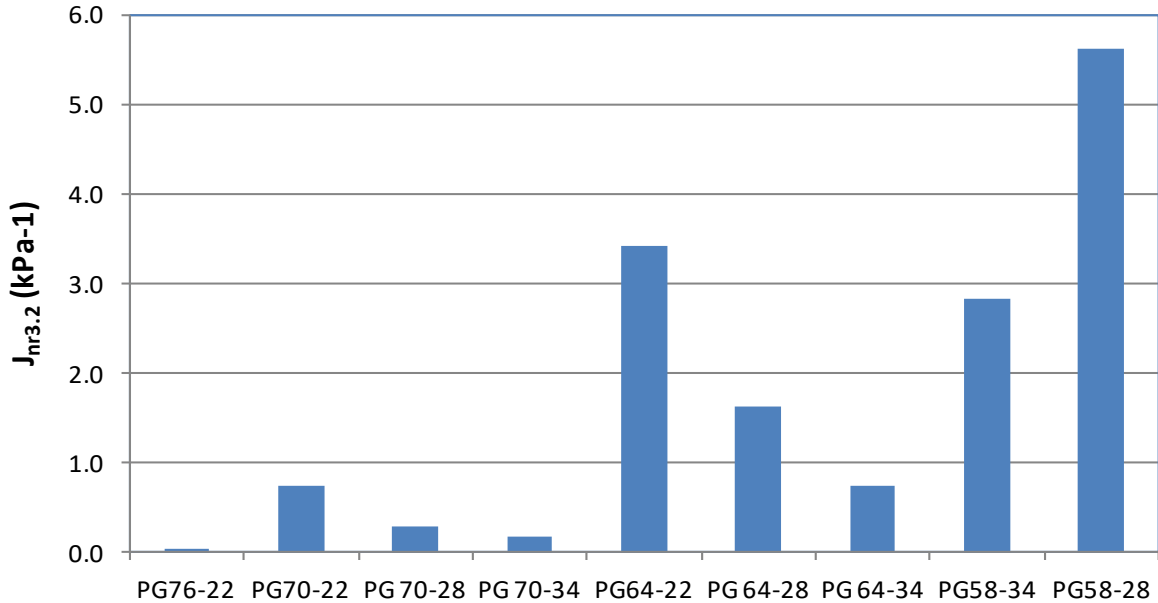


Figure 1. MSCR Test Results of Nine Asphalt Binders.

CORRELATION BETWEEN MSCR BINDER TEST AND ASPHALT MIX RUTTING TEST

Materials and Asphalt Mix Rutting Test

Five asphalt binders and three aggregates were selected for this evaluation. The five binders are PG64-22, PG64-28, PG64-34, PG70-22, and PG76-22; the three aggregates include limestone, crushed gravels, and granite. A full factorial design with a total of 15 mixes was used for this study. For each aggregate type, the same asphalt binder content and gradation were used for all the mixes, and the only variable was the asphalt binder type. Table 1 shows the optimum asphalt binder for each mix. Figure 2 shows the gradations of the mixes.

Table 1. Optimum Asphalt Content of Each Mix.

Aggregates	PG64-22	PG64-28	PG64-34	PG70-22	PG76-22
Limestone (Type D)	4.8%	4.8%	4.8%	4.8%	4.8%
Crushed gravel (Type C)	4.6%	4.6%	4.6%	4.6%	4.6%
Granite (Superpave D)	5.5%	5.5%	5.5%	5.5%	5.5%

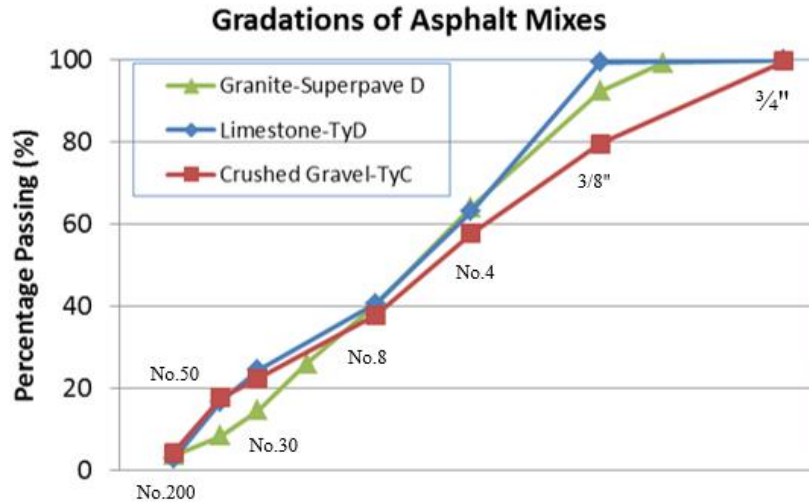


Figure 2. Aggregate Gradations of Mixes Used in This Study.

HWTT is the standard test for evaluating the rutting resistance of asphalt mixes in Texas. So HWTT was selected here to assess the validity of the MSCR binder test. HWTT was conducted at a temperature of 50°C following TEX-242-F, *Test Procedure for Hamburg Wheel-Tracking Test (HWTT)*. A Superpave gyratory compactor was used to mold cylindrical specimens with a diameter of 150 mm and a height of 62 mm. A masonry saw was used to cut along the edge of the cylindrical specimens. The target air void of specimens was 7 percent \pm 1 percent. To evaluate the rutting susceptibility and moisture resistance, specimens were submerged under water at a temperature of 50°C during the test, and a linear variable differential transducer device measured deformations of specimens. The stop criterion was a rut depth of 12.5 mm or 20,000 passes.

Test Results and Analysis

Figure 3, Figure 4, and Figure 5 show the HWTT results of 15 mixes (5 binders and 3 types of aggregates). When examining the results, the following observations are made:

- First, the three PG64-XX binders (PG64-22, PG64-28, and PG64-34) have different rutting performances under the HWTT, regardless of aggregate types, although they have the same high-temperature PG grade. The mixes with the PG64-34 binder have superior rutting performance to those with either PG64-22 or PG64-28 binder. Therefore, the MSCR test and associated specification are better than the current $G^*/\sin \delta$ -based PG specification.
- The PG64-34 and PG70-22 binders graded as PG64-V showed similar performance in terms of rutting only when the stripping part of the HWTT curves is ignored. Additionally, regardless of aggregate types, the PG76-22 binder (graded as PG64-E) mixes had the least rut depth. Thus, the MSCR test and associated specifications work as they should.
- There is not much difference in rutting performance between the mixes with PG64-22 and PG64-28 binders, which proves that the current $G^*/\sin \delta$ -based PG specification works just fine.

In summary, the MSCR test and associated specification seem to work better than the current $G^*/\sin \delta$ -based PG specification. However, caution should be exercised when grading the slightly modified asphalt binders (e.g., PG64-28).

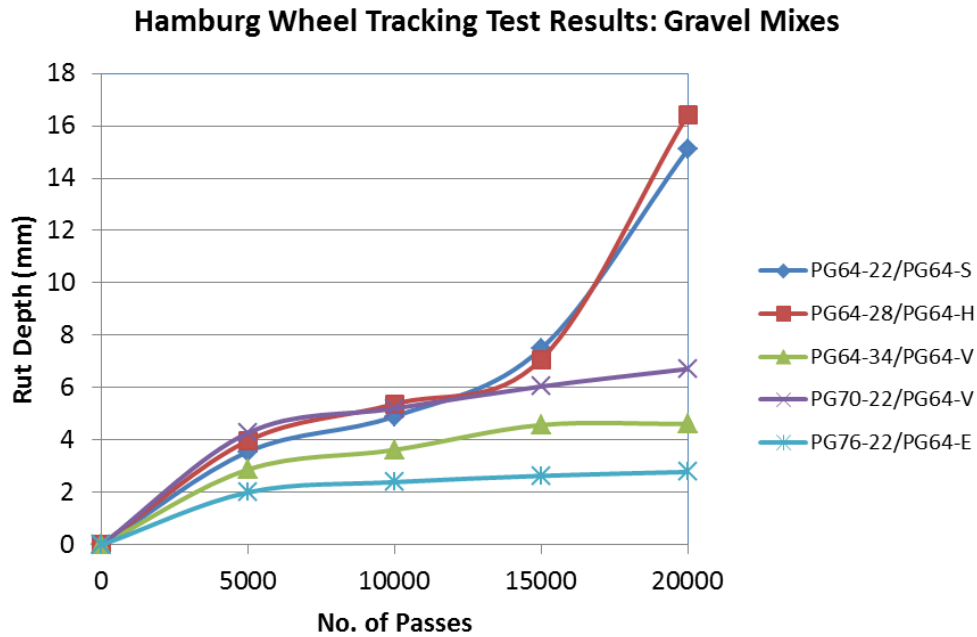


Figure 3. HWTT Results of Gravel Mixes with Five Binders.

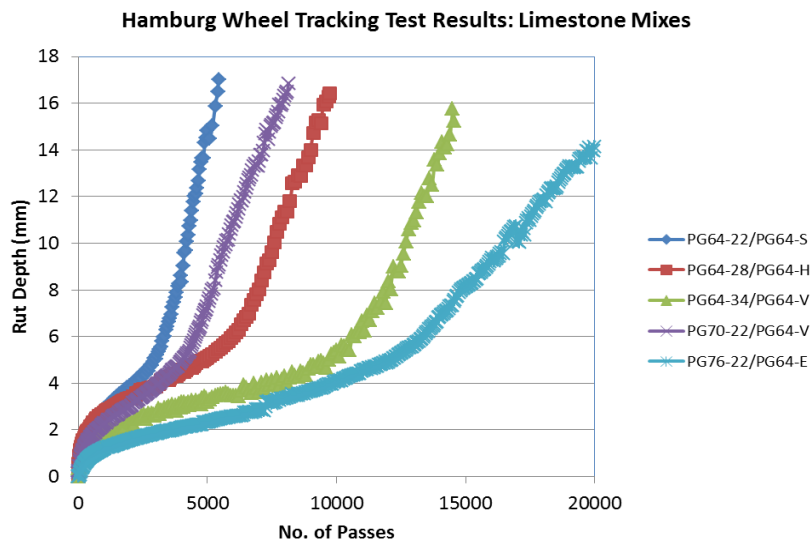


Figure 4. HWTT Results of Limestone Mixes with Five Binders.

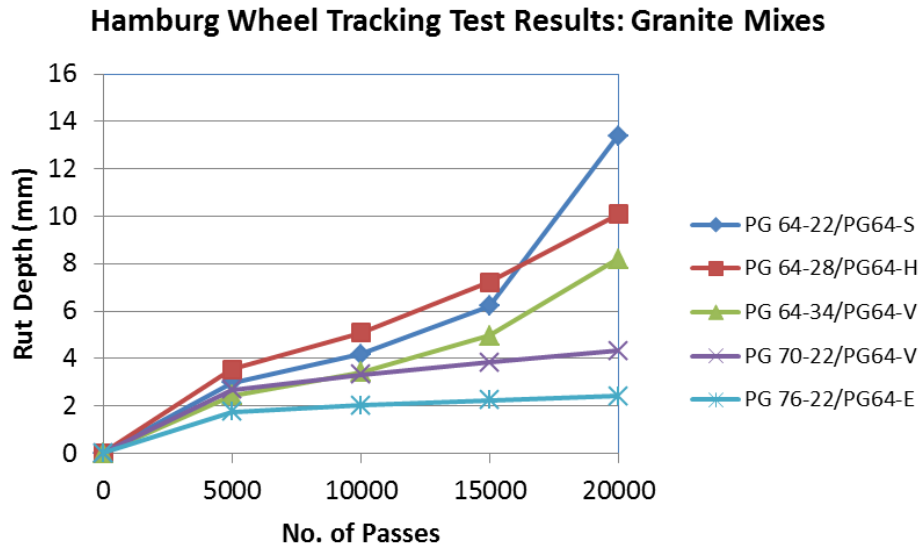
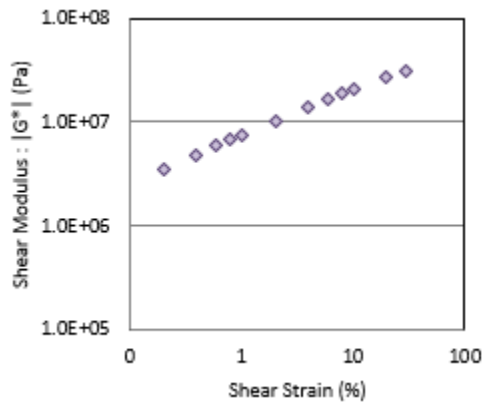


Figure 5. HWTT Results of Granite Mixes with Five Binders.

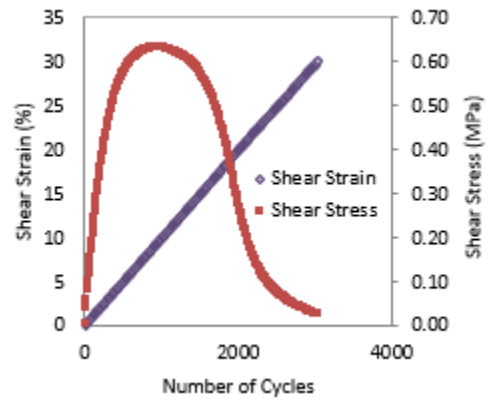
FATIGUE CRACKING RESISTANCE: LAS TESTS AND LIMITATIONS

In addition to asphalt binder rutting resistance, another critical aspect of asphalt binder performance is its fatigue cracking resistance. The research team used the AASHTO TP 101, *Standard Method of Test for Estimating Fatigue Resistance of Asphalt Binders Using the Linear Amplitude Sweep*, to evaluate the fatigue cracking resistance of engineered binders at intermediate temperature. LAS tests are conducted using a DSR instrument. From these tests, characteristic stiffness versus damage evolution curves are obtained, which are then used to estimate the number of cycles required to fail asphalt binders at constant shear strains. There are two steps in this test.

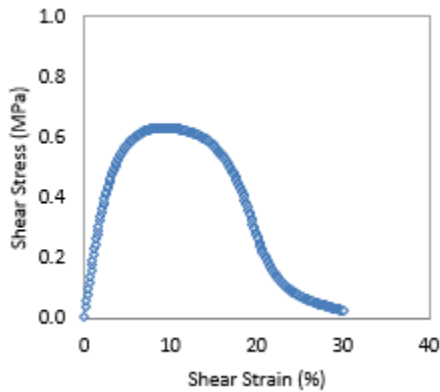
In the first step, asphalt binder samples are first subjected to linear viscoelastic frequency sweep tests at constant shear strain, temperature, and frequency (see Figure 6[a]). The shear stress and shear strain history data recorded during the frequency sweep test (see Figure 6[a]) are then analyzed to obtain the linear viscoelastic properties of the asphalt binder — $|G^*|_{LVE}$ and m . In the second step, the same samples are subjected to cyclic shear tests at the same temperature used in the frequency sweep test (see Figure 6[b]). During this second step, the shear strain increases from 0 to 30 percent every 100 cycles for 3100 cycles of loading. The shear stress versus shear strain history data recorded during the cyclic sweep test (see Figure 6[b] and Figure 6[c]) and the linear viscoelastic properties obtained from the first step are then used together to determine the characteristic damage behavior (i.e., C versus D curves) of asphalt binder samples based on the viscoelastic continuum damage (VECD) mechanics model (see Figure 6[d]).



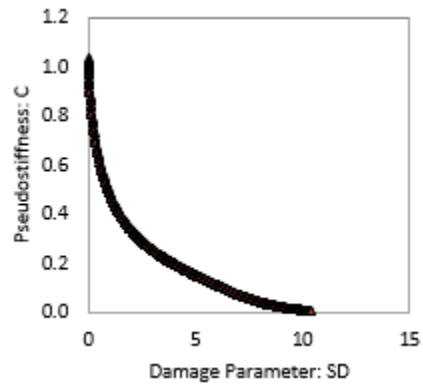
(a) Frequency Sweep Step



(b) LAS Step



(c) Shear Stress \times Shear Strain Curve



(d) Characteristic Curve

Figure 6. LAS Test and Analysis: An Illustration.

Effect of Binder Sources and PGs

For this part of the study, original PG64-34, PG64-28, PG64-22, and PG70-22 asphalt binders were rolling thin film oven (RTFO)-aged and subjected to LAS tests following AASHTO TP 101. Figure 7 presents the estimated fatigue lives of these binders at a controlled shear strain of 2.5 and 5.0 percent. The figure clearly shows that fatigue lives predicted from LAS-VECD analysis for these binders generally follow the relationship one would expect fatigue life would have with PG, except for PG70-22.

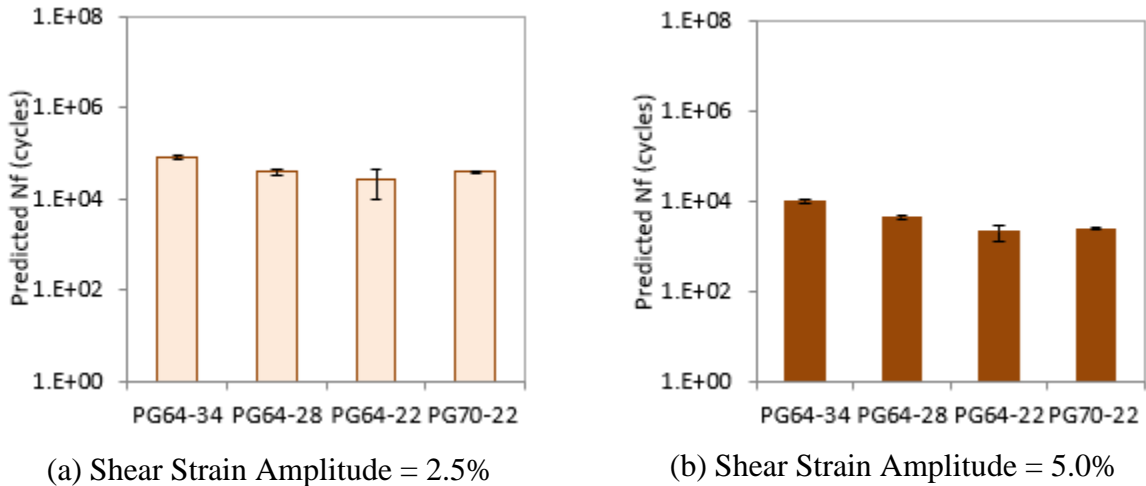
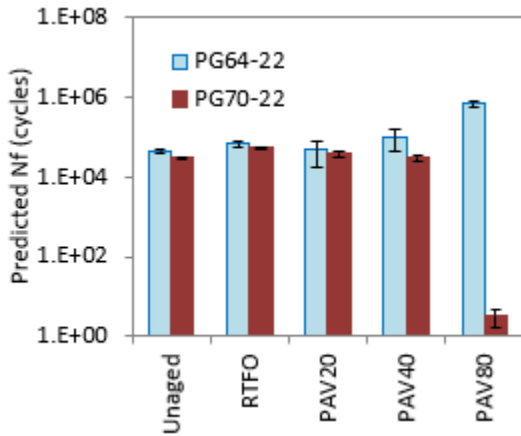


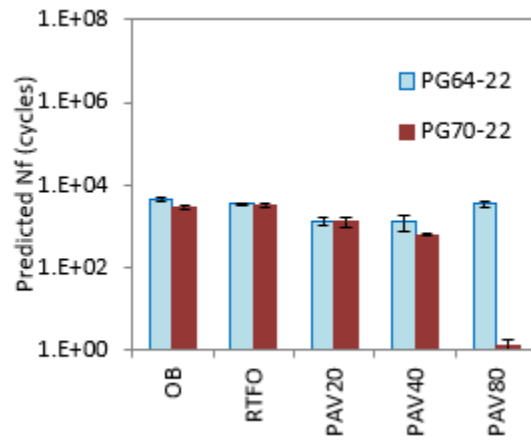
Figure 7. LAS Test Results: Original Binders.

Effect of Aging

For this part of the study, original PG64-22 and PG70-22 binders were aged following the sequences: unaged original binder (OB), RTFO + 0 h pressure aging vessel (PAV) aging, RTFO + 20 h PAV, RTFO + 40 h PAV, and RTFO + 80 h PAV (referred to as OB, RTFO, PAV20, PAV40, and PAV80, respectively). The aged and unaged samples of PG64-22 and PG70-22 binders were then subjected to LAS tests following AASHTO TP 101. Figure 8 presents the fatigue lives of these binders estimated at different aging and loading conditions. The figure clearly shows that fatigue lives predicted from LAS-VECD analysis for both binder grades do not follow the relationship one would expect fatigue life would have with aging. The inconsistency between estimated and expected trends might be due to using the VECD model to predict fatigue life even in severely aged asphalt binders. Using the VECD model in such estimations cannot be justified when the cracks are not homogeneously smeared in the continuum, and the size of continuum is not significantly larger than the size of individual cracks. Since one cannot guarantee both these conditions are met when binders are severely aged, one cannot also justify the use of VECD in severely aged binders. Therefore, there is a need to develop a test method that can discriminate asphalt binders based on their resistance to fatigue cracking at intermediate temperatures even when the binders are severely aged.



(a) Shear Strain Amplitude = 2.5%

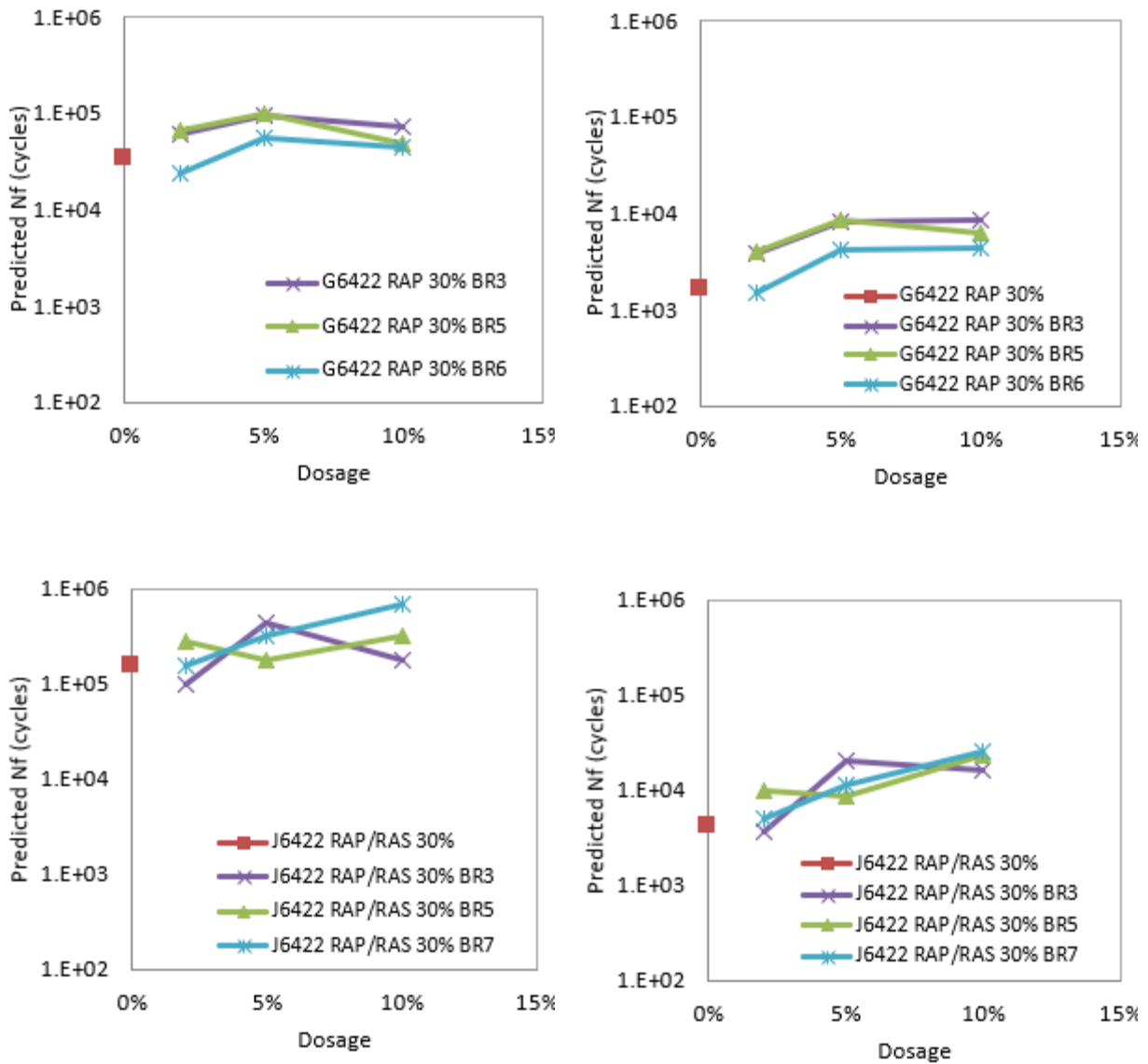


(b) Shear Strain Amplitude = 5.0%

Figure 8. LAS Test Results: Effect of Chemical Aging.

Effect of Engineering Agents

Researchers used materials obtained from two real field projects to evaluate the effect of engineering agents on the fatigue cracking resistance of asphalt binders at intermediate temperatures following LAS tests. From the materials obtained from one of these two field projects, PG64-22 asphalt binder from source G (G6422); 30 percent recycled asphalt pavement (RAP)–extracted asphalt binder; and 2, 5, and 10 percent bio-rejuvenators (BR3, BR5, and BR6) were used. From the materials obtained from the other field project, PG64-22 asphalt binder from source J (J6422); 18 percent RAP and 11 percent RAP-extracted asphalt binders; and 2, 5, and 10 percent bio-rejuvenators (BR3, BR5, and BR6) were used. The blends were tested at 15°C under the PLAS test using two replicates per blend. Figure 9 shows the predicted fatigue lives for binders engineered with bio-rejuvenators at different control strain rates. The results did not show consistent trends.



(a) Shear Strain Amplitude = 2.5%

(b) Shear Strain Amplitude = 5.0%

Figure 9. LAS Test Results: Effect of Engineering Agents.

NEW FATIGUE CRACKING RESISTANCE: PLAS TESTS

Hintz and Bahia (2013) discussed crack propagation of asphalt binders under the time sweep test in which a constant shear strain is applied to asphalt binder samples (8 mm in diameter and 2 mm in thickness) using a DSR. Texas A&M Transportation Institute (TTI) researchers used a power-law relationship between energy release rate, J , and crack growth rate, \dot{c} , proposed previously by Schapery (1984) to describe asphalt binder propagation under DSR testing. Specifically, for DSR testing, Hintz and Bahia (2013) defined the energy release rate, J , as in Equation 1.

$$J = \frac{|G^*|\gamma^2 h}{2r^2(r-c)} \left(r - c + z \left(1 - e^{-\frac{c}{z}} \right) \right)^3 \left(1 - e^{-\frac{c}{z}} \right) \quad (1)$$

Herein, $|G^*|$ is shear modulus, γ is shear strain under the time sweep test, c is crack length, r is sample radius, h is sample height or thickness, and z is a numerical factor equal to 0.1 for this case. When dealing with concrete fracture, Bazant and Prat (1988) proposed an alternative cracking growth rate equation (Equation 2).

$$\dot{c} = A \left(\frac{J}{J_f} \right)^n \quad (2)$$

Herein, \dot{c} is crack growth (or propagation) rate, J is energy release rate, J_f is fracture energy determined from a monotonic test, and A and n are parameters determined by repetitive laboratory testing (e.g., the time sweep test). The previous equation shows that parameter $\frac{J}{J_f}$ has a significant influence on the crack growth rate although it does not represent the whole cracking process. The larger the $\frac{J}{J_f}$ value, the faster the crack growth. Thus, some characterizing parameters for asphalt binder fatigue resistance can potentially be derived from parameter $\frac{J}{J_f}$ shown in Equation 3.

$$\frac{J}{J_f} = \frac{|G^*|\gamma^2 h}{2r^2(r-c)J_f} \left(r - c + z \left(1 - e^{-\frac{c}{z}} \right) \right)^3 \left(1 - e^{-\frac{c}{z}} \right) \quad (3)$$

This equation shows that parameter $\frac{J}{J_f}$ is directly proportional to $\frac{|G^*|\gamma^2}{J_f}$ for a specific crack length, c . The parameters r , h , and z are constants. Therefore, the cracking growth rate is highly related to the parameter $\frac{|G^*|\gamma^2}{J_f}$. For a time sweep test, the smaller $\frac{|G^*|\gamma^2}{J_f}$, the slower crack growth, the better fatigue crack resistance.

To recap, the new cracking parameter $\frac{|G^*|\gamma^2}{J_f}$ is derived based on fracture mechanics and the time sweep test at a constant shear strain, γ .

The time sweep test itself is too long, and the LAS test was developed as an accelerated asphalt binder fatigue test. Thus, the new asphalt binder fatigue cracking test is proposed based on the latest LAS test. Since the characterizing parameter $\frac{|G^*|\gamma^2}{J_f}$ is not a fundamental indicator but an index parameter, the shear modulus can be approximately calculated from the measured shear stress versus shear strain curve of the LAS test. Thus, the initial frequency sweep test in the current LAS test becomes unnecessary. The new asphalt binder fatigue cracking test is a PLAS test running at a selected temperature using oscillatory shear in strain-control mode at a frequency of 10 Hz. The loading scheme consists of a continuous oscillatory strain sweep. Loading is increased linearly from 0 to 30 percent throughout 3000 cycles, as shown in Figure 6(a) and Figure 6(b).

Figure 10 shows peak shear strain and peak shear stress recorded every 10 load cycles (or every 1 sec). The proposed PLAS test differs from the time sweep test in which the cyclic shear strain is constant. Thus, the characterizing parameter $\frac{|G^*|\gamma^2}{J_f}$ cannot be used for the PLAS test. An alternative fatigue resistant energy index (FREI) is proposed in Equation 4.

$$FREI = \frac{J_{f-\tau_{max}}}{G_{0.5\tau_{max}}} \cdot (\gamma_{0.5\tau_{max}})^2 \quad (4)$$

Herein, $J_{f-\tau_{max}}$ is the shear fracture energy calculated until maximum shear stress (see Figure 10), $G_{0.5\tau_{max}}$ is the calculated shear modulus at the point of half of the maximum shear stress, and $\gamma_{0.5\tau_{max}}$ is the shear strain at the point of half of the maximum shear stress.

FREI is a kind of reciprocal of parameter $\frac{|G^*|\gamma^2}{J_f}$, but there are some differences. FREI characterizes the resistance of asphalt binder to fatigue cracking. The larger the FREI, the better fatigue cracking resistance. Other rationales for FREI definition are as follows:

- **$J_{f-\tau_{max}}$** : It is well known that materials with larger fracture energy normally have better cracking resistance. Unlike a regular fracture energy calculation, only the first half (until maximum shear stress) of the stress versus strain curve is used for calculating $J_{f-\tau_{max}}$. The reasons for that are that the stress/strain conditions asphalt binders experience in the real-world asphalt binder pavements are far less severe than the maximum shear stress/strain although it may be higher than the stress/strain conditions of asphalt binder concrete as a whole; and the shear strain after the peak stress may not be the real strain asphalt binder experience due to potential macrocrack in the DSR asphalt binder specimen and consequently unknown true radius of the asphalt binder specimen.
- **$\gamma_{0.5\tau_{max}}$** : Unlike the shear strain in the time sweep test, which is constant, $\gamma_{0.5\tau_{max}}$ is the shear strain at the point of half of the maximum shear stress. For any two asphalt binders, larger $\gamma_{0.5\tau_{max}}$ means better flexibility and relaxation capability of asphalt binder when both asphalt binders reach their half of maximum shear load bearing capacities. That is the main reason for switching $\gamma_{0.5\tau_{max}}$ to the numerator from the denominator (reciprocal of parameter $\frac{|G^*|\gamma^2}{J_f}$ original derivation for the time sweep test).
- **$G_{0.5\tau_{max}}$** : Larger shear modulus often makes asphalt binders more prone to cracking when all other factors are the same. The value of $G_{0.5\tau_{max}}$ is not equal to the asphalt binder shear modulus value measured at the small strain level. Instead, TTI researchers chose the shear modulus $G_{0.5\tau_{max}}$ at the point of half of the maximum shear stress because the researchers believe that the asphalt binders often experience higher shear strain than those used in the frequency sweep test for determining shear modulus.

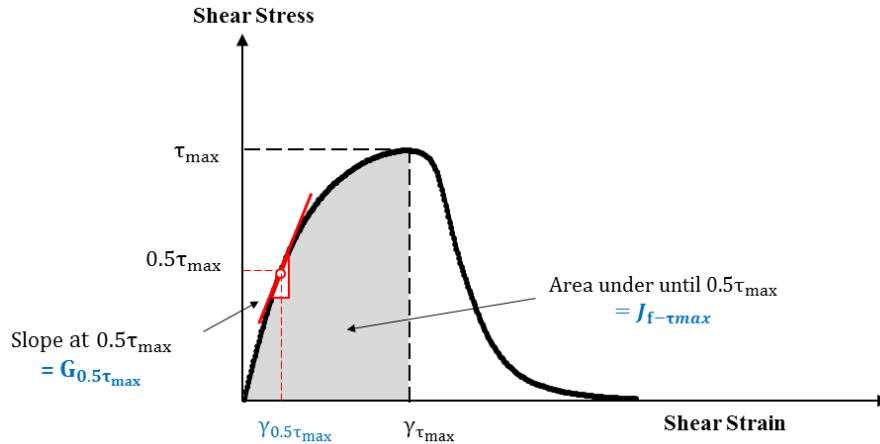


Figure 10. PLAS Test and Analysis: An Illustration.

Asphalt binder aging through oxidation makes asphalt binders more brittle and consequently less cracking resistant (Glover et al. 2005, Peterson 2009, Vallerga 1981). The more severe the aging, the worse the asphalt binder fatigue resistance. Recently, bio-rejuvenators have been used with RAP materials to compensate for aged asphalt binders in RAP or reclaimed asphalt shingles (RAS). One of the main purposes of using bio-rejuvenators is to restore the lost chemical balance between asphaltenes and maltenes within aged asphalt binders so that the rejuvenated asphalt binders become more flexible and better fatigue resistant (Epps et al. 1980). The ensuing sections illustrate the success of the parameter FREI in discriminating the effect of the source and PG of asphalt binders, the durations of chemical aging, and the sources and dosages of engineering agents.

Effect of Binder Sources and PGs

For this part of the study, original PG64-34, PG64-28, PG64-22, and PG70-22 asphalt binders were first RTFO aged and then subjected to LAS tests following AASHTO TP 101. For each OB, two replicates were used. Figure 11 presents PLAS test results of these original binders. The figure clearly shows that fatigue lives predicted from LAS-VECD analysis for these binders generally follow the relationship one would expect fatigue life would have with PG.

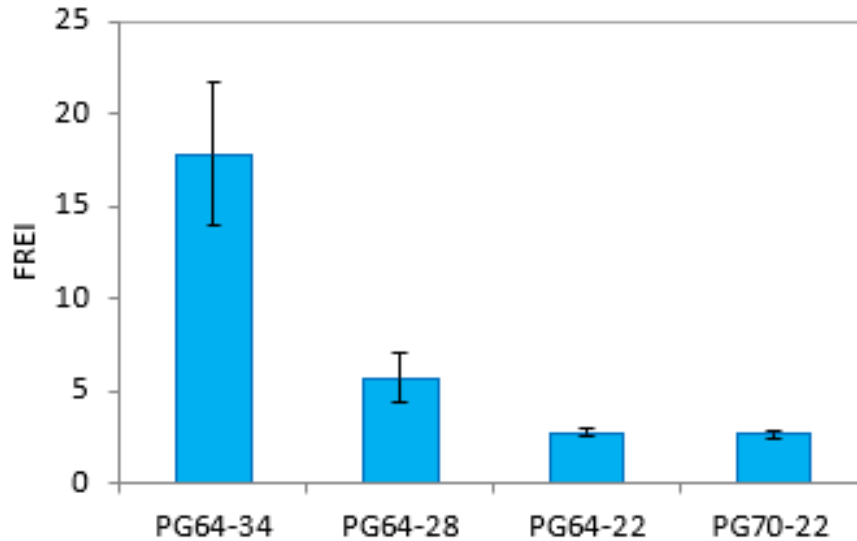


Figure 11. PLAS Test Results: Original Binders.

Effect of Aging

The same two asphalt binders used to identify the deficiency of the LAS test were used to evaluate the effect of aging on fatigue cracking resistance of asphalt binders at intermediate temperature using the PLAS test. For each asphalt binder, the PLAS test was performed at 15°C for five aging conditions: OB, RTFO, PAV20, PAV40, and PAV80. For each aging condition, two replicates were used. Figure 12 shows the averaged FREI value for each asphalt binder at each specific aging condition. The figure indicates that the FREI is a true indicator of asphalt binder fatigue resistance—the aged binders have lower values of FREI and, thereby, poorer fatigue resistance.

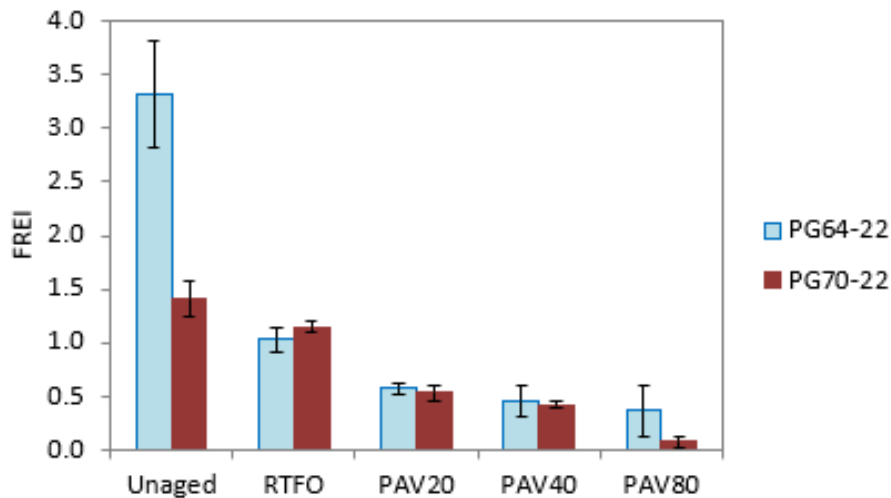


Figure 12. PLAS Test Results: Effect of Chemical Aging.

Effect of Engineering Agents

Using the PLAS test, materials from the two real field projects described before were used to evaluate the effect of engineering agents on FREI or fatigue cracking resistance of asphalt binders at intermediate temperature. Figure 13 shows the averaged FREI value for each bio-rejuvenator at each specific dosage rate. The figure clearly shows that FREI has a good correlation with the dosage of bio-rejuvenator; the FREI value becomes higher with a higher dosage of bio-rejuvenator, suggesting that an increase in bio-rejuvenator dosage makes asphalt binder more ductile and thereby more able to resist fatigue cracking at intermediate temperatures. The figure also shows that FREI clearly discriminates the effectiveness of different sources of these agents.

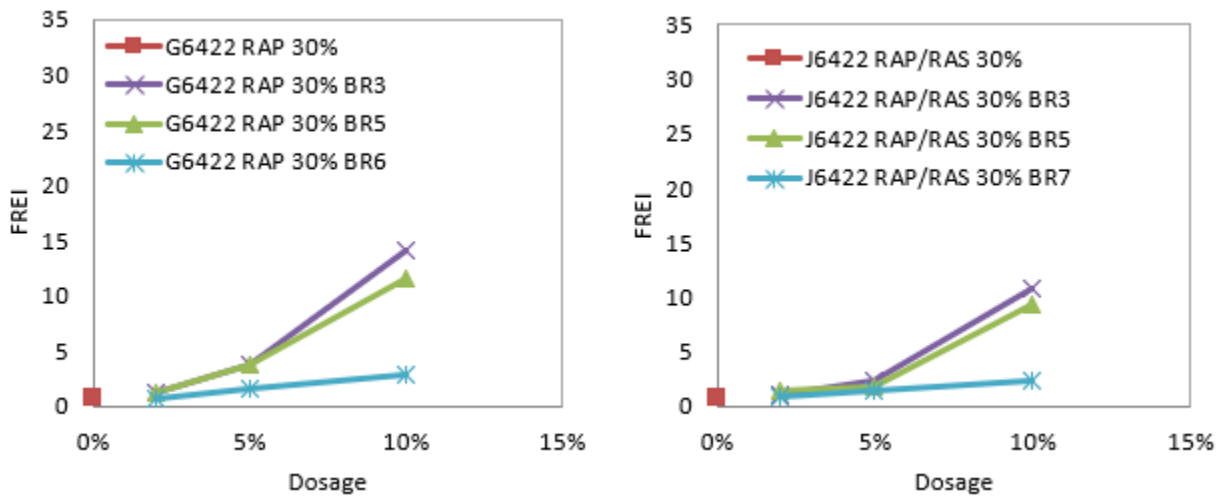


Figure 13. PLAS Test Results: Effect of Engineered Binders.

The juxtaposition of the LAS and PLAS test reveals that PLAS is more effective than the LAS test in discriminating the effect of the sources and PG of asphalt binder sources, the conditions of chemical aging, and the source and dosage of engineering agents.

Correlation with Laboratory Mixture Cracking Tests

Many tests have been developed to evaluate the cracking resistance of asphalt binder mixtures (Zhou et al. 2016b). Based on previous work (Zhou et al. 2016a), the Texas OT (Tex-248-F 2014) and the I-FIT (Al-Qadi et al. 2015) were selected for this study. The Texas OT uses the number of cycles to fail (OT cycles) to discriminate the cracking resistance of asphalt binder mixtures. The higher the number of OT cycles, the better the cracking resistance. The I-FIT uses the flexibility index (FI) to discriminate the cracking resistance of asphalt binder mixtures. The larger the FI value, the better the cracking resistance.

The same limestone aggregates with the same gradation plus four different asphalt binders were used to produce four virgin asphalt binder mixtures. The nominal maximum aggregate size for the mixtures was 9.5 mm, and the same optimum asphalt binder content of 5.7 percent was used for all four mixtures. For each mixture, five replicates of OT and four replicates of I-FIT specimen at 7.0 ± 0.5 percent air voids were prepared through the Superpave gyratory compactor

and saw cutting. Before the compaction, each loose mix was conditioned in the oven for 4 h at 135°C. Both tests were run at a room temperature of 25°C following the Tex-248-F (2014) and the procedure proposed by Al Qadi et al. (2015). Figure 14 shows the averaged OT cycles and FI values for four different mixtures used in this study. Both mixture cracking tests indicated that the asphalt binder PG64-34 had the best cracking resistance, followed by PG64-28, PG64-22, and PG70-22.

The same four asphalt binders were characterized under the PLAS test at 15°C. Figure 14 also presents the calculated FREI for each asphalt binder. A comparison of the calculated FREI values and those mixture cracking results clearly shows that the rankings of cracking resistance between the PLAS test and mixture cracking tests on these four asphalt binders are the same (from the best to the worst): PG64-34, PG64-28, PG-64-22, and PG70-22.

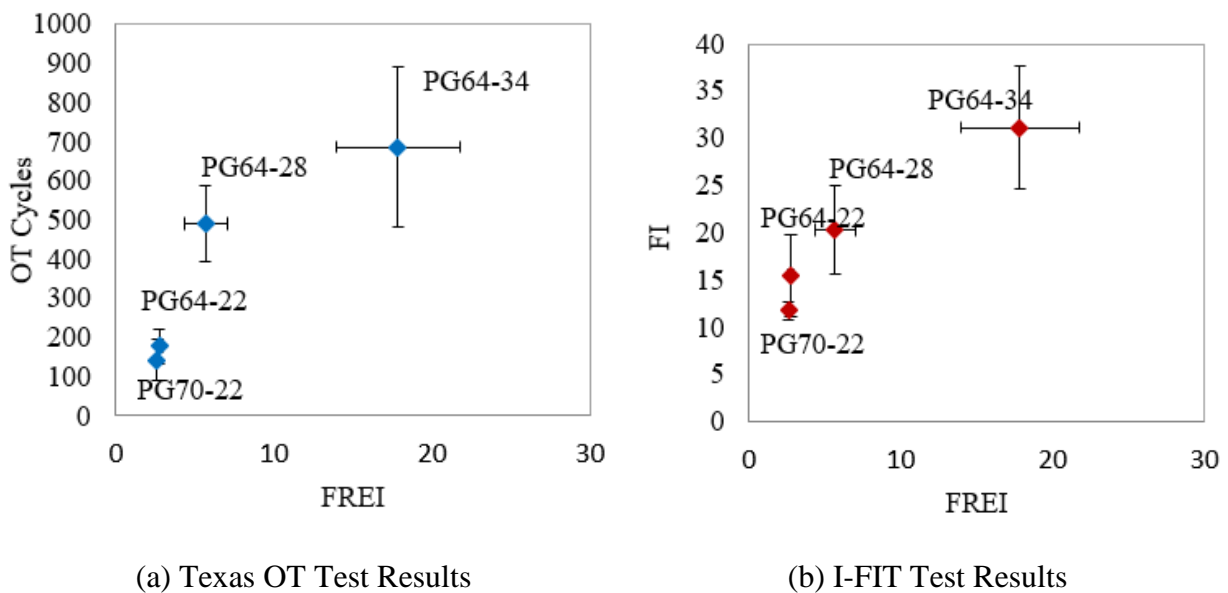


Figure 14. PLAS Test Results: Correlation with Mixture Cracking Results.

Correlation with Full-Scale Accelerated Pavement Tests

To further validate the asphalt binder PLAS test, TTI researchers employed the fatigue data from FHWA-ALF testing on polymer-modified asphalt binders (Gibson et al. 2012). Twelve full-scale lanes of pavement with various modified asphalt binders were constructed at FHWA-ALF under Pooled Fund Study TPF-5(019) in summer 2002. Figure 15 shows the layout of the 12 test lanes. All 12 lanes have an asphalt binder layer and a granular base (GB) course over a uniformly prepared subgrade. The pavements were loaded with super single tires (74 kN [16.6 kips] and 827.4 kPa [120 psi]) at 19°C (66°F). Lanes 2 to 6 had clear bottom-up fatigue cracking, so these five lanes were used for validating the asphalt binder PLAS test.

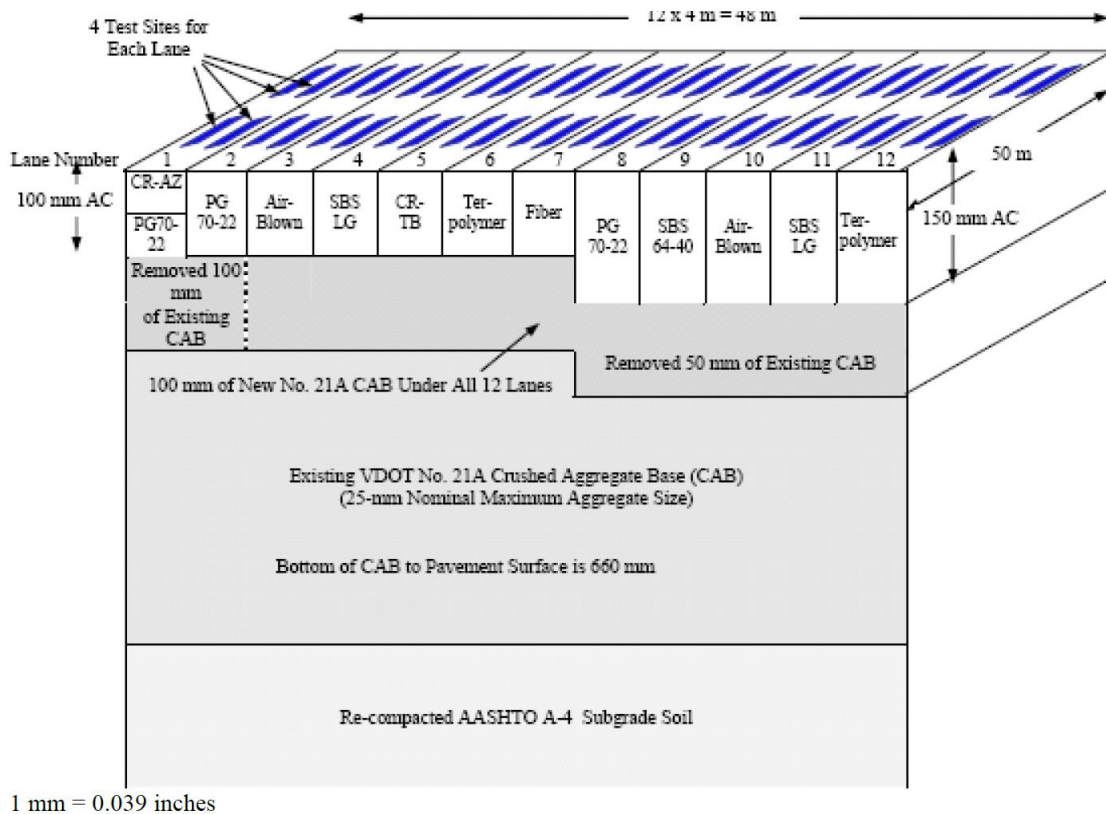


Figure 15. Three-Dimensional Layout of the FHWA-ALF Test Section (Gibson et al. 2012).

Although the FHWA-ALF testing was completed long ago, original asphalt binders from Lanes 2, 3, 4, 5, and 6 were stored and available for validation. To match the FHWA-ALF testing temperature, the PLAS tests on the RTFO-aged original asphalt binders were run at 19°C as well. Figure 16 compares the asphalt binder fracture index (FREI), and the load passes to a 25 percent cracked area measured from FHWA-ALF. The PLAS test results match the overall trend of the FHWA-ALF fatigue data. An imperfect relationship shown in Figure 16 is expected because many factors impact field fatigue performance. The asphalt binder is not the only one, as mentioned in this report's introduction. Thus, the full-scale field fatigue data results also indicated that the PLAS test is effective for evaluating asphalt binder fatigue resistance.

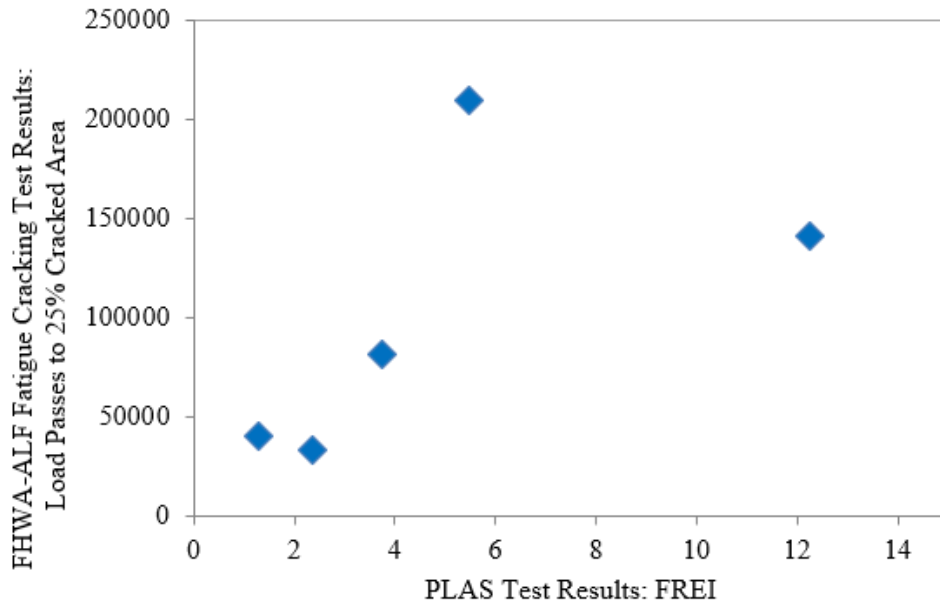


Figure 16. PLAS Test Results: Correlation with FHWA-ALF Cracking Test Results.

SUMMARY AND CONCLUSION

Lab tests were performed to evaluate and compare different binders' rutting and cracking resistance. Based on the test results, the following summary and conclusions are offered:

- Nine asphalt binders ranging from the softest (PG58-34) to the hardest (PG76-22) were selected for the evaluation. The MSCR and PG grading tests were performed at 64°C, the temperature pavements experienced in Texas, based on AASHTO TP 70. HWTT was selected here to assess the validity of the MSCR binder test. According to the HWTT results of 15 mixes (5 binders and 3 types of aggregates), the mixes with the PG64-34 binder have superior rutting performance to those with either PG64-22 or PG64-28 binder. The MSCR test and associated specification are better than the current $G^*/\sin \delta$ -based PG specification.
- Regarding the cracking resistance evaluation, the juxtaposition of the LAS and PLAS test reveals that the PLAS test is more effective than the LAS test in discriminating the effect of the sources and PG of asphalt binder sources, the conditions of chemical aging, and the source and dosage of engineering agents.
- A comparison of the calculated FREI values and those mixture cracking results clearly shows that the rankings of cracking resistance between the PLAS test and mixture cracking tests are the same (from the best to the worst).
- The PLAS test results match the overall trend of the FHWA-ALF fatigue data. The full-scale field fatigue data results indicated that the PLAS test effectively evaluated asphalt binder fatigue resistance.

CHAPTER 3. FIELD PERFORMANCE OF TEST SECTIONS WITH PGXX-22, PGXX-28, AND PGXX-34 BINDERS

INTRODUCTION

Multiple field test sections were constructed under this project to confirm the benefits of soft, highly modified binders in the colder areas of Texas. TTI researchers have been surveying cracking and rutting distresses of these sections periodically since their initial construction. This chapter describes the construction and field performance of each field test section.

SH 15 TEST SECTIONS IN AMARILLO DISTRICT

General Description

Four test sections were constructed on SH 15 near Perryton, Texas, under Project 0-6674 (Hu et al. 2014). The starting point of the first section is about 4.3 miles away from the intersection of SH 15 and US 83 (see point A in Figure 17) and is right across milepost number 368. Each of these sections is bound northeast and measures 1000 ft in length.

The sections were constructed by replacing 1 in. of existing pavement with 1.5 in. of Type D and 1 in. of Type F mix. The Type D overlay was prepared with different percentages or grades of asphalt binder as follows:

- Section 1: 5.5 percent PG58-28 (control mix).
- Section 2: 5.8 percent PG58-28.
- Section 3: 5.8 percent PG64-34.
- Section 4: 5.5 percent PG64-34.

Section 1 used the control mix prepared with PG58-28 asphalt binder, while Section 2 used the mix with the same asphalt binder but with higher asphalt binder content. Section 3 and Section 4 used the softer but highly modified PG64-34 asphalt binder but slightly different asphalt binder contents. The mix designs followed the TxDOT specification.

The sections were constructed on October 7, 2013. The average paving temperature was measured as 245°F. The temperature measurement was taken directly from the material behind the paver.

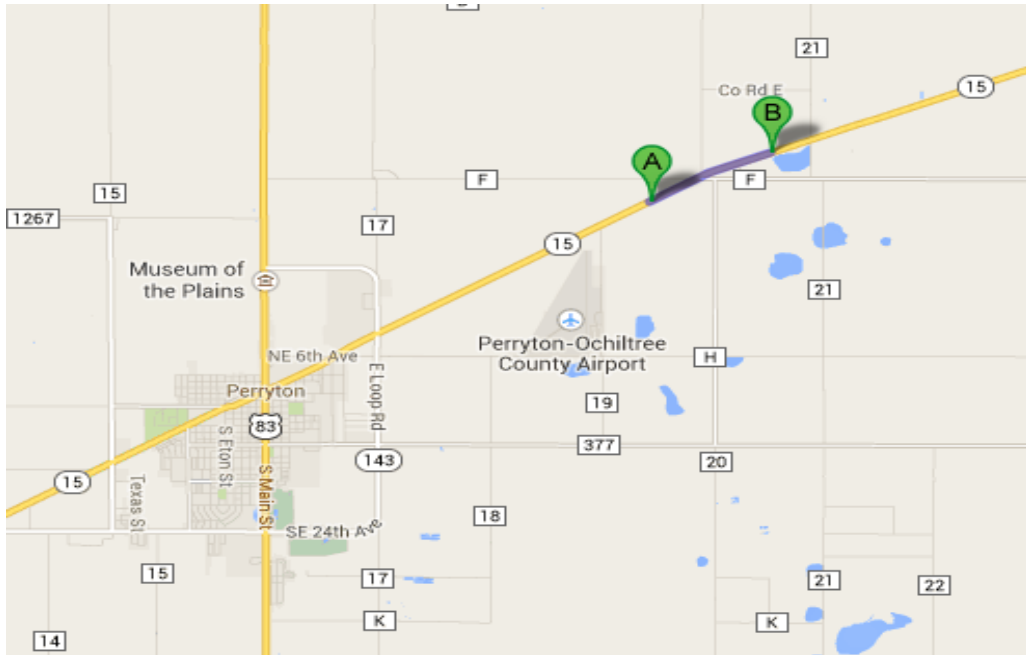


Figure 17. SH 15 Test Sections: Location Map via Google.

Field Survey

The last survey of these sections under Project 0-6674 was conducted on June 7, 2014. At the time, no cracking or rutting issues were observed. Since then, the sections have been surveyed six more times, in March 2015, September 2015, March 2016, September 2016, March 2017, and January 2018. Figure 18 through Figure 21 present the conditions of sections as observed in recent surveys.

Rutting

Researchers detected rutting in each section for the first time in January 2018. The detected rut depth was only about 1/16 in., as shown in Figure 18 through Figure 21. They had not observed any rutting before this survey.

Cracking

Section 1: Researchers spotted cracking in this section for the first time in March 2016 (see Figure 22). At the time, 14 transverse cracks totaled 213 ft/mile, and 8 different stretches of alligator cracking totaled 20.5 percent of the total lane area. In September 2017, researchers found that almost all cracks healed, most likely due to heat in the summer. In March 2017, cracks reappeared with much higher severity, with a total of 22 transverse cracks that totaled 3052 ft/mile and 13 different stretches of alligator cracking that totaled 25.5 percent of the total lane area. The most recent survey conducted on January 10, 2018, showed that cracks have interconnected throughout the section covering both wheel paths, as shown in Figure 18.

Section 2: Researchers observed cracking in this section for the first time in March 2016 (see Figure 22). At the time, there were only 2 transverse cracks that totaled 26 ft/mile and

1 longitudinal crack that totaled 29 ft/mile. In March 2017, researchers detected more cracks: 10 transverse cracks totaled 179 ft/mile, 7 longitudinal cracks totaled 183 ft/mile, and 2 stretches of alligator cracking totaled 3.3 percent of the total lane area. Healing was not observed in this section. In January 2018, researchers found that the transverse cracks covered the full width of the sections and that cracks have interconnected with each other, more noticeably in the inner wheel path throughout the section, as shown in Figure 19.

Section 3: Researchers observed cracking in this section for the first time in September 2016 (see Figure 22). At the time, only 1 stretch of alligator cracking totaled 1.8 percent of the total area. In March 2017, researchers detected 3 new transverse cracks that totaled 53 ft/mile and 7 new stretches of alligator cracking that totaled 18.4 percent of the total lane area. A recent survey in March 2018 showed that all these cracks have interconnected, as shown in Figure 20.

Section 4: Researchers observed cracking in this section for the first time in March 2017 (see Figure 22). At the time, they detected 3 transverse cracks totaling 54 ft/mile and 6 stretches of alligator cracks totaling 21.3 percent of the total lane area. The survey in January 2018 showed that transverse cracks have extended full width, and alligator cracks have interconnected with each other, as shown in Figure 21.



Alligator Cracking: 03/07/2017



Transverse Cracking: 03/07/2017



Overall Cracking: 01/10/2018



Rutting (1/16 in.): 01/10/2018

Figure 18. SH 15 Test Section 1: Survey Pictures.



Alligator Cracking: 03/07/2017



Transverse Cracking: 03/07/2017



Longitudinal Cracking: 03/07/2017



Cracking: 01/10/2018



Rutting (1/16 in.): 01/10/2018

Figure 19. SH 15 Test Section 2: Survey Pictures.



Alligator Cracking: 03/07/2017



Transverse Cracking: 03/07/2017



Overall Cracking: 01/10/2018



Rutting (1/16 in.): 01/10/2018

Figure 20. SH 15 Test Section 3: Survey Pictures.



Alligator Cracking: 03/07/2017



Transverse Cracking: 03/07/2017



Overall Cracking: 01/10/2018



Rutting (1/16 in.): 01/10/2018

Figure 21. SH 15 Test Section 4: Survey Pictures.

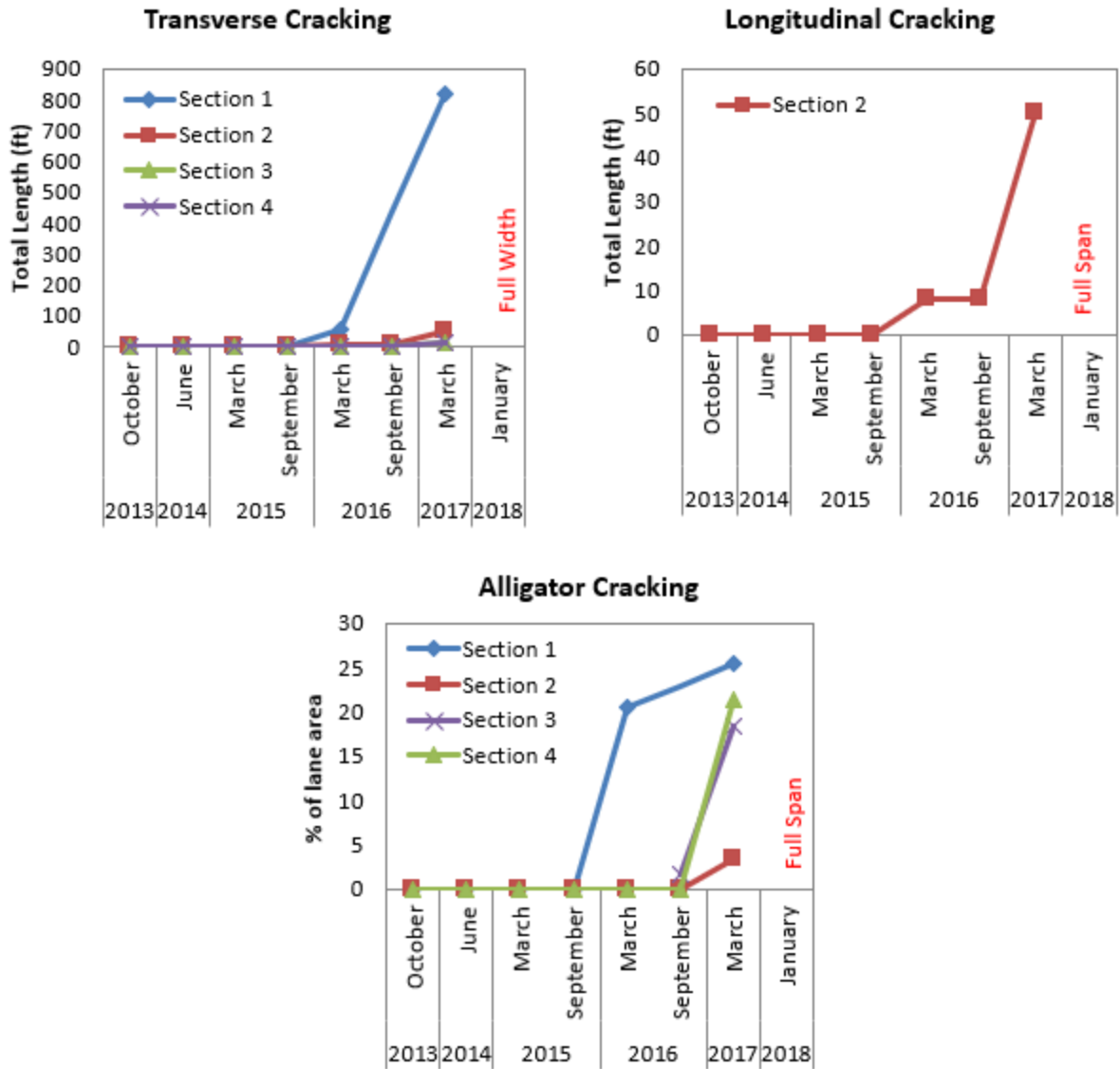


Figure 22. SH 15 Test Sections: Survey Results.

The fact that alligator, longitudinal, and transverse cracking appears later and with smaller severity values in Sections 3 and 4 than in Sections 1 and 2 (Figure 22) suggests that PG64-34 was able to delay the initiation and the propagation of cracking as expected.

US 62 TEST SECTIONS IN CHILDRESS DISTRICT

General Description

Three sections were constructed on the eastbound side of US 62 close to Childress, Texas, under Project 0-6674 (Hu et al. 2014). Figure 23 shows the starting point of Section 1 (point A) and the end point of Section 3 (point B). Each section is bound northeast and measures about 1500 ft in length. Milepost number 442 lies just next to the starting point of Section 3.

The sections were constructed by replacing 8 in. of existing pavement with 2 in. of Type D mix and 3 in. of Type B mix. The 3 in. of Type B mix was used throughout the project; the only difference is the surface Type D mix. The Type D mix in these three sections differed either in asphalt binder grade or in the use of reclaimed materials as follows:

- Section 1: PG64-34 + RAP/RAS.
- Section 2: PG70-28 (control mix).
- Section 3: PG70-28 + RAP/RAS.

Section 1 uses the mix prepared with PG64-34 asphalt binder together with reclaimed materials, Section 2 uses the mix prepared with virgin mix and a PG70-28 asphalt binder (without RAP/RAS), and Section 3 uses the mix prepared with PG70-28 asphalt binder together with reclaimed materials. The only difference between Sections 1 and 3 is the asphalt binder type: PG64-34 in Section 1 versus PG70-28 in Section 3.

The construction of the overlay was conducted on October 3, 2013. The average paving temperature was measured behind the paver as 320°F.



Figure 23. US 62 Test Sections: Location Map via Google.

Field Survey

The last survey of these sections under Project 0-6674 was conducted on June 6, 2014. At the time, neither cracking nor rutting was detected in any of these sections. Since then, the sections have been surveyed six more times: March 2015, September 2015, March 2016, September 2016, March 2017, and January 2018. Figure 24 through Figure 26 present the conditions of sections as observed in recent surveys.

Rutting

None of these sections has exhibited any noticeable rutting as of January 10, 2018 (see Figure 24 through Figure 26).

Cracking

Section 1: Researchers first observed cracks in this section in March 2017 (see Figure 27). At the time, 10 longitudinal cracks totaled 1181 ft/mile, and only 2 transverse cracks totaled 76 ft/mile. In January 2018, 20 longitudinal cracks that totaled 2192 ft/mile were observed. The total number and length of transverse cracks remained intact.

Section 2: Researchers first observed transverse cracks in this section in March 2015 (see Figure 27). These cracks increased from 44, totaling 239 ft/mile in March 2015 to 163 cracks totaling 886 ft/mile in January 2018. Similarly, researchers observed longitudinal cracks in this section first in January 2018. Three longitudinal cracks totaled 134 ft/mile.

Section 3: Researchers first observed transverse cracks in this section in March 2015 (see Figure 27). The total number of these cracks remained almost the same, from 19 cracks that totaled 588 ft/mile in March 2015 to 20 cracks that totaled 1170 ft/mile in January 2018. Similarly, researchers observed longitudinal cracks in this section first in January 2018. Ten longitudinal cracks totaled 3917 ft/mile.



Longitudinal Cracking: 01/10/2018

Transverse Cracking: 01/10/2018



Rutting (None): 01/10/2018

Figure 24. US 62 Test Section 1: Survey Pictures.



Longitudinal Cracking: 01/10/2018



Transverse Cracking: 01/10/2018



Rutting (None): 01/10/2018

Figure 25. US 62 Test Section 2: Survey Pictures.



Longitudinal: 01/10/2018



Transverse Cracking: 01/10/2018



Rutting: 01/10/2018 (None)

Figure 26. US 62 Test Section 3: Survey Pictures.

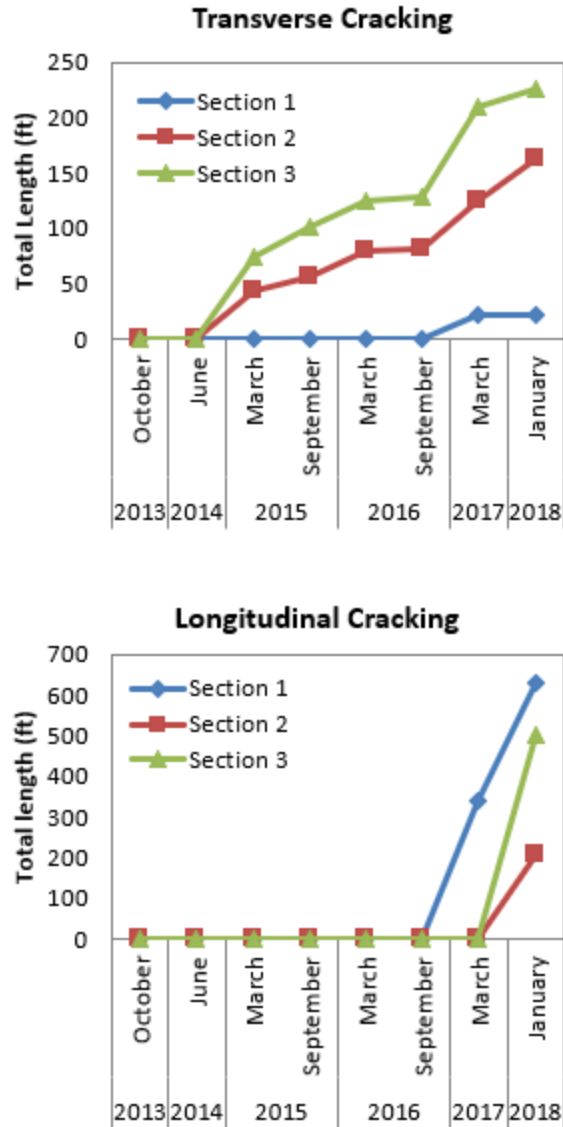


Figure 27. US 62 Test Sections: Survey Results.

Considering both transverse and longitudinal cracking, it is clear that Section 1 has less total cracking length than Sections 2 and 3. Such observation indicated that PG64-34 was able to impede the initiation and propagation of such cracks in this case.

LOOP 820 TEST SECTIONS IN FORT WORTH DISTRICT

General Description

Four sections located on the westbound side of Loop 820 in Fort Worth, Texas, were built in July 2012. These sections were side by side on four lanes on Loop 820. The lanes start 61 ft away from the first pole after the Quebec Bridge (point A in Figure 28) and end very close to milepost 9 (point B in Figure 28), measuring 992 ft in length.

Each of these lanes/sections was constructed with 2-in.-thick Type D mix containing different combinations of asphalt binder, reclaimed materials, and warm-mix additive from Advera as follows:

- Section 0: PG64-22 + 13% RAP + 5% RAS + Advera (control mix).
- Section 1: PG64-22 + 13% RAP + 5% RAS pre-blended with Advera.
- Section 2: PG64-28 + 13% RAP + 5% RAS + Advera.
- Section 3: PG64-22 (0.4 percent more) + 13% RAP + 5% RAS + Advera.

As seen, Section 0 uses the control mix prepared with PG64-22 asphalt binder, 13 percent RAP, 5 percent RAS, and the warm-mix additive of Advera. Section 1 uses the mix prepared with the same materials as the control mix, except that RAS was pre-blended with Advera additive before mixing with other components of the mix. Section 2 uses a mix similar to the control mix, except that the PG64-22 asphalt binder is replaced with PG64-28. Section 3 uses a mix very similar to the control mix, except that it contains 0.4 percent more asphalt binder than the control mix. Section 0 (innermost lane) is next to the left shoulder or central median, while Section 3 (slowest lane) is next to the right shoulder.

Sections 1–3 were constructed in the night of July 19, 2012. The average paving temperatures measured behind the paver were 262°F, 268°F, and 272°F for Sections 1, 2, and 3, respectively.

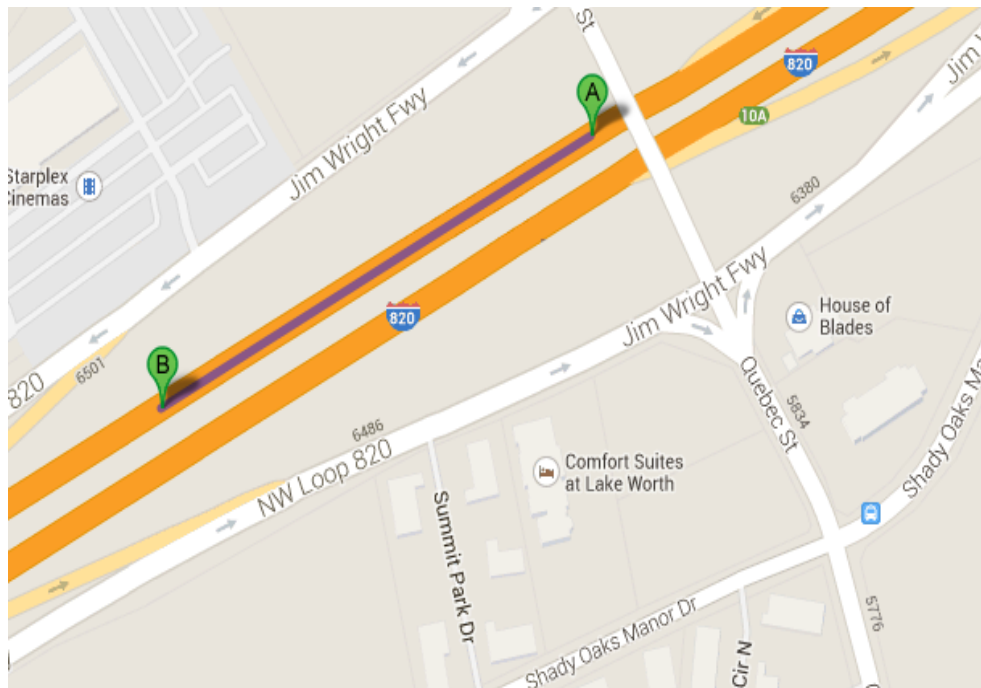


Figure 28. Loop 820 Test Sections: Location Map via Google.

Field Survey

The last survey of these sections for Project 0-6674 was conducted on June 12, 2014. The survey found no cracking or rutting issues in any of these sections, except for some segregation issues in Section 4. Since then, the sections have been surveyed four more times: March 2016, November

2016, July 2017, and March 2018. Figure 29 presents the conditions of these sections as observed in recent surveys.



View from Quebec Bridge on 03/26/2018

Figure 29. Loop 820 Test Sections 0 to 3: Survey Pictures.

Rutting

None of these sections has exhibited any noticeable rutting as of March 26, 2018 (see Figure 29).

Cracking

Loop 820 is a very busy road; four test sections were paved side by side, resulting in a survey problem. It was possible to determine the cracking conditions of Sections 0 and 3 clearly, but the conditions of Sections 1 and 2 could not be well observed. Many efforts were made, but no fruitful result was obtained. Thus, TTI researchers had to turn to Google Maps for an overall comparison. Figure 30 shows overall pavement conditions. Section 1 has the most reflective cracking, followed by Section 0; Section 2 has the least reflective cracking, and Section 3 has the second least reflective cracking. Such observation indicated that using soft but modified asphalt binder could improve cracking resistance; adding more virgin asphalt binder into the mix can also increase the cracking resistance of asphalt binder mixes with RAP/RAS.



Satellite View Accessed on 06/25/2018 via Google Maps

Figure 30. Loop 820 Test Sections: Cracking Conditions.

FAIRGROUND ROAD TEST SECTIONS IN ODESSA DISTRICT

General Description

Two test sections were constructed on North Fairground Road in Midland, Texas, in October 2016 for this part of the project. Section 1 was northbound, while Section 2 was southbound (see Figure 31). A different asphalt binder grade was used in each of these test sections while keeping the mix design the same as follows:

- Section 1: 5.7% PG64-22 + 14% RAP (control mix).
- Section 2: 5.7% PG64-28 + 14% RAP.

Section 1 used the control mix prepared with PG64-22 asphalt binder (unmodified) by weight of total mix, while Section 2 used the mix prepared with PG64-28 asphalt binder (softer, modified). In both sections, 5.7 percent asphalt binder and 14.0 percent RAP content were used. The mix designs follow the TxDOT specification. The sections were constructed on October 26, 2016. The average paving temperature was measured as 300°F. The temperature measurement was taken directly from the material behind the paver. TTI researchers used several permanent reference objects to locate the test sections for performance monitoring.

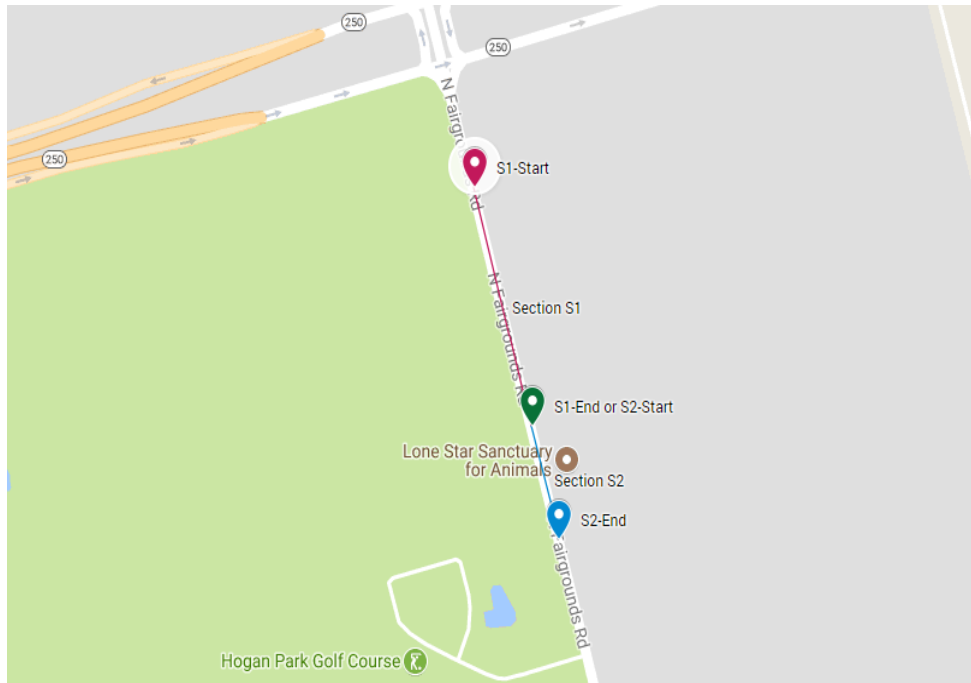


Figure 31. North Fairground Road Test Sections: Location Map via Google.

Field Survey

Since the construction, the sections have been surveyed twice, on July 3, 2017, and March 27, 2018. Figure 32 and Figure 33 present the conditions of sections as observed in these two surveys. These sections have shown no distress to date except for one pull-up in Section 1.

Rutting

Both these sections have exhibited no sign of rutting as of March 27, 2018 (Figure 32 and Figure 33).

Cracking

Both these sections have exhibited no sign of any type of cracking as of March 27, 2018 (Figure 32 and Figure 33).



Rutting/Cracking: None; Pull-Up: One
07/03/2017



Rutting/Cracking: None, Pull-Up: One
03/27/2018

Figure 32. North Fairground Road Test Section 1: Survey Pictures.



Rutting/Cracking/Pull-Up: None
03/07/2017



Rutting/Cracking/Pull-Up: None
03/27/2018

Figure 33. North Fairground Road Test Section 2: Survey Pictures.

FM 468 TEST SECTIONS IN LAREDO DISTRICT

General Description

Two test sections were constructed on FM 468 near Cotulla, Texas, for this project. Section 1 was westbound, while Section 2 was eastbound (see Figure 34).

A different asphalt binder grade was used in each of these test sections while keeping the mix design the same as follows:

- Section 1: 5.8 percent PG64-22 + 17% RAP (control mix).
- Section 2: 5.8 percent PG64-28 + 17% RAP.

Section 1 used the control mix prepared with PG64-22 asphalt binder (unmodified) by weight of total mix, while Section 2 used the mix prepared with PG64-28 asphalt binder (softer, modified).

Both mixes contain 5.8 percent asphalt binder and 17.0 percent RAP content by total weight of mix. The mix designs follow the TxDOT specification.

The sections were constructed on December 9, 2015. The average paving temperature was measured as 275°F. The temperature measurement was taken directly from the material behind the paver. TTI researchers used several reference objects to locate the test sections for the distress survey.

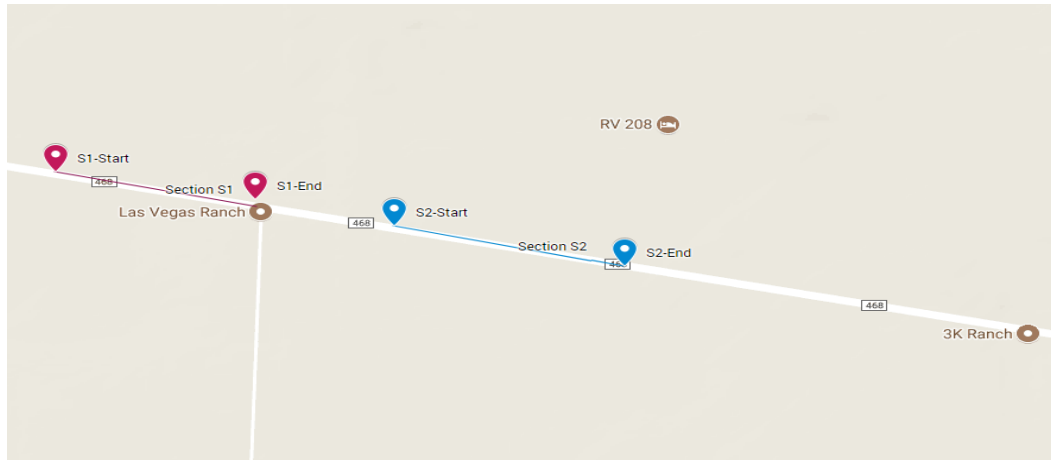


Figure 34. FM 468 Test Sections: Location Map via Google.

Field Survey

Since the construction, the sections have been surveyed three times, on April 8, 2016, October 9, 2017, and March 29, 2018. Figure 35 and Figure 36 present the conditions of these two sections observed in these surveys.

In the first survey, researchers did not observe any rutting or cracking in either of these sections on that date. Researchers found that Section 2 had been accidentally removed in the second survey. Therefore, the survey was conducted in Section 1 afterward.

Rutting

Both sections showed no sign of rutting in the first survey conducted on April 8, 2016. When the sections were surveyed on October 9, 2017, both showed some rutting. Section 1 showed 1/16 to 8/16 in. of rut depth in outer wheel paths and 1/16 to 5/16 in. of rut depth in the inner wheel paths (see Figure 35). Similarly, Section 2 showed 1/16 to 2/16 in. in depth in outer wheel paths and 1/16 in. in the inner wheel paths (see Figure 36). When these sections were surveyed on March 29, 2018, they showed that rut depths barely increased in both these sections, possibly due to lower temperatures that are prevalent from October to March.

Two important facts are noteworthy. First, the rutting was more severe in outer wheel paths than in inner wheel paths, and second, rut depth rutting was more severe in the section with modified PG64-28 asphalt binder than the section with unmodified PG64-22 asphalt binder.

Cracking

As of March 29, 2018, both these sections have exhibited no sign of cracking (see Figure 35 and Figure 36).



No Cracking: 03/29/2017



Rutting in Outer Wheel Path: 1/16–8/16 in.
10/09/2017



Rutting in Inner Wheel Path: 1/16–8/16 in.
10/09/2017



Rutting in Outer Wheel Path: 1/16–8/16 in.
03/29/2018



Rutting in Inner Wheel Path: 1/16–8/16 in.
03/29/2018

Figure 35. FM 468 Test Section 1: Survey Pictures.



No Cracking

03/29/2017



Rutting in Outer Wheel Path: 1/16–2/16 in.

10/09/2017



Rutting in Inner Wheel Path: 1/16 in.

10/09/2017



Rutting in Outer Wheel Path: 2/16–3/16 in.

03/29/2018



Rutting in Inner Wheel Path: 1/16 in.

03/29/2018

Figure 36. FM 468 Test Section 2: Survey Pictures.

SH 7 TEST SECTIONS IN BRYAN DISTRICT

General Description

Project SH 7 in the Bryan District is in Robertson County from the Robertson County line to FM 937 for a length of 5.10 miles. Figure 37 shows the project location. The existing maintenance strategy was to mill and inlay 2-in. asphalt overlay with Superpave-C mix with PG64-22. After discussing with the Bryan District and the contractor, the mix design for the test section was kept the same as the control mix except for switching the virgin binder to PG64-28 from PG64-22. Table 2 shows the mix compositions. The existing pavement condition of SH 7 looked poor. Distress, including fatigue cracking and transverse cracking, was observed. Even after the 2-in. milling in the night of June 18, 2020, some cracking could still be clearly observed, as shown in Figure 38.

The construction of the field test sections on westbound SH 7 started in the morning of June 19, 2020, but the paving direction was toward the east. The test section with PG64-28 was paved first, followed by the test section with PG64-22. The construction process included asphalt tack coat (Figure 39), paving (Figure 40), and compaction (Figure 41).

The plant mixes were collected at the asphalt plant. Their cracking and rutting resistance was evaluated using the IDEAL cracking test (IDEAL-CT), IDEAL rutting test (IDEAL-RT), and HWTT. Table 3 presents the test results.

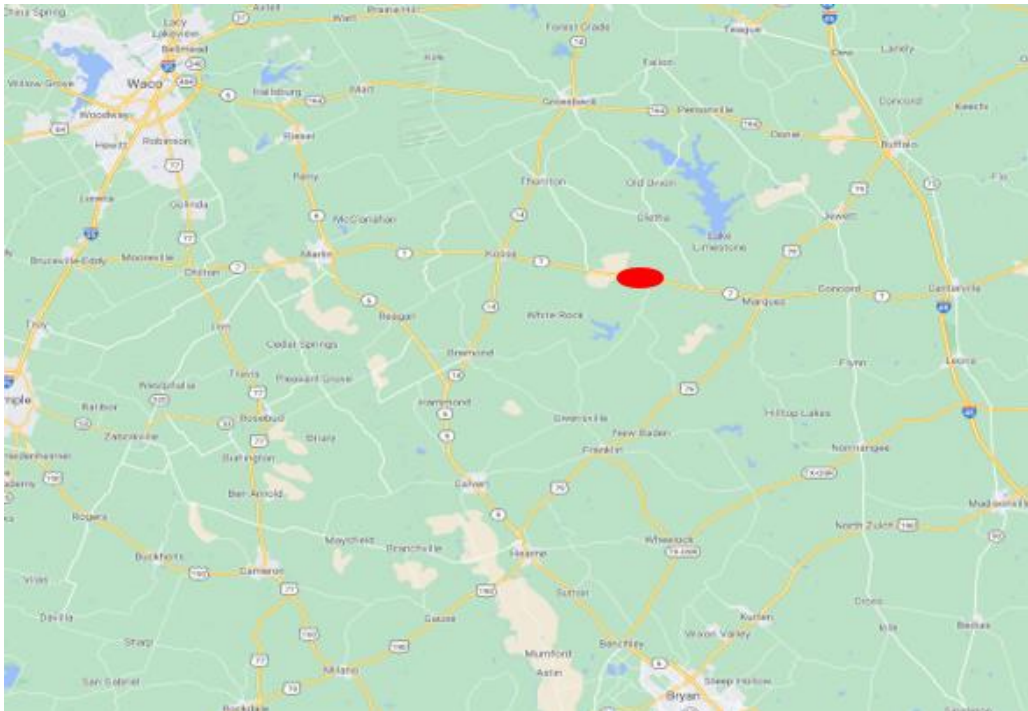


Figure 37. Location of Project SH 7.

Table 2. Compositions of Asphalt Mixes Used on SH 7.

Sections	% Rock					RAP %	Asphalt Concrete (AC) %	PG
	Type C	Grade 4	F-Rock	Washed Screenings	Sand			
Control section	8.9	27.6	19.2	17.5	6.8	20.0	4.6	PG64-22
Test section	8.9	27.6	19.2	17.5	6.8	20.0	4.6	PG64-28



Figure 38. Example of SH 7 Pavement Condition after the 2-In. Milling.



Figure 39. Applying Tack Coat.



Figure 40. Paving Asphalt Mix.



Figure 41. Compacting the Mat.

Table 3. Laboratory Test Results of SH 7 Mixes.

Test	Mix with PG64-22 (Control Mix)	Mix with PG64-28
IDEAL-CT	33.6	82.0
IDEAL-RT	88.6	66.1
Hamburg rut depth after 15,000 passes (mm)	6.0	15.0

Field Survey

Since the construction in June 2020, the research team has continuously monitored the sections. The latest field survey was completed on May 5, 2022. No rutting was observed in either test section (Figure 42). Two cracks were observed on the control test section with PG64-22, as shown in Figure 43. No cracking was seen on the test section with PG64-28 (Figure 44).



Figure 42. No Rutting on Both Test Sections on SH 7.



Figure 43. Cracking Observed on Control Section with PG64-22.



Figure 44. No Cracking on Test Section with PG64-28.

SH 214 TEST SECTIONS IN LUBBOCK DISTRICT

General Description

Project SH 214 is located in Yoakum County from the Yoakum County line to US82, as shown in Figure 45. The existing pavement has multiple seal coats with transverse cracking (Figure 46). The original pavement rehabilitation strategy includes a 0.75-in. level-up with Ty-D, fabric interlayer (to stop cracking), and a 1.75-in. overlay with stone-matrix asphalt (SMA)-C and PG70-28. After discussions with the Lubbock District and the contractor, all the level-up layer and fabric and SMA-C mix designs were kept the same for the test section. The only change was to the virgin binder of the SMA-C mix, switching to PG64-34 from PG70-28. Table 4 lists the mix compositions.

The construction of the field test sections on southbound SH 214 started in the morning of October 8, 2020. The test section with PG64-34 was paved first, followed by the test section with PG70-28. The construction process included asphalt tack coat (Figure 47), fiberglass fabric interlayer (Figure 48), paving (Figure 49), and compaction (Figure 50).



Figure 45. Location of Project SH 214.



Figure 46. Pavement Condition of SH 214.

Table 4. Compositions of Asphalt Mixes Used on SH 214.

Sections	% Rock					AC %	Binder PG
	SAC-C	SAC-B	D/F Blend	Mam Sand	MF		
Control section	37.0	27.5	15.0	15.5	5.0	6.6	PG70-28
Test section	37.0	27.5	15.0	15.5	5.0	6.6	PG64-34



Figure 47. Applying Tack Coat.



Figure 48. Paving Fiberglass Fabric Interlayer.



Figure 49. Paving Asphalt Mix.



Figure 50. Compacting the Mat.

The plant mixes were collected at the asphalt plant, and their cracking and rutting resistance was evaluated using IDEAL-CT, OT, and HWTT. Table 5 presents the test results.

Table 5. Laboratory Test Results of SH 214 SMA Mixes.

Test	SMA with PG70-28 (Control Mix)	SMA with PG64-34
IDEAL-CT	1299.6	2229.0
OT-Crack Progression Rate (CPR)	0.227	0.254
OT-Critical Fracture Energy (CFE)	0.823	1.147
Hamburg rut depth after 20,000 passes (mm)	8.8	11.4

Field Survey

Since the construction in April 2021, researchers have continuously monitored the sections. The latest field survey was completed on May 10, 2022. Neither rutting nor cracking was observed in either test section, as shown in Figure 51 through Figure 54.



Figure 51. No Rutting on the Test Section with PG64-34 on SH 214.



Figure 52. No Cracking on the Test Section with PG64-34 on SH 214.



Figure 53. No Rutting on the Test Section with PG70-28 on SH 214.

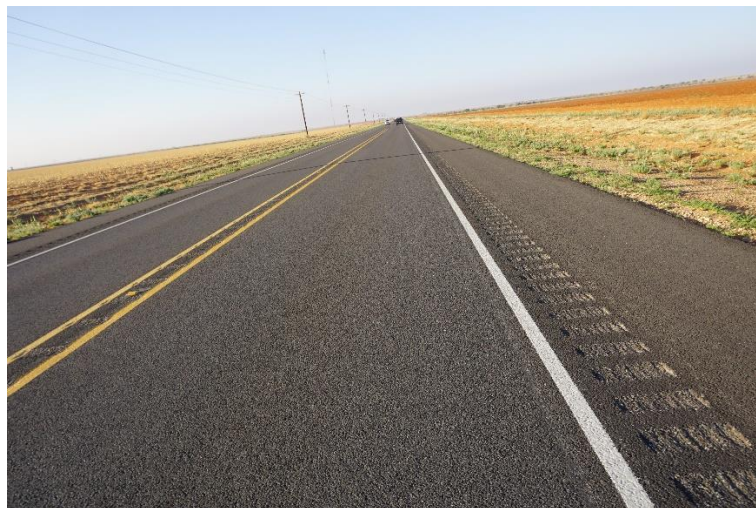


Figure 54. No Cracking on the Test Section with PG70-28 on SH 214.

APT TEST SECTIONS IN DALLAS DISTRICT

General Description

The Dallas accelerated pavement testing (APT) test sections are located at the University of Texas at Arlington APT test site (Figure 55). There are eight sections and seven asphalt mixtures (Figure 56). These eight sections have the same pavement structure: 3-in. asphalt layer, 10-in. granular base (GB), and subgrade. The base and subgrade are supposed to be the same; the only difference is the asphalt mixes used in the asphalt layer. Two of the eight sections are related to Project 5-6674-01, Sections O and P with Mixes 2 and 4. The general properties of Mixes 2 and 4 are shown in Table 6, which shows the percentages of rocks, asphalt content, and added RAP and RAS content in the mixtures.

Mix 2 with PG70-22 was paved on September 3, 2020, and Mix 4 with PG64-28 was paved on September 4, 2020. The paving and compaction process is shown in Figure 57 and Figure 58, respectively.

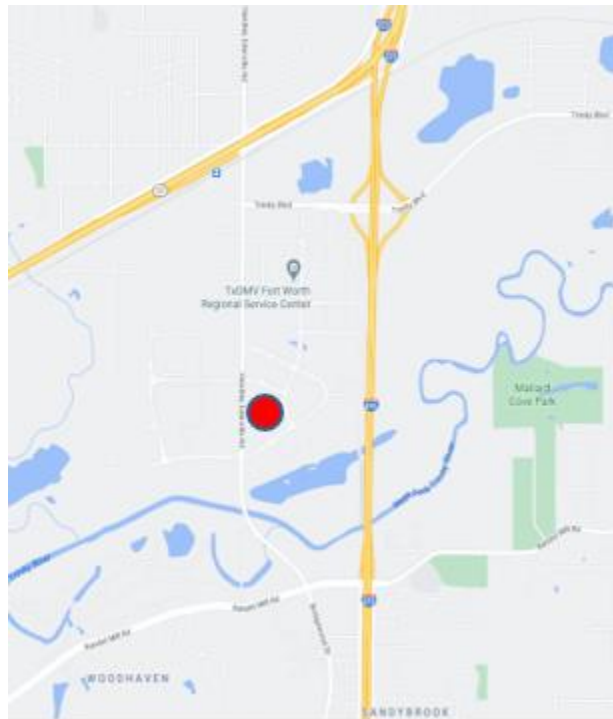


Figure 55. Location of Dallas APT Test Sections.

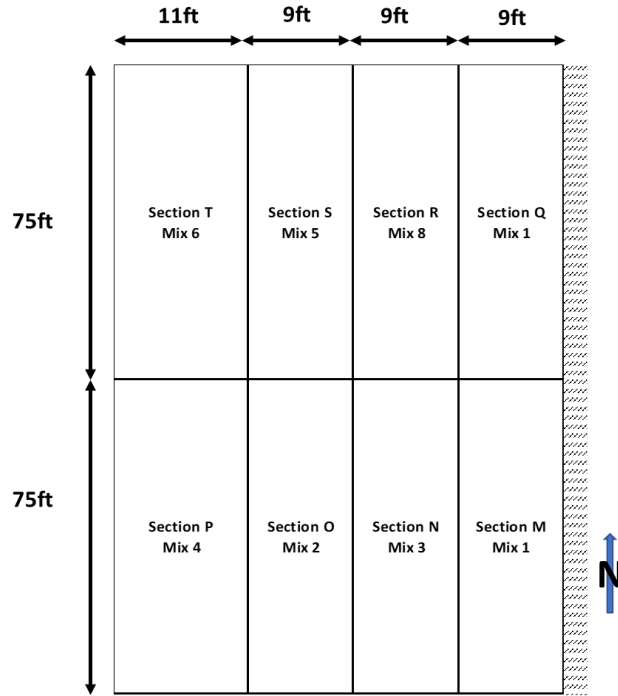


Figure 56. Schematic Drawing of the Test Sections.

Table 6. Compositions of Asphalt Mixes: 2 and 4.

Mix (Section)	% Rock			RAP %	AC %	Binder PG
	Type C	Type D	Man Sand			
2 (O)	25.0	30.0	30.0	15.0	4.8	PG70-22
4 (P)	25.0	30.0	30.0	15.0	4.8	PG64-28



Figure 57. Paving Operation at Dallas Test Sections.



Figure 58. Compacting Test Sections at Dallas Test Sections.

APT Test Results

The plant mixes were collected at the asphalt plant, and their cracking and rutting resistance was evaluated using IDEAL-CT, IDEAL-RT, OT, and HWTT. Table 7 presents the test results.

Table 7. Laboratory Test Results of Dallas APT Mixes.

Test	Mix 2 with PG70-22 (Control Mix)	Mix 4 with PG64-28
IDEAL-CT	93.9	150.5
IDEAL-RT	82.5	60.8
OT-CPR	0.57	0.350
OT-CFE	1.94	1.93
Hamburg rut depth after 15,000 passes (mm)	5.4	12.7

These two test sections were loaded under the APT testing facility. Figure 59 shows the pavement distress after 100,000 loading passes. Mix 4 with PG64-28 performed much better than Mix 2 with PG64-22.

Dallas APT Test Sections at UT Arlington Campus

- Mix 2: PG70-22 with 15% RAP -64% fatigue cracking after 350,000 passes
- Mix 4: PG64-28 with 15% RAP -57% fatigue cracking after 350,000 passes



Figure 59. Fatigue Cracking on Test Section O with PG70-22 (Left) and Section P with PG64-28 (Right).

FM 2105 TEST SECTIONS IN SAN ANGELO DISTRICT

General Description

Project FM 2105 is located in north San Angelo (Figure 60). It is a reconstruction job with a 2-in. Superpave-C mix and PG70-22 over a 3-in. dense-graded Ty-B mix. The test section is associated with a surface layer of Superpave-C mix. After discussing with San Angelo District and the contractor, the mix design for the test section was kept the same as the control mix except for switching the virgin binder to PG64-28 from PG64-22. Table 8 shows the mix compositions.

The field test sections were paved on the westbound of FM 2105 on April 1, 2021. The test section with PG70-28 was first paved, followed by the control section with PG70-22. The construction process included 1) asphalt tack coat (Figure 61), 2) paving the mixes (Figure 62), and 3) compaction (Figure 63).

The plant mixes were collected at the asphalt plant, and their cracking and rutting resistance was evaluated using IDEAL-CT, IDEAL-RT, and HWTT. Table 9 presents the test results.

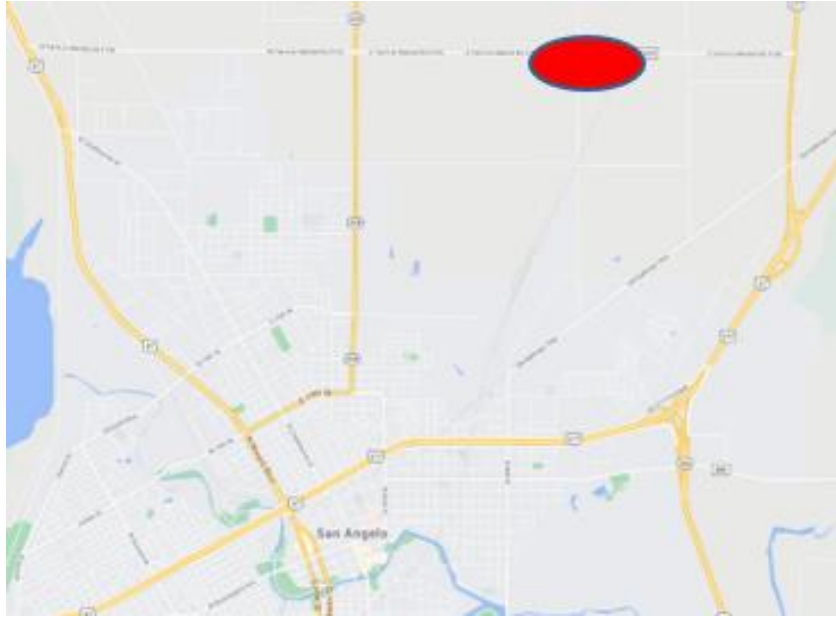


Figure 60. Location of FM 2105 Test Sections.

Table 8. Compositions of Asphalt Mixes Used on FM 2105.

Sections	% Rock					RAP %	AC %	Binder PG
	C-Rock	Ty-D	Ty-FF	Air Classifier	Hot-Mix Screenings			
Control section	20.0	27.0	16.0	10.0	17.1	9.9	5.2	PG70-22
Test section	20.0	27.0	16.0	10.0	17.1	9.9	5.2	PG70-28



Figure 61. Applying Tack Coat on FM 2105.



Figure 62. Paving Operation on FM 2105.



Figure 63. Compacting Test Sections on FM 2105.

Table 9. Laboratory Test Results of FM 2105 Mixes.

Test	Mix with PG70-22 (Control Mix)	Mix with PG70-28
IDEAL-CT	51.6	40.9
IDEAL-RT	95.2	106.1
Hamburg rut depth after 20,000 passes (mm)	5.4	5.5

Field Survey

Since the construction in April 2021, the research team has continuously monitored the sections. The latest field survey was completed on May 11, 2022. Neither rutting nor cracking was observed in either test section, as shown in Figure 64 through Figure 67.



Figure 64. No Rutting on the Test Section with PG70-28 on FM 2105.



Figure 65. No Cracking on the Test Section with PG70-28 on FM 2105.



Figure 66. No Rutting on the Test Section with PG70-22 on FM 2105.



Figure 67. No Cracking on the Test Section with PG70-22 on FM 2105.

SH 71 TEST SECTIONS IN AUSTIN DISTRICT

General Description

Project SH 71 is located in Burnet County from US 281 to the Blanco County line for a length of 10.1 miles. The field test section was paved on southbound SH 71, 1.75 miles south of US 281 at the intersection with CR 401, as shown in Figure 68. It was an asphalt overlay with TOM mix. After discussions with the San Angelo District and the contractor, the mix design for the test section was kept the same as the control mix except for switching the virgin binder to PG70-28 from PG70-22. Table 10 shows the mix compositions.

The field test sections were paved on eastbound SH 71 on June 11, 2021. The test section with PG70-28 was first paved, followed by the control section with PG70-22. Figure 69 and Figure 70 show the construction process.

The plant mixes were collected at the asphalt plant, and their cracking and rutting resistance was evaluated using IDEAL-CT, OT, and HWTT. Table 11 presents the test results.

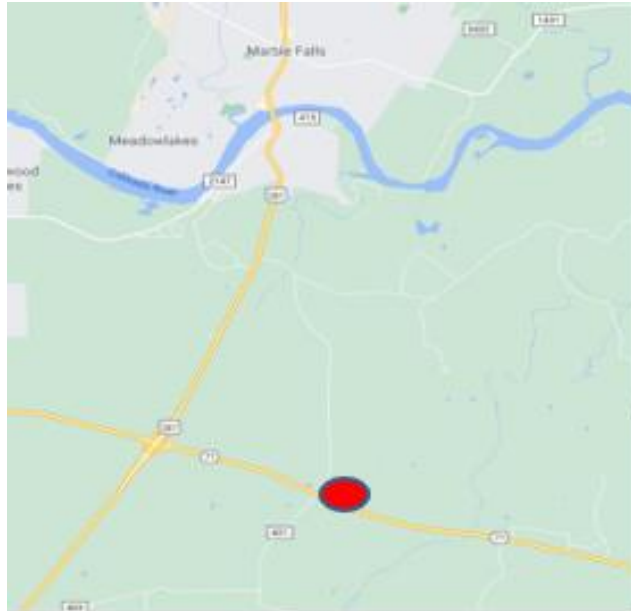


Figure 68. Location of SH 71 Test Sections.

Table 10. Compositions of Asphalt Mixes Used on SH 71.

Sections	% Rock			AC %	Binder PG
	Grade 5	F-Rock	Screenings		
Control section	44.0	38.0	18.0	6.4	PG70-22
Test section	44.0	38.0	18.0	6.4	PG70-28



Figure 69. Paving Operation on SH 71.



Figure 70. Compaction Operation on SH 71.

Table 11. Laboratory Test Results of SH 71 Mixes.

Test	Mix with PG70-22 (Control Mix)	Mix with PG70-28
IDEAL-CT	358.3	380.3
OT-CPR	0.29	0.27
OT-CFE	1.98	1.69
Hamburg rut depth after 20,000 passes (mm)	5.9	6.9

Field Survey

Since the construction in June 2021, the research team has been monitoring the sections. The latest field survey was completed on May 4, 2022. Neither rutting nor cracking was observed in either test section, as shown in Figure 71 through Figure 74.



Figure 71. No Rutting on the Test Section with PG70-28 on SH 71.



Figure 72. No Cracking on the Test Section with PG70-28 on SH 71.



Figure 73. No Rutting on the Test Section with PG70-22 on SH 71.



Figure 74. No Cracking on the Test Section with PG70-22 on SH 71.

SUMMARY AND CONCLUSIONS

Multiple field test sections were constructed under this project to confirm the benefits of soft, highly modified binders in the colder areas of Texas. TTI researchers have been surveying cracking and rutting distresses of these sections periodically since their initial construction. This section describes the construction and field performance of each field test section.

This study conducted cracking and rutting surveys on field test sections in 10 districts. For the test sections constructed in 2020 and 2021, the corresponding plant mixes were collected at the asphalt plant. Their cracking and rutting resistance was evaluated using the IDEAL-CT, IDEAL-RT, and HWTT tests. The results were as follows:

- In the Amarillo District, four test sections were constructed on SH 15 near Perryton. The binders were PG58-28 versus PG64-34. The fact that alligator, longitudinal, and transverse cracking appears later and with smaller severity values in Sections 3 and 4

than in Sections 1 and 2 suggests that PG64-34 was able to delay the initiation and the propagation of cracking as expected.

- In the Childress District, three sections were constructed on the eastbound side of US 62. The binders were PG70-28 versus PG74-34. Considering both transverse and longitudinal cracking, it is clear that Section 1 has less total cracking length than Sections 2 and 3. Such observations indicate that PG64-34 was able to impede the initiation and propagation of such cracks in this case.
- In the Fort Worth District, four sections were constructed on the westbound side of Loop 820. The binders were PG64-24 versus PG64-28. The four test sections were paved side by side, resulting in a survey problem since Loop 820 is a very busy road. It was possible to determine the cracking conditions of Sections 0 and 3 clearly, but the conditions of Sections 1 and 2 could not be well observed. TTI researchers had to turn to Google Maps for an overall comparison. Section 1 has the most reflective cracking, followed by Section 0; Section 2 has the least reflective cracking, and Section 3 has the second least reflective cracking. Such observations indicate that using soft but modified asphalt binder (PG64-28) could improve cracking resistance; adding more virgin asphalt binder into the mix can also increase the cracking resistance of asphalt binder mixes with RAP/RAS.
- In the Odessa District, two test sections were constructed on North Fairground Road. The binders were PG64-22 versus PG64-28. Both sections have exhibited no sign of rutting or cracking as of March 27, 2018.
- In the Laredo District, two test sections were constructed on FM 468 near Cotulla. The binders were PG64-24 and PG64-28. Two important facts are noteworthy. First, the rutting was more severe in outer wheel paths than in inner wheel paths; second, the rut depth of the rutting was more severe in the section with modified PG64-28 asphalt binder than the section with unmodified PG64-22 asphalt binder. Both sections have exhibited no sign of cracking.
- In the Bryan District, two test sections were constructed on SH 7 in June 2020. The binders were PG64-22 versus PG64-28. The latest field survey was completed on May 5, 2022. Two cracks were observed on the control test section with PG64-22. No cracking was seen on the test section with PG64-28. No rutting was observed in either test section.
- In the Lubbock District, two test sections were constructed on SH 214 in April 2021. The binders were PG70-28 versus PG64-34. The latest field survey was completed on May 10, 2022. Neither rutting nor cracking was observed in either test section.
- In the Dallas District, two test sections were loaded under the APT testing facility. The binders were PG70-22 versus PG64-28. After 100,000 loading passes, the mix with PG64-28 performed much better than the mix with PG64-22.
- In the San Angelo District, two test sections were constructed on FM 2105 in April 2021. The latest field survey was completed on May 11, 2022. Neither rutting nor cracking was observed in either test section.
- In the Austin District, two test sections were constructed on SH 71 in June 2021. The latest field survey was completed on May 4, 2022. Neither rutting nor cracking was observed in either test section.

Overall, the survey result of field test sections shows that soft, highly modified binders (PGxx-28 or PGxx-34) have better cracking resistance, and their benefits in the colder areas of Texas are confirmed.

CHAPTER 4. REVISED STATEWIDE ASPHALT BINDER SELECTION CATALOG

INTRODUCTION

This chapter first describes the current statewide PG binder selection catalog. One important factor, the existing pavement condition, was not considered when selecting a binder for an overlay using the current catalog.

To develop the binder selection catalog for overlay, researchers simulated the cracking performance of 2700 different cases of overlays. These cases involve a full factorial combination of five climatic zones, four levels of traffic volume, three overlay thicknesses, three types of existing pavement structures, three types of aggregates, and five asphalt binders.

By incorporating the binder selection method for overlay into the current PG binder selection catalog, researchers recommend a new statewide asphalt binder selection catalog. The recommended PGs for counties in each district were updated accordingly.

STATEWIDE PG BINDER SELECTION CATALOG CURRENTLY USED IN TEXAS

TxDOT currently selects asphalt binder PG grade for any pavement in Texas using two major phases.

The *first phase* of this method involves selecting the high- and low-temperature PGs of asphalt binder based on the location of the project and the desired level of confidence (i.e., 95 or 98 percent confidence). Confidence level refers to the chances that the normal variations in temperature 20 mm below the pavement surface will never exceed the range of the selected binder grade. TxDOT provides color-coded location maps for a given confidence level to aid in this step. Figure 75 presents the color-coded location map with recommended starting binder PG.

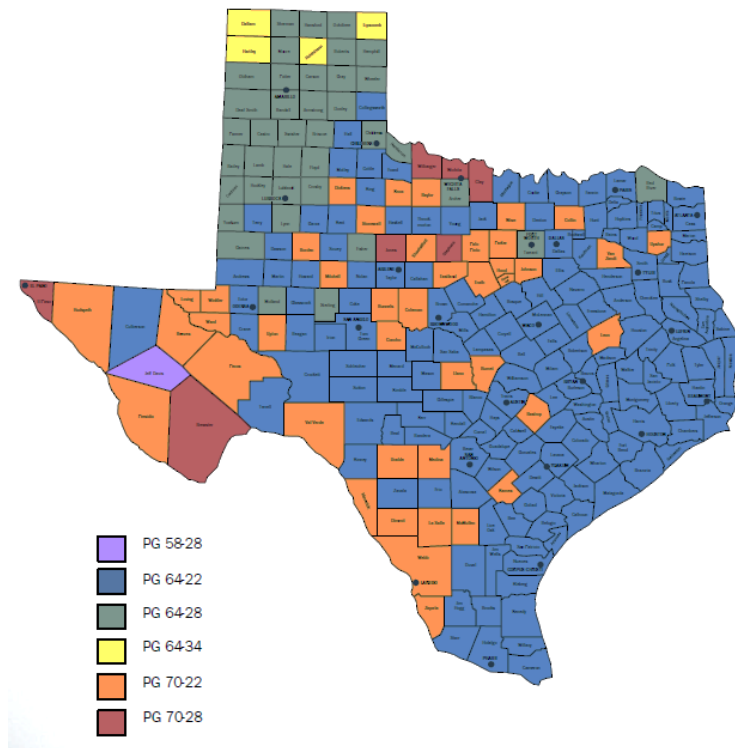


Figure 75. Asphalt Binder Grade Recommendation: TxDOT Method.

The *second phase* of TxDOT’s current method for asphalt binder PG selection involves four different steps for adjusting the starting binder PG. Each step deals with a different factor (traffic volume, traffic speed, pavement layer, and the use of recycled material) that influences the overall performance of asphalt pavement. Figure 76 presents these steps with each factor’s corresponding impact on the starting binder PG. In some cases, these factors change the starting binder PG up to two grades.

TxDOT’s current method recommends that the high-temperature PG be 64 at the minimum and 76 at the maximum, and the low-temperature PG be –34 at the minimum and –22 at the maximum. However, in some special locations, the recommendations are slightly different. The method recommends a high-temperature PG of 58 in select hot climates, such as Jeff Davis County in the El Paso District, and a low-temperature PG of –34 in select cold climates, such as counties north of IH 40, namely in Dallam, Hartley, Hutchinson, and Lipscomb Counties in the Amarillo District.

Despite these safeguards, TxDOT’s current method does not consider whether the proposed project involves the construction of new pavement or an asphalt overlay over an existing pavement when recommending binder PG.

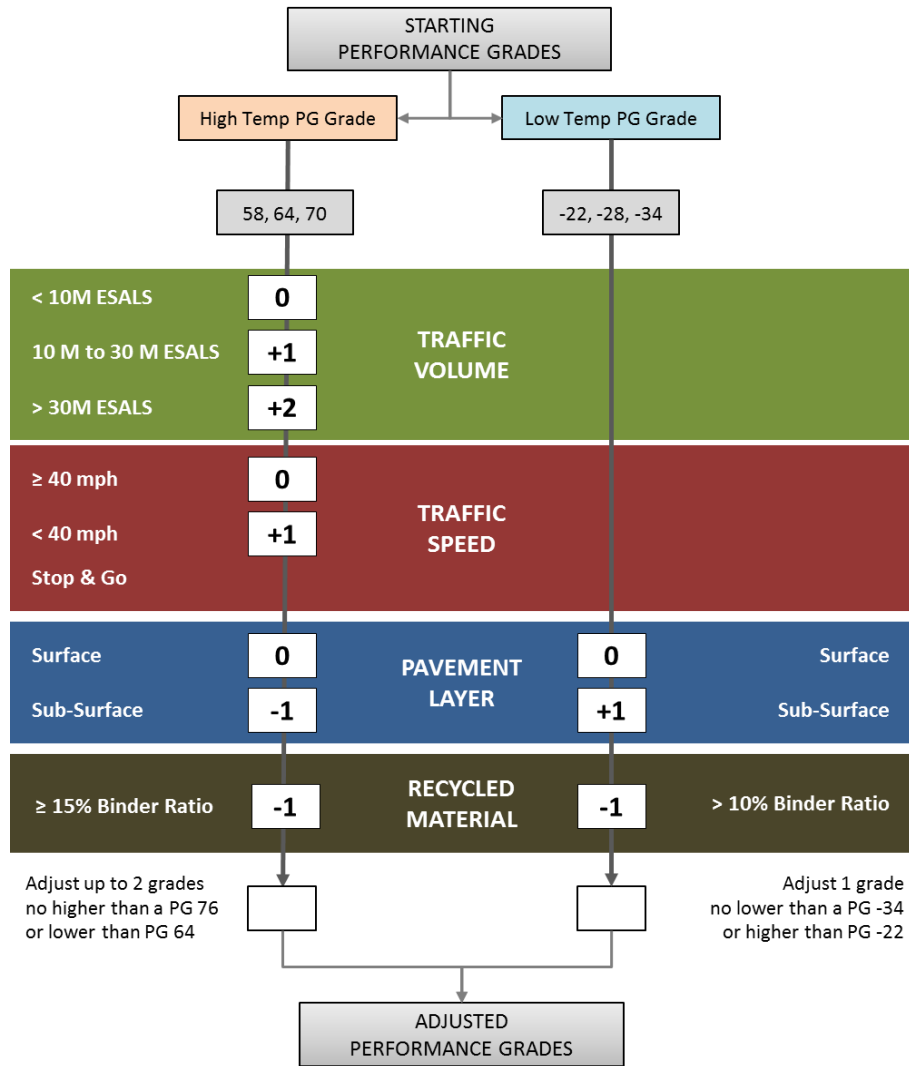


Figure 76. Asphalt Binder Grade Adjustment: TxDOT Method.

STATEWIDE ASPHALT BINDER SELECTION CATALOG FOR OVERLAY

To make TxDOT’s current binder grade selection method more robust, researchers first established that the existing pavement layer, overlay thickness, traffic level, environmental zones (or climate), aggregate type, and asphalt binder PG influence the cracking performance of the overlays. For this purpose, researchers simulated the cracking performance of 2700 different cases of overlays involving five different zones for climates, four different levels of traffic volume, three different overlay thicknesses, three different types of existing pavement structures, three different types of aggregate types, and five different grades of asphalt binder (see Table 12). Researchers used the Texas Asphalt Concrete Overlay Design and Analysis System for these simulations. The simulation results also determined the binder PG that would provide the best possible outcome in terms of cracking performance in each district in Texas.

Table 12. Overlay Performance Simulation Factorial.

Factor	Details
Environmental zone-1	Amarillo representing dry-cold zone
Environmental zone-2	Odessa representing dry-warm zone
Environmental zone-3	Austin representing moderate zone
Environmental zone-4	Paris representing wet-cold zone
Environmental zone-5	Beaumont representing wet-warm zone
Existing pavement structure-1	Conventional AC over GB
Existing pavement structure-2	Existing JPCP over GB
Existing pavement structure-3	Thinner existing AC over cement-treated base
Traffic level-1	3 million
Traffic level-2	5 million
Traffic level-3	10 million
Traffic level-4	30 million
Overlay thickness-1	2 inch
Overlay thickness-2	3 inch
Overlay thickness-3	4 inch
Overlay mixture with limestone-1	PG64-34
Overlay mixture with limestone-2	PG64-28
Overlay mixture with limestone-3	PG64-22
Overlay mixture with limestone-4	PG70-22
Overlay mixture with limestone-5	PG76-22
Overlay mixture with gravel-1	PG64-34
Overlay mixture with gravel-2	PG64-28
Overlay mixture with gravel-3	PG64-22
Overlay mixture with gravel-4	PG70-22
Overlay mixture with gravel-5	PG76-22
Overlay mixture with granite-1	PG64-34
Overlay mixture with granite-2	PG64-28
Overlay mixture with granite-3	PG64-22
Overlay mixture with granite-4	PG70-22
Overlay mixture with granite-5	PG76-22

Table 13 presents the recommended binder grades for each district in Texas based on these simulations. The table shows that each county in a given district is recommended the same binder PG. When recommended binders in Table 13 and Figure 76 are compared, the binder recommended by this new approach is usually softer than the binder recommended by TxDOT's current method. This difference highlights that binder recommendations for each county must be updated when an overlay construction is considered.

NEW STATEWIDE ASPHALT BINDER SELECTION CATALOG

Using TxDOT's current catalog, TTI researchers identified the counties in each district with different recommended PGs and then updated them with newly recommended PGs. Table 14 presents the recommended high- and low-temperature PG for brand new pavement construction and new overlay construction over existing pavement layers. Researchers second TxDOT's current protocol that the starting binder PG needs to be adjusted for traffic volume, traffic speed, pavement layer, and the use of recycled material, whichever is applicable. Therefore, researchers modified the two phases of TxDOT's current binder PG selection method as follows.

The *first phase* of the new approach involves selecting the high- and low-temperature PGs of asphalt binder based on the project's location, the desired level of confidence, and the type of construction. The type of construction (new versus overlay) specifically plays a critical role in recommending low-temperature PG for the project. Researchers developed color-coded location maps for a 98 percent confidence level to aid in selecting the recommended PG for any given project in Texas:

- Figure 77: PG for new pavement construction.
- Figure 78: PG for asphalt overlay over existing AC.
- Figure 79: PG for asphalt overlay over existing jointed plain concrete pavements (JPCP).

The *second phase* of the new approach involves adjusting the starting binder PG using four different steps. As in Texas's current approach, each of these steps deals with a different factor (traffic volume, traffic speed, pavement layer, and the use of recycled material) that might influence the overall performance of asphalt pavement. The adjustment for the pavement layer might not be applicable for overlay design. Figure 80 illustrates each step included in Phase I and II of the new approach.

Table 13. Asphalt Binder Grade Recommendation.

<i>No.</i>	<i>District</i>	<i>Aggregate</i>	<i>Conventional Existing AC Pavement</i>	<i>Existing JPCP</i>
1	Paris	Gravel	PG64-28	PG64-34
2	Fort Worth	Limestone	PG64-22 (Higher % AC) or PG64-28	PG64-34
3	Wichita Falls	Gravel	PG64-28	PG64-34
4	Amarillo	Gravel	PG64-28	PG64-34 (Higher % AC)
5	Lubbock	Gravel	PG64-28	PG64-34 (Higher % AC)
6	Odessa	Gravel	PG64-28	PG64-28
7	San Angelo	Gravel	PG64-28	PG64-28
8	Abilene	Gravel	PG64-28	PG64-34 (Higher % AC)
9	Waco	Limestone	PG64-22 (Higher % AC) or PG64-28	PG64-28
10	Tyler	Limestone	PG64-22 (Higher % AC) or PG64-28	PG64-34
11	Lufkin	Limestone	PG64-22 (Higher % AC) or PG64-28	PG64-28
12	Houston	Limestone	PG64-22 (Higher % AC) or PG64-28	PG64-28
13	Yoakum	Gravel	PG64-28	PG64-28
14	Austin	Limestone	PG64-22 (Higher % AC) or PG64-28	PG64-28
15	San Antonio	Limestone	PG64-22 (Higher % AC) or PG64-28	PG64-28
16	Corpus Christi	Gravel	PG64-22	PG64-22
17	Bryan	Limestone	PG64-22 (Higher % AC) or PG64-28	PG64-28
18	Dallas	Limestone	PG64-22 (Higher % AC) or PG64-28	PG64-28
19	Atlanta	Granite	PG70-22	PG64-28
20	Beaumont	Granite	PG70-22	PG64-28
21	Pharr	Gravel	PG64-22	PG64-22
22	Laredo	Gravel	PG64-22	PG64-22
23	Brownwood	Limestone	PG64-22 (Higher % AC) or PG64-28	PG64-28
24	El Paso	Limestone	PG64-22 (Higher % AC) or PG64-28	PG64-28
25	Childress	Gravel	PG64-28	PG64-34 (Higher % AC)

Table 14. Asphalt Binder Grade Recommendation: New Catalog.

No.	District	Counties	PGH:	PGL:	PGL: Overlay	
			New & Overlay	New	Existing AC	Existing JPCP
1	Paris	Red River	64	-28	-28	-34
		Delta, Fannin, Franklin, Grayson, Hunt, Hopkins, Lamar, Rains	64	-22	-28	-34
2	Fort Worth	Tarrant	64	-28	-28	-34
		Jack	64	-22	-28	-34
		Erath, Hood, Johnson, Palo Pinto, Parker, Somervell, Wise	70	-22	-28	-34
3	Wichita Falls	Archer	64	-28	-28	-34
		Cooke, Montague, Throckmorton, Young	64	-22	-28	-34
		Baylor	70	-22	-28	-34
4	Amarillo	Clay, Wichita, Wilbarger	70	-28	-28	-34
		Armstrong, Carson, Deaf Smith, Gray, Hansford, Hemphill, Moore, Ochiltree, Oldham, Potter, Randall, Roberts, Sherman	64	-34	-34	-34
		Dallam, Hartley, Hutchinson, Lipscomb	64	-28	-28	-34
5	Lubbock	Bailey, Castro, Cochran, Crosby, Floyd, Garza, Hale, Hockley, Lamb, Lubbock, Lynn, Parmer, Swisher, Yoakum	64	-28	-28	-34
		Dawson, Gaines, Terry	64	-22	-28	-34
6	Odessa	Midland	64	-28	-28	-28
		Andrews, Crane, Ector, Martin, Terrell	64	-22	-28	-28
		Loving, Pecos, Reeves, Upton, Ward, Winkler	70	-22	-28	-28
7	San Angelo	Sterling	64	-28	-28	-28
		Coke, Crockett, Edwards, Glasscock, Irion, Kimble, Menard, Reagan, Real, Schleicher, Sutton, Tom Green	64	-22	-28	-28
		Concho, Runnels	70	-22	-28	-28
8	Abilene	Fisher	64	-28	-28	-34
		Callahan, Haskell, Howard, Kent, Nolan, Scurry, Taylor	64	-22	-28	-34
		Borden, Mitchell, Shackelford, Stonewall	70	-22	-28	-34
9	Waco	Jones	70	-28	-28	-34
		Bell, Bosque, Coryell, Falls, Hamilton, Hill, Limestone, McLennan	64	-22	-28	-28
10	Tyler	Anderson, Cherokee, Gregg, Henderson, Rusk, Smith, Wood	64	-22	-28	-34
		Van Zandt	70	-22	-28	-34
11	Lufkin	Angelina, Houston, Nacogdoches, Polk, Sabine, San Augustine, San Jacinto, Shelby, Trinity	64	-22	-28	-28
12	Houston	Brazoria, Fort Bend, Galveston, Harris, Montgomery, Waller	64	-22	-28	-28
13	Yoakum	Austin, Calhoun, Colorado, DeWitt, Fayette, Gonzales, Jackson, Lavaca, Matagorda, Victoria, Wharton	64	-22	-28	-28
14	Austin	Blanco, Caldwell, Gillespie, Hays, Lee, Mason, Travis, Williamson	64	-22	-28	-28
		Bastrop, Burnet, Llano	70	-22	-28	-28
15	San Antonio	Atascosa, Bandera, Bexar, Comal, Frio, Guadalupe, Kendall, Kerr, Wilson	64	-22	-28	-28
		McMullen, Medina, Uvalde	70	-22	-28	-28

<i>No.</i>	<i>District</i>	<i>Counties</i>	<i>PGH: New & Overlay</i>	<i>PGL: New</i>	<i>PGL: Overlay Existing AC</i>	<i>Existing JPCP</i>
16	Corpus Christi	Aransas, Bee, Goliad, Jim Wells, Kleberg, Live Oak, Nueces, Refugio, San Patricio	64	-22	-22	-22
		Karnes	70	-22	-22	-22
17	Bryan	Brazos, Burleson, Freestone, Grimes, Madison, Milam, Robertson, Walker, Washington	64	-22	-28	-28
		Leon	70	-22	-28	-28
18	Dallas	Dallas, Denton, Ellis, Kaufman, Navarro, Rockwall	64	-22	-28	-28
		Collins	70	-22	-28	-28
19	Atlanta	Bowie, Camp, Cass, Harrison, Marion, Morris, Panola, Titus	64	-22	-22	-28
		Upshur	70	-22	-22	-28
20	Beaumont	Chambers, Hardin, Jasper, Jefferson, Liberty, Newton, Orange, Tyler	64	-22	-22	-28
21	Pharr	Brooks, Cameron, Hidalgo, Jim Hogg, Kenedy, Starr, Willacy	64	-22	-22	-22
		Zapata	70	-22	-22	-22
22	Laredo	Duval, Kinney, Zavala	64	-22	-22	-22
		Dimmit, La Salle, Maverick, Val Verde, Webb	70	-22	-22	-22
23	Brownwood	Brown, Comanche, Lampasas, McCulloch, Mills, San Saba	64	-22	-28	-28
		Coleman, Eastland	70	-22	-28	-28
		Stephens	70	-28	-28	-28
24	El Paso	Jeff Davis	58	-28	-28	-28
		Culberson	64	-22	-28	-28
		Hudspeth, Presidio	70	-22	-28	-28
		Brewster, El Paso	70	-28	-28	-28
25	Childress	Briscoe, Childress, Donley, Hardeman, Wheeler	64	-28	-28	-34
		Collingsworth, Cottle, Foard, Hall, Motley, King	64	-22	-28	-34
		Dickens, Knox	70	-22	-28	-34

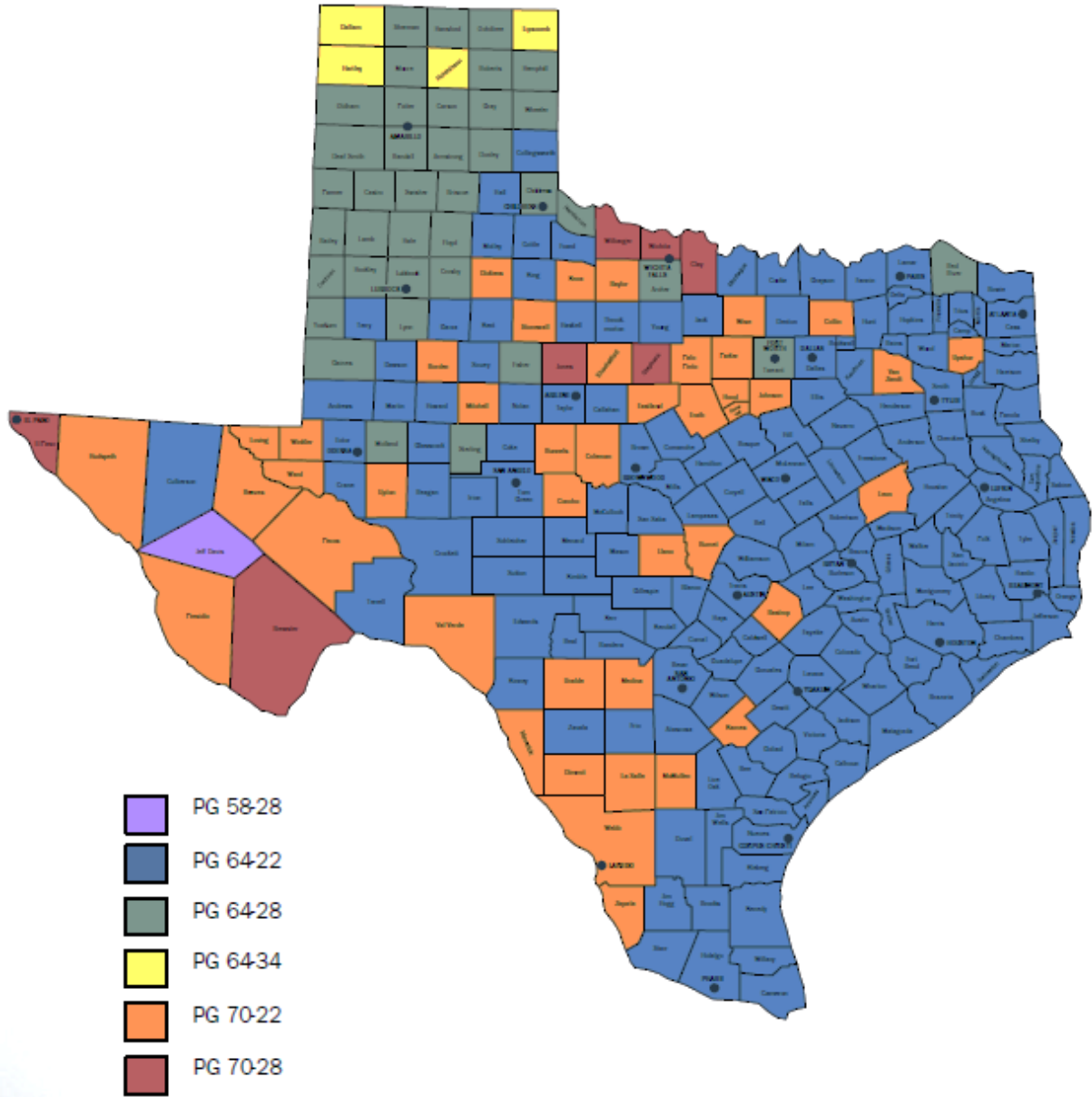


Figure 77. PG Recommendation for New Construction.

PG GRADE RECOMMENDATION
BASED ON CLIMATE - 98% CONFIDENCE

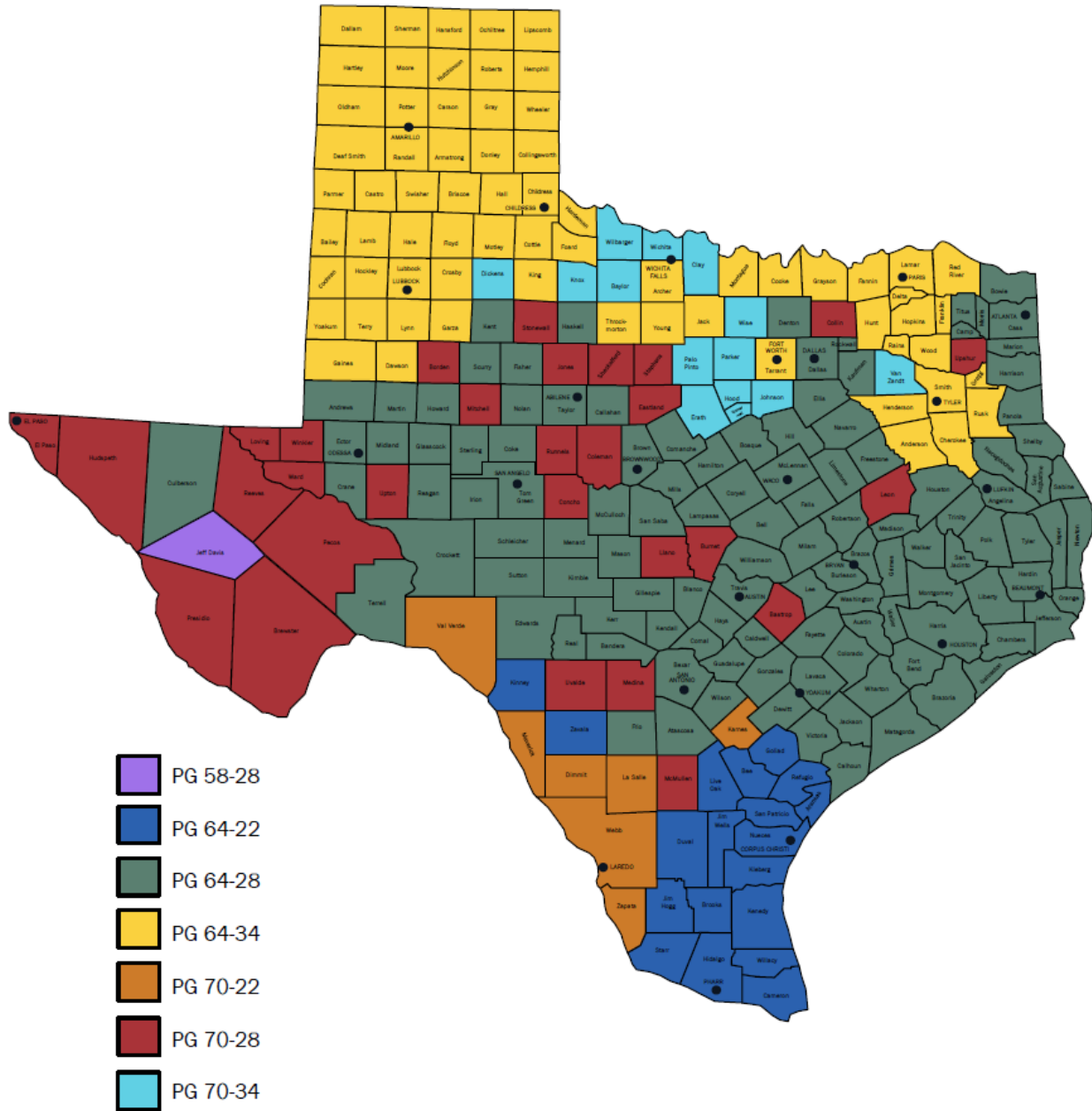


Figure 79. PG Recommendation for Asphalt Overlay over JPCP.

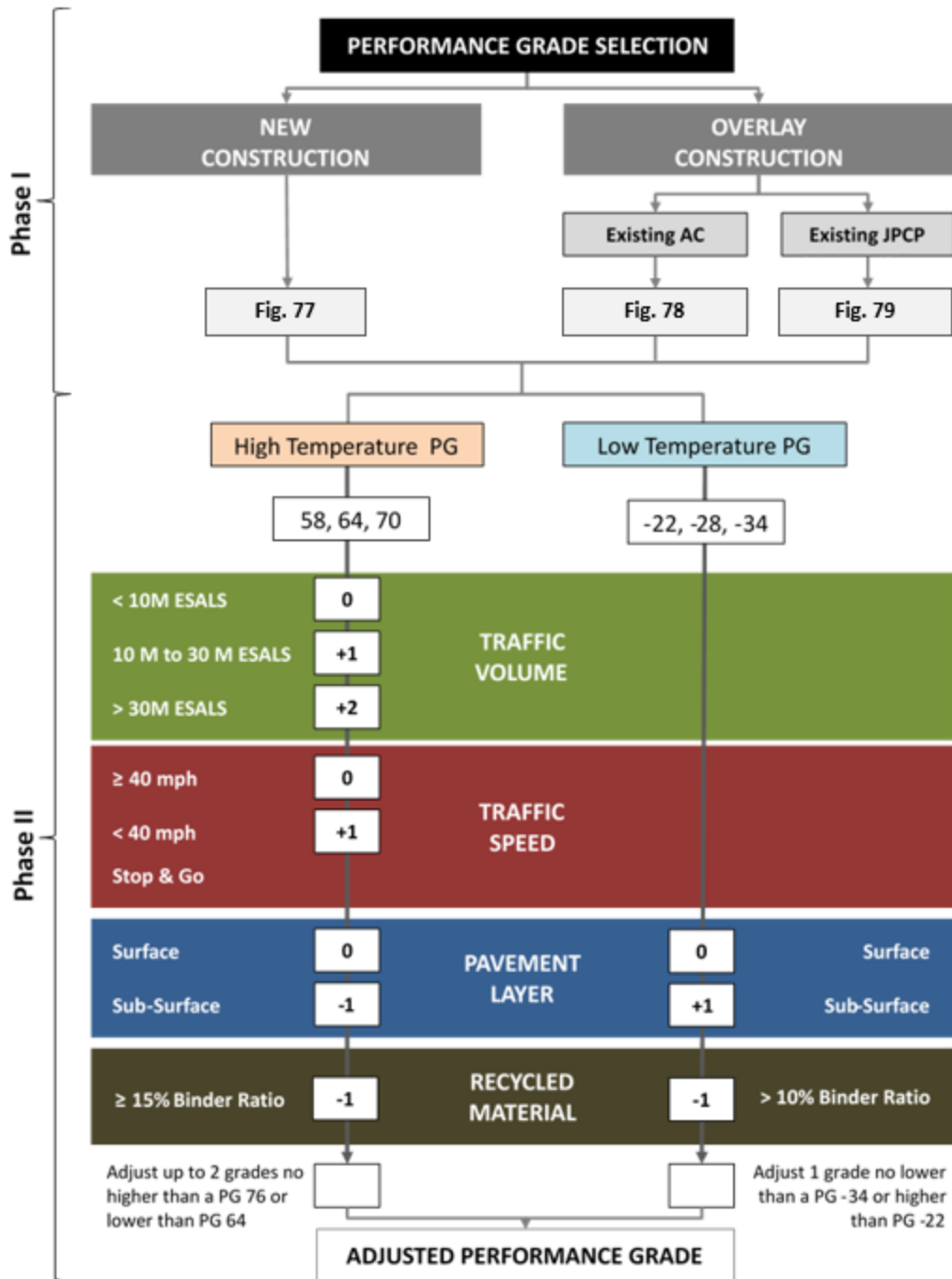


Figure 80. Asphalt Binder PG Recommendation and Adjustment: New Method.

SUMMARY AND CONCLUSION

TxDOT’s current binder PG selection method does not consider whether the proposed project involves the construction of new pavement or an asphalt overlay over an existing pavement when recommending binder PG.

By simulating 2700 cases of overlays and comparing their cracking performances, researchers established a statewide binder selection method and catalog for overlays. The simulation results

determined the binder PG that would provide the best possible outcome in terms of cracking performance in each district in Texas.

Further, the binder selection catalog for overlay was combined into the current Texas PG binder selection catalog, and a new statewide asphalt binder selection catalog was proposed. The binder recommended by this new approach is usually softer than the binder recommended by TxDOT's current method. This difference highlights that binder recommendations for each county must be updated when an overlay construction is considered.

CHAPTER 5. BINDER QUALITY: AGING AND CRACKING RESISTANCE

INTRODUCTION

Asphalt binder is one of the most expensive and critical materials used in the construction and maintenance of asphalt pavements in Texas, costing taxpayers hundreds of millions of dollars annually. The impact of asphalt binders on asphalt mix performance includes three aspects: asphalt binder type selection, asphalt binder content, and asphalt binder quality. Chapter 4 provides a revised binder type selection catalog, while asphalt binder content is determined through balanced mix design methods. It has been widely recognized that asphalt binders with the same PG can perform very differently. This problem is attributed to the fact that refining and manufacturing of asphalt binders have changed considerably in recent years, primarily concerning greenhouse gas emissions. In addition, the crude source of the asphalt binders and modification technologies continue to change. Thus, the binder quality issue still needs serious attention. This chapter addresses the binder quality issue through laboratory experiments on binder aging and mix cracking resistance.

LABORATORY MIX AND BINDER TEST PLAN

As listed in Table 15, a total of 13 representative overlay mixes from Texas and Massachusetts were used in this study. The 13 mixes cover various aspects of asphalt mixes:

- Mix types (12.5 mm Superpave versus 12.5 mm SMA).
- Recycled materials (Mixes 1, 2, 7–12).
- Rejuvenator (Mix 2).
- Binder content (Mix 3 versus Mix 4).
- Binder source (Mix 5 versus Mix 6; Mix 9 versus Mix 10; Mix 11 versus Mix 12).
- Aggregate water absorption (Mix 5 versus Mix 12).

For the nine Texas mixes, six levels of loose mix conditioning listed as follows were considered; for the four Massachusetts mixes, five loose mix conditionings (all six except the 4 h at 135°C) were employed:

- Short-term conditioning: 2 h at the compaction temperature.
- AASHTO R30 conditioning: 4 h at 135°C.
- Mid-term conditioning: 2 h at the compaction temperature, and then 20 h at 100°C and 2 h at the compaction temperature.
- 24 h at 95°C conditioning: 2 h at the compaction temperature, and then 24 h at 95°C and 2 h at the compaction temperature.
- 72 h at 95°C conditioning: 2 h at the compaction temperature, and then 72 h at 95°C and 2 h at the compaction temperature.
- 144 h at 95°C conditioning: 2 h at the compaction temperature, and then 144 h at 95°C and 2 h at the compaction temperature.

Table 15. Thirteen Mixes for Evaluating the Short- and Mid-Term Conditioning Protocols.

Mixture Type		Virgin Binder	RAP/RAS	Rejuvenator	Total Asphalt Content (%)
1	12.5 mm Superpave	PG70-22-Source 1	10% RAP	None	5.3
2	12.5 mm Superpave	PG64-22-Source 2	15% RAP/2% RAS	Bio-rejuvenator	5.2
3	9.5 mm Superpave	PG76-22-Source 3	None	None	5.0
4	9.5 mm Superpave	PG76-22-Source 3	None	None	5.5
5	9.5 mm Superpave	PG64-22-Source 4	None	None	5.5
6	9.5 mm Superpave	PG64-22-Source 5	None	None	5.5
7	12.5 mm Superpave	PG64-28-Source 6	15% RAP	None	5.2
8	12.5 mm Superpave	PG64-28-Source 6	15% RAP	None	5.0
9	9.5 mm Superpave	PG64-28-Source 6	15% RAP	None	6.0
10	9.5 mm Superpave	PG64-28-Source 7	15% RAP	None	6.0
11	12.5 mm Superpave*	PG64-22-Source 3	20% RAP	None	4.6
12	12.5 mm Superpave*	PG64-22-Source 4	20% RAP	None	4.6
13	12.5 mm SMA	PG76-22-Source 3	None	None	6.3

* Mixes 11 and 12 had a water absorption of 2.0 percent, and the rest of the mixes had a water absorption of 0.8–1.0 percent.

Note: The mix compaction temperatures are highly related to virgin binders. In this study, the compaction temperatures used are 149°C, 135°C, 135°C, and 122°C for mixes with binders PG76-22, PG70-22, PG64-28, and PG64-22, respectively.

IDEAL-CT was selected to evaluate the cracking resistance evolutions of all 13 mixes. For every mix under each level of conditioning, three IDEAL-CT specimens with 150 mm in diameter and 62 mm in height were molded at 7 ± 0.5 percent air voids using a Superpave gyratory compactor, and a total of 222 specimens were prepared. Each specimen was conditioned in a temperature chamber for 2 h at 25°C and then tested at a 50 mm/min loading rate at 25°C following ASTM D8225-19. The cracking tolerance index (CT_{Index}) is the cracking resistance parameter. The larger the CT_{Index} , the better the cracking resistance of the mix. The authors also collected the broken specimens after the testing for asphalt binder extraction, so comparing PAV aging and the different aging protocols became possible. The following two test procedures were used to conduct the asphalt binder extraction and recovery processes:

- Tex-210-F, Determining Asphalt Content of Bituminous Mixtures by Extraction: Part I—Centrifuge Extraction Method Using Chlorinated Solvent.
- ASTM D5404 Standard Practice for Recovery of Asphalt from Solution Using the Rotary Evaporator.

Only part of the broken specimens of Massachusetts mixes was kept due to limited storage space.

In addition to asphalt mix testing, asphalt binder rheology and associated aging characteristics of each virgin binder were characterized through a frequency sweep test using DSR. The frequency sweep test was conducted under 6 temperatures (64, 50, 45, 25, 15, and 5°C) and 19 frequencies (from 1 to 100 rad/sec.). For virgin binders, five aging conditions were used: OB, RTFO aged binder, PAV-20 h, PAV-40 h, and PAV-60 h aged binders. Furthermore, the same frequency sweep test was conducted on each extracted and recovered asphalt binder. The extracted and recovered binders under six conditioning protocols were tested without further aging.

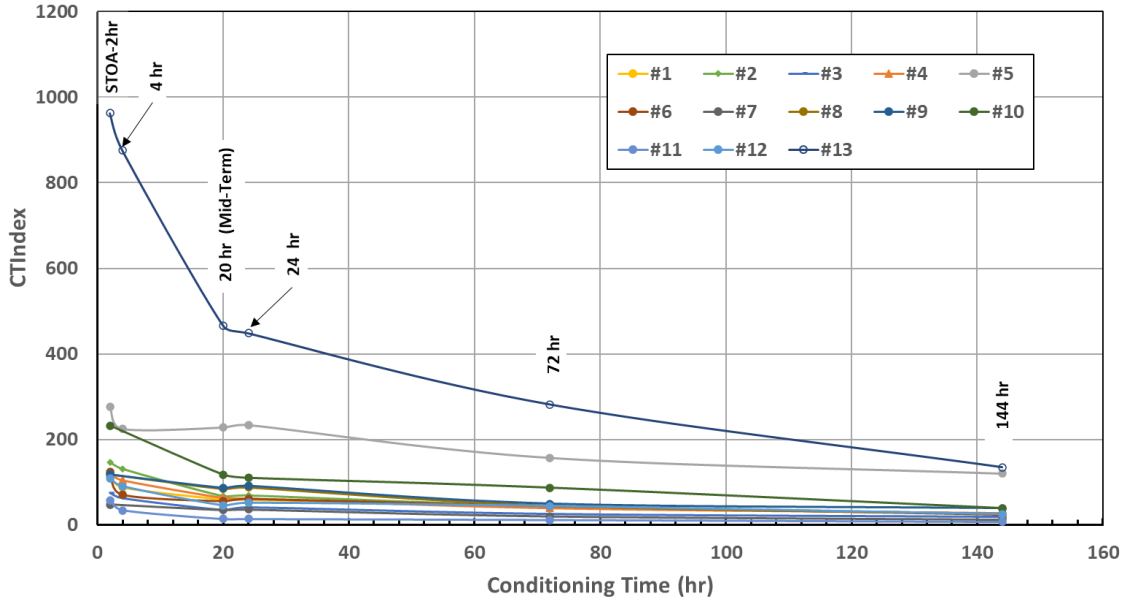
LABORATORY TEST RESULTS AND DISCUSSION

Figure 81(a) shows the average CT_{Index} values of each mix under six different conditioning levels. Mix 13, the 12.5-mm SMA, has the best cracking resistance, followed by Mix 5, which is

the 9.5-mm Superpave with PG64-22-Source 5; and Mix 11 has the worst cracking resistance among the 13 mixes. All other mixes fell in between them. To see the impact of conditioning level on the cracking resistance of the 13 asphalt mixes more clearly, researchers normalized the CT_{Index} values of each specific mix to its CT_{Index} value at the conditioning level of 2 h at the compaction temperature. For example, the CT_{Index} values of Mix 11 at the conditioning levels of 2 h at the compaction temperature and 4 h at 135°C are 963 and 876, respectively; the corresponding normalized CT_{Index} values become 1 and 0.91. Figure 81(b) shows the normalized CT_{Index} curves for all 13 mixes. Specifically, Figure 82 further details the impact of factors: mix type, binder content, rejuvenator, binder source, and asphalt absorption on the cracking resistance evolution of asphalt mixes. Three observations are made from Figure 81 and Figure 82:

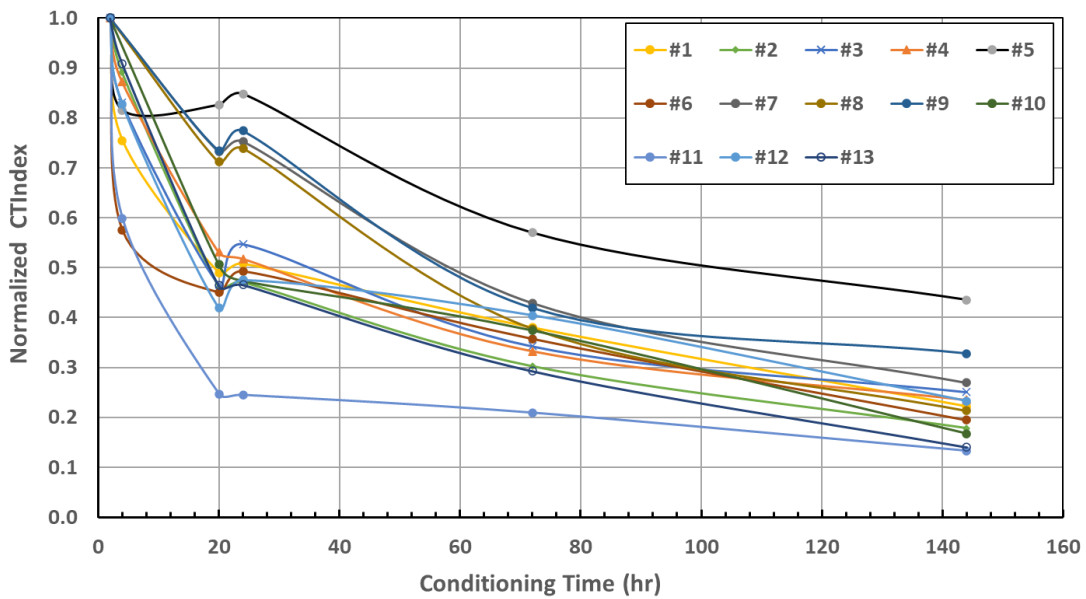
- Overall, the longer the conditioning time, the poorer the cracking resistance of each asphalt mix. At the same time, not all 13 mixes followed the same CT_{Index} reduction curve.
- Critical factors influencing cracking resistance evolution:
 - Mix type and asphalt binder content had no significant impact on cracking resistance evolution. As shown in Figure 82(a), Mix 12 (12.5-mm SMA with a 6.3 percent asphalt binder content) had a similar normalized CT_{Index} curve to that of Mix 4 (12.5 mm Superpave with 5.5 percent asphalt binder content); Mixes 3 and 4 presented in Figure 82(b) are similar except that Mix 4 had 0.5 percent more asphalt.
 - Rejuvenator did not negatively impact the mix cracking resistance evolution with conditioning time compared to other mixes, as illustrated in Figure 82(c).
 - RAP content had little negative influence on the mix cracking resistance evolution with conditioning time; Figure 82(d) shows similar CT_{Index} evolution curves for Mixes 1, 3, 4, 10, 12, and 13.
 - Binder source had the biggest influence on mix cracking resistance evolution with conditioning time, as displayed in Figure 82(e), regardless of asphalt binder content (5.5 percent, 6.0 percent, and 4.7 percent asphalt content for Mixes 5 and 6, 9 and 10, and 11 and 12, respectively), aggregate gradation (9.5 mm versus 12.5 mm Superpave), and aggregate absorption (1.0 percent versus 2 percent water absorption).
 - Asphalt absorption (Figure 82[f]) greatly impacted cracking resistance evolution, specifically in the early conditioning stage. As listed in Table 15, Mixes 5 and 12 have three major differences: asphalt binder content, RAP content, and aggregate absorption. As concluded previously, neither asphalt binder nor RAP content significantly impacted cracking resistance evolution with conditioning time. Thus, the difference shown in Figure 82(f) is likely caused by aggregate absorption.

IDEAL-CT Test Results vs. Conditioning Time



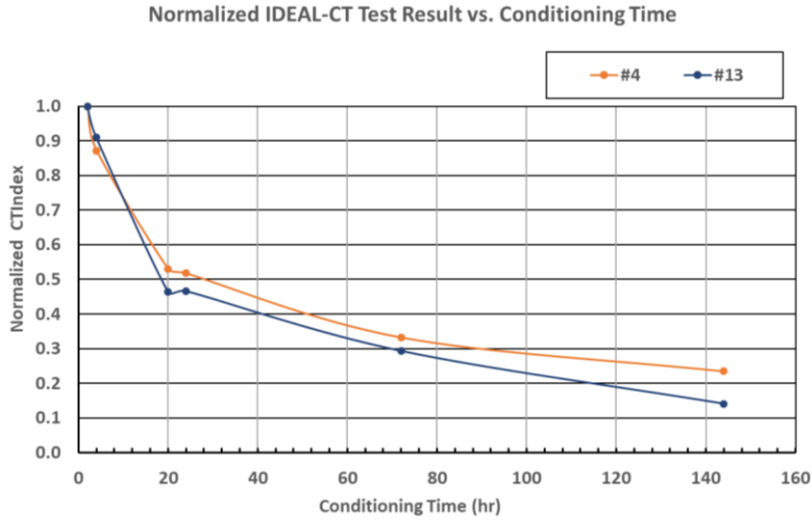
(a) Cracking resistance with conditioning

Normalized IDEAL-CT Test Result vs. Conditioning Time

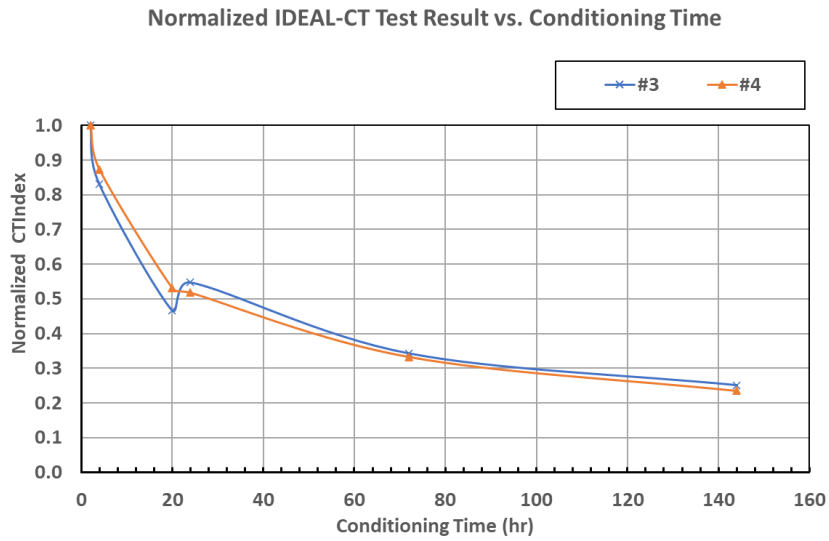


(b) Normalized cracking resistance with conditioning

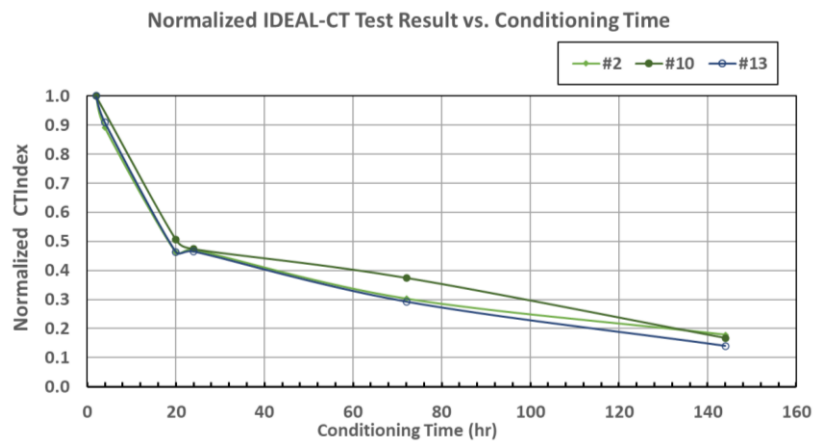
Figure 81. Cracking Resistance Evolution of Each Mix with Conditioning Time (or Level).



(a) Mix Type: SMA versus Superpave

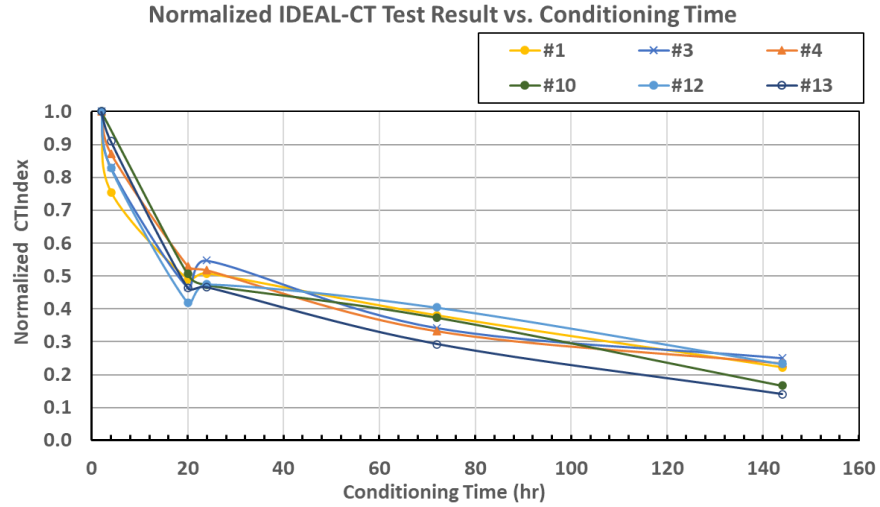


(b) Asphalt Binder Content: 5.0 versus 5.5%

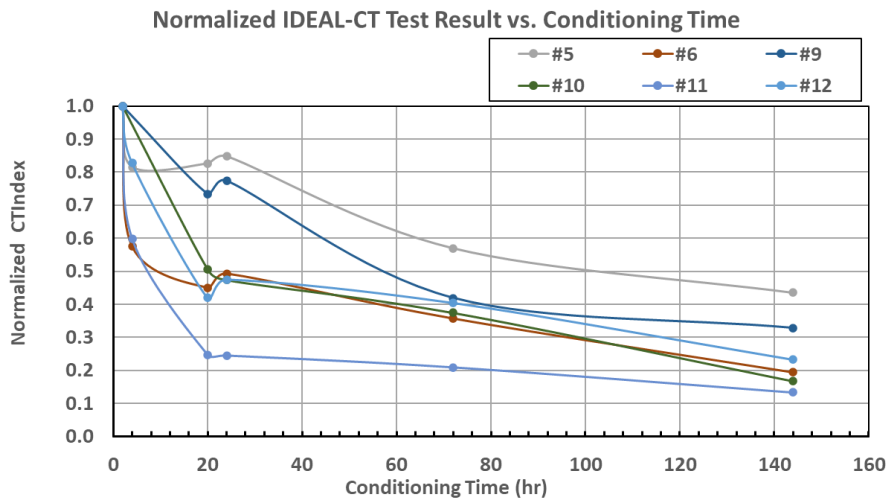


(c) Rejuvenator versus others

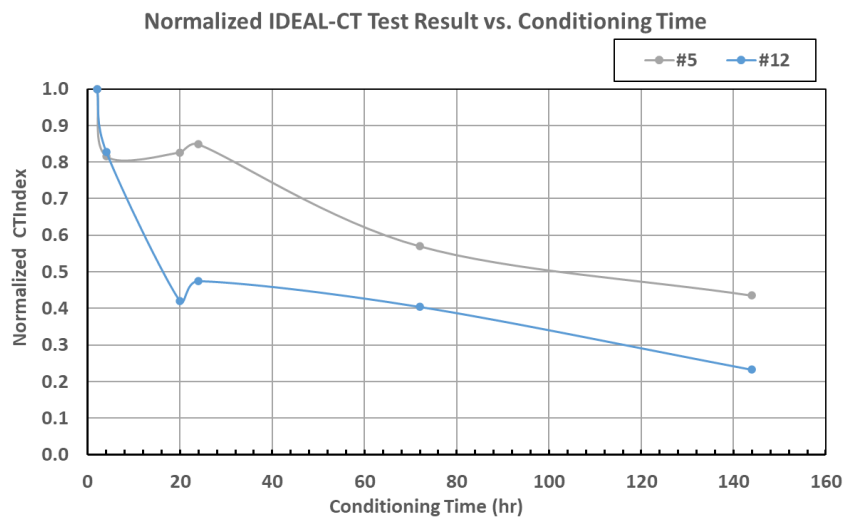
Figure 82. Cracking Resistance Evolution or Each Mix with Conditioning Time (or Level).



(d) RAP content: 0 versus 15% versus 20%



(e) Binder source: Mixes 5 versus 6; 9 versus 10; 11 versus 12



(f) Asphalt absorption: Mixes 5 versus 12

Figure 82. Cracking Resistance Evolution of Each Mix with Conditioning Time (or Level). Continued.

- Reasonableness of the mid-term conditioning protocol (20 h at 100°C):
 - 4 h at 135°C is not long enough for mid-term conditioning since some mixes had dramatic CT_{Index} reductions when conditioned for 20 h at 100°C. Meanwhile, conditioning for 72 h at 95°C may be too long since the normalized CT_{Index} values became very close to each other among all 13 mixes except for Mix 5, with the best binder quality, and Mix 11, with very poor binder quality and the highest asphalt absorption. The normalized CT_{Index} values at the 144 h at 95°C conditioning were closely interwoven. Thus, either 72 h at 95°C or 144 h at 95°C conditioning cannot differentiate the mixes.
 - The best choice for mid-term conditioning is the 20 h at 100°C or the 24 h at 95°C, where the 13 mixes have the biggest separation, actually into four groups: Group 1 with Mix 5; Group 2 with Mixes 7, 8, and 9; Group 3 with Mix 11; and Group 4 with the rest of them. Compared to the 24 h at 95°C, the 20 h at 100°C is preferred in terms of its practicality and consistency with binder PAV aging standard. Furthermore, these major groups of mix cracking resistance evolution curves matched the binder quality groups to be discussed in the next section. Therefore, it is logical and reasonable to select the 20 h at 100°C as the mid-term loose mix conditioning protocol.

BINDER TEST RESULTS AND DISCUSSION

Figure 83 presents the frequency sweep test results of extracted and recovered binders from Mixes 2, 3, 4, 5, 6, 11, and 13 under six conditioning protocols. The extracted and recovered binders from other mixes are not available. Figure 84 displays the frequency sweep test results of several virgin binders in this study under five aging conditions. In general, with the increasing aging severity, the complex shear modulus (G^*) versus phase angle (δ) curve moves toward the left, regardless of the virgin binders or the extracted and recovered binders. Additionally, the authors investigated two specific issues, as described below:

- The extracted and recovered binder modulus evolution versus mix CT_{Index} evolution under six conditioning protocols: Figure 81(b) presents the normalized CT_{Index} evolution of different mixes under six conditioning protocols. To compare those normalized CT_{Index} curves with the extracted and recovered binders, one has to do two things: First, pick up a binder parameter from the measured shear modulus and phase angle curve. Second, normalize it to one 2 h at compaction temperature, just like CT_{Index} normalization. Researchers first explored the Glower-Rowe (G-R) parameter, which can be calculated based on the frequency sweep test data. However, researchers found that the accuracy of the calculated G-R value was doubtful in some cases because either G^* or phase angle master curves are not always smooth. Thus, this study chose an alternative binder parameter—shear modulus at 45°C at 10 rad/sec—for comparing with mix CT_{Index} . Figure 85 shows the normalized G^* value at 45°C at 10 rad/sec and the corresponding mix CT_{Index} under six condition protocols for Mixes 2, 3, 4, 5, 6, 11, and 13. All mixes, except Mix 6, have a very consistent evolution curve between mix and binder properties. This observation validated the CT_{Index} test results presented in Figure 81 and Figure 82 and confirmed the importance of asphalt binder quality and aging resistance.
- Loose mix conditioning protocols versus binder aging (RTFO, PAV20, and PAV40): Figure 86 presents the comparison between loose mix conditioning protocols and asphalt

binder RTFO, PAV20, and PAV40 aging for three virgin mixes: Mixes 4, 5, and 6. Three observations can be made from Figure 86:

- The 2 h loose mix conditioning at compaction temperature is equivalent to asphalt binder RTFO aging.
- The 72 h loose mix conditioning at 95°C is equivalent to asphalt binder PAV 20 h aging at 100°C.
- The 144 h loose mix conditioning at 95°C is equivalent to asphalt binder PAV 40 h aging at 100°C.

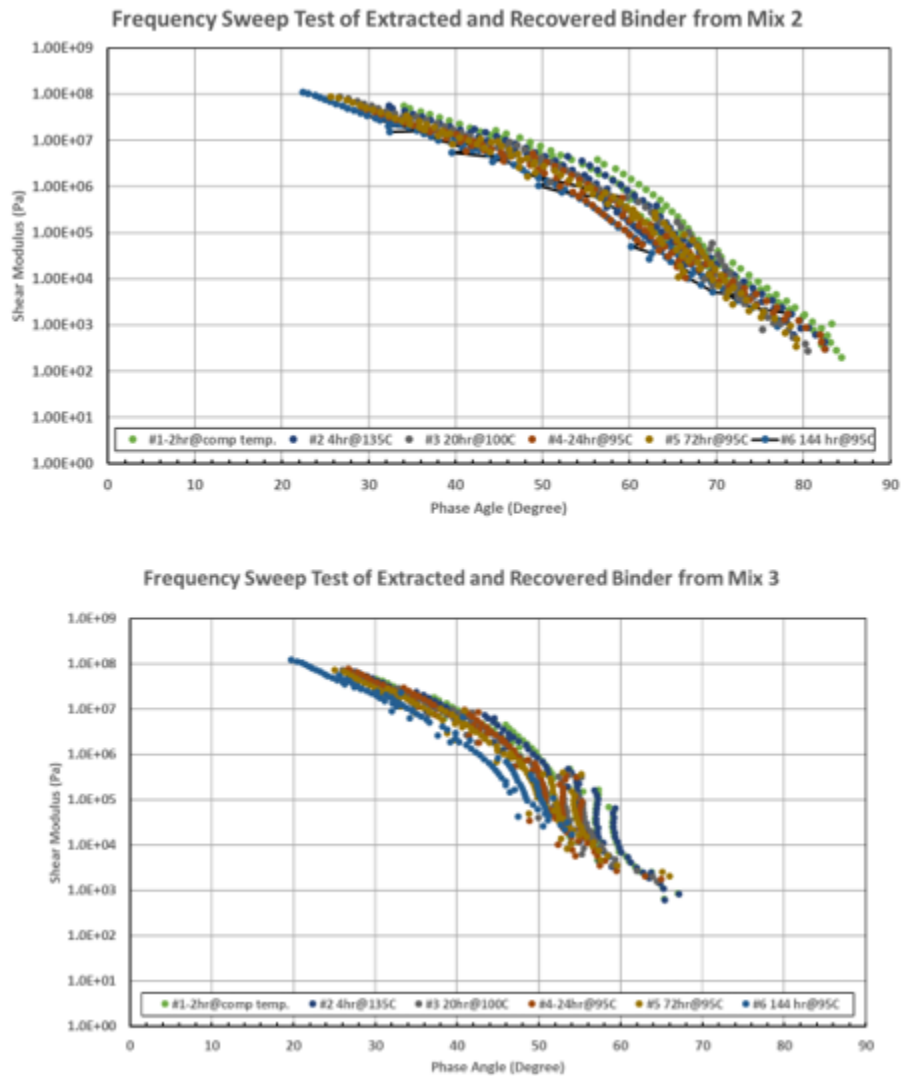


Figure 83. Extracted and Recovered Binders: Shear Modulus versus Phase Angle in Black Space.

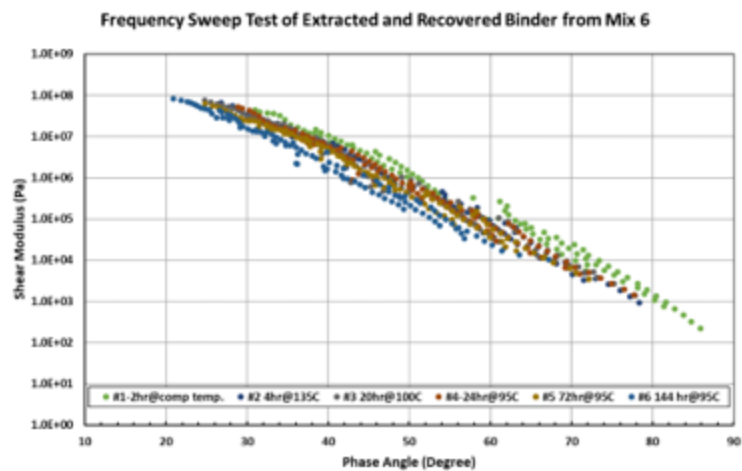
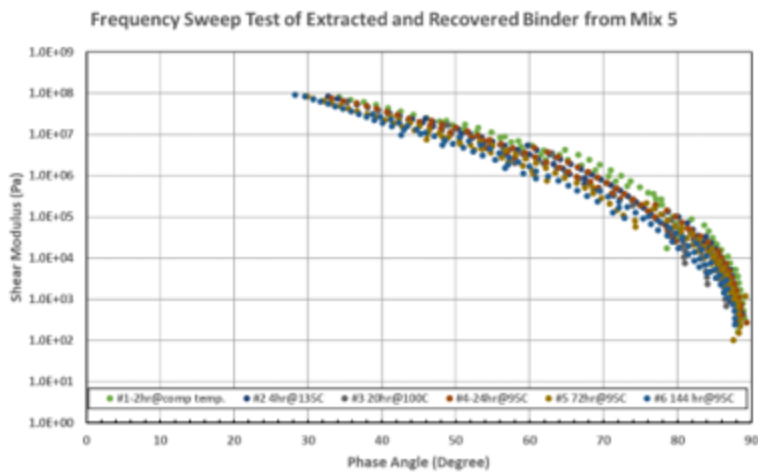
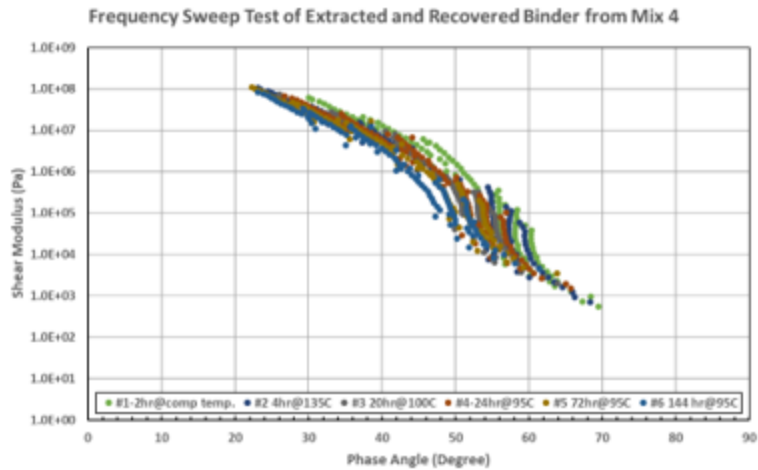


Figure 83. Extracted and Recovered Binders: Shear Modulus versus Phase Angle in Black Space. Continued.

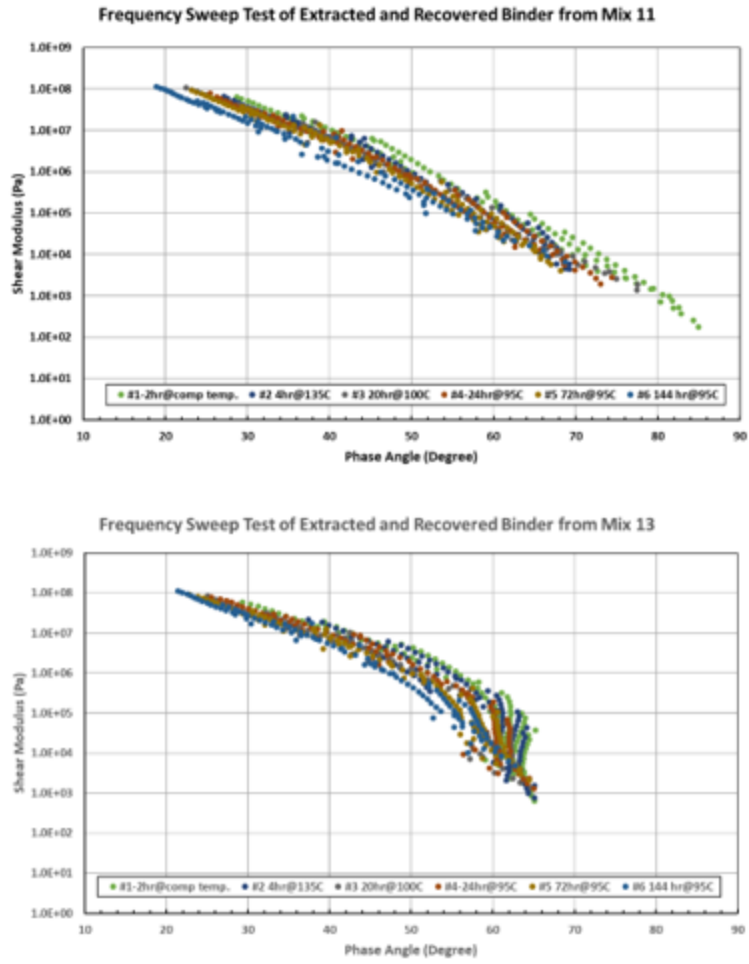


Figure 83. Extracted and Recovered Binders: Shear Modulus versus Phase Angle in Black Space. Continued.

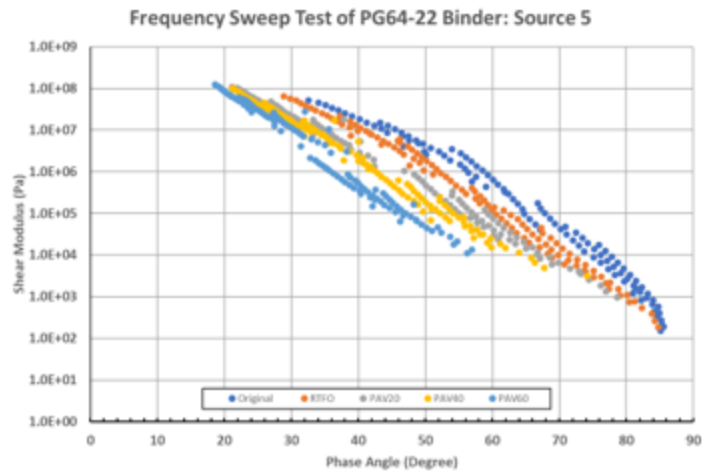
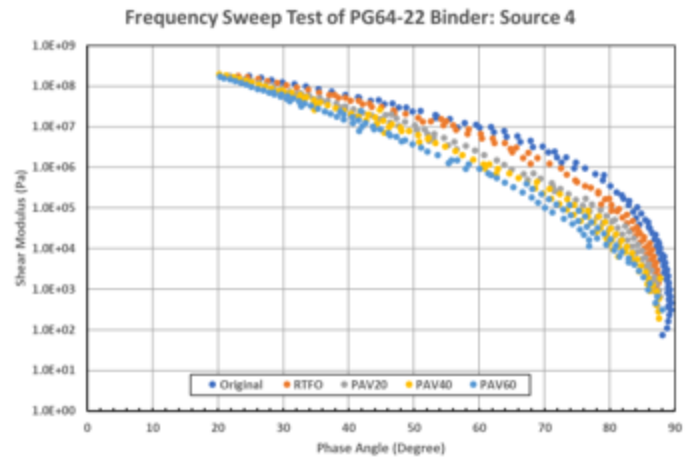
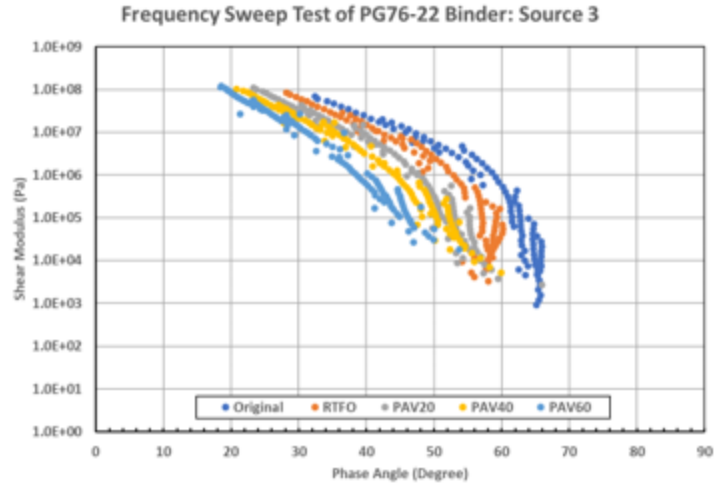


Figure 84. Virgin Binders: Shear Modulus versus Phase Angle in Black Space.

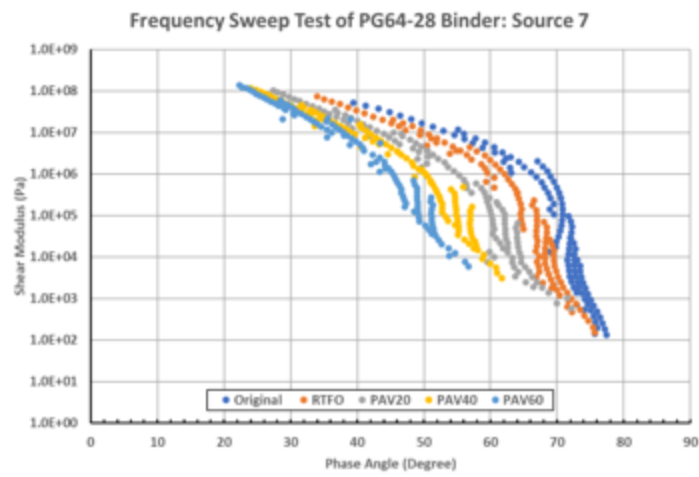
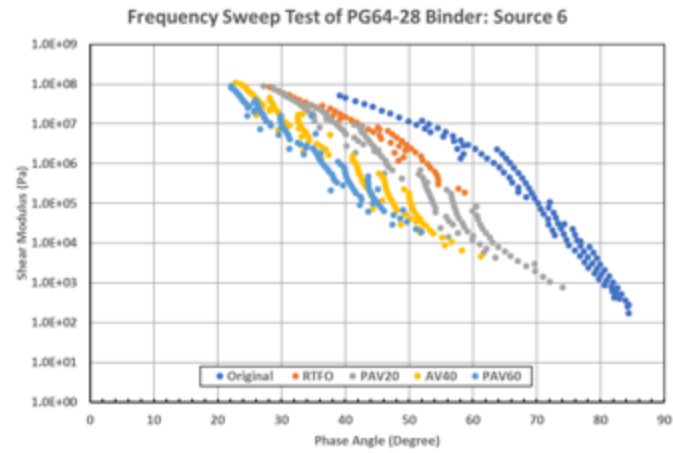


Figure 84. Virgin Binders: Shear Modulus versus Phase Angle in Black Space. Continued.

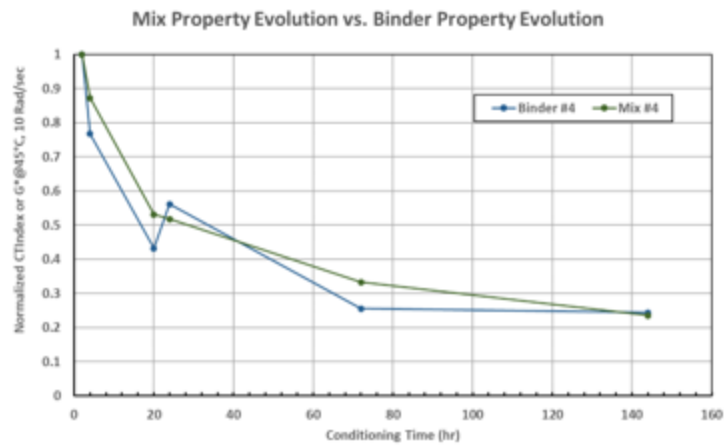
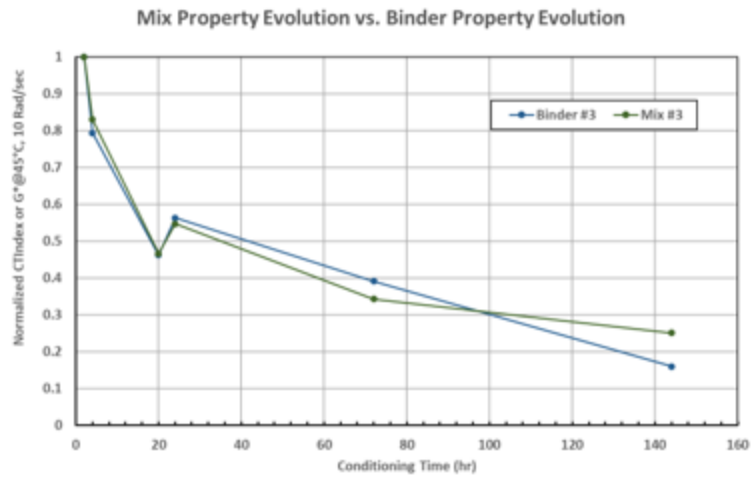
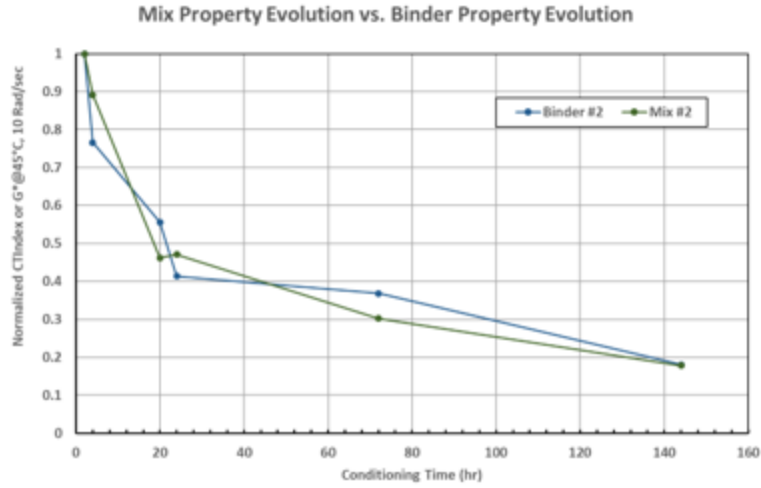


Figure 85. Comparison between Mix and Binder Property Evolution under Six Conditioning Protocols.

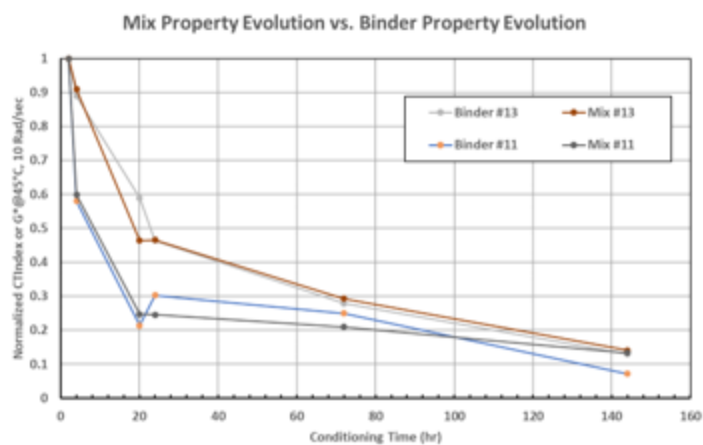
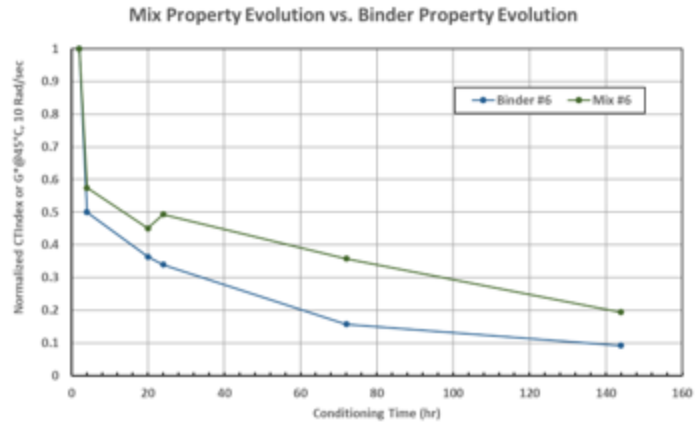
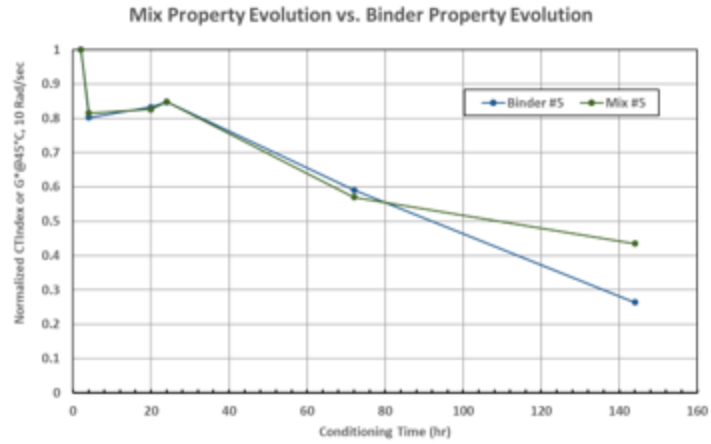


Figure 85. Comparison between Mix and Binder Property Evolution under Six Conditioning Protocols. Continued.

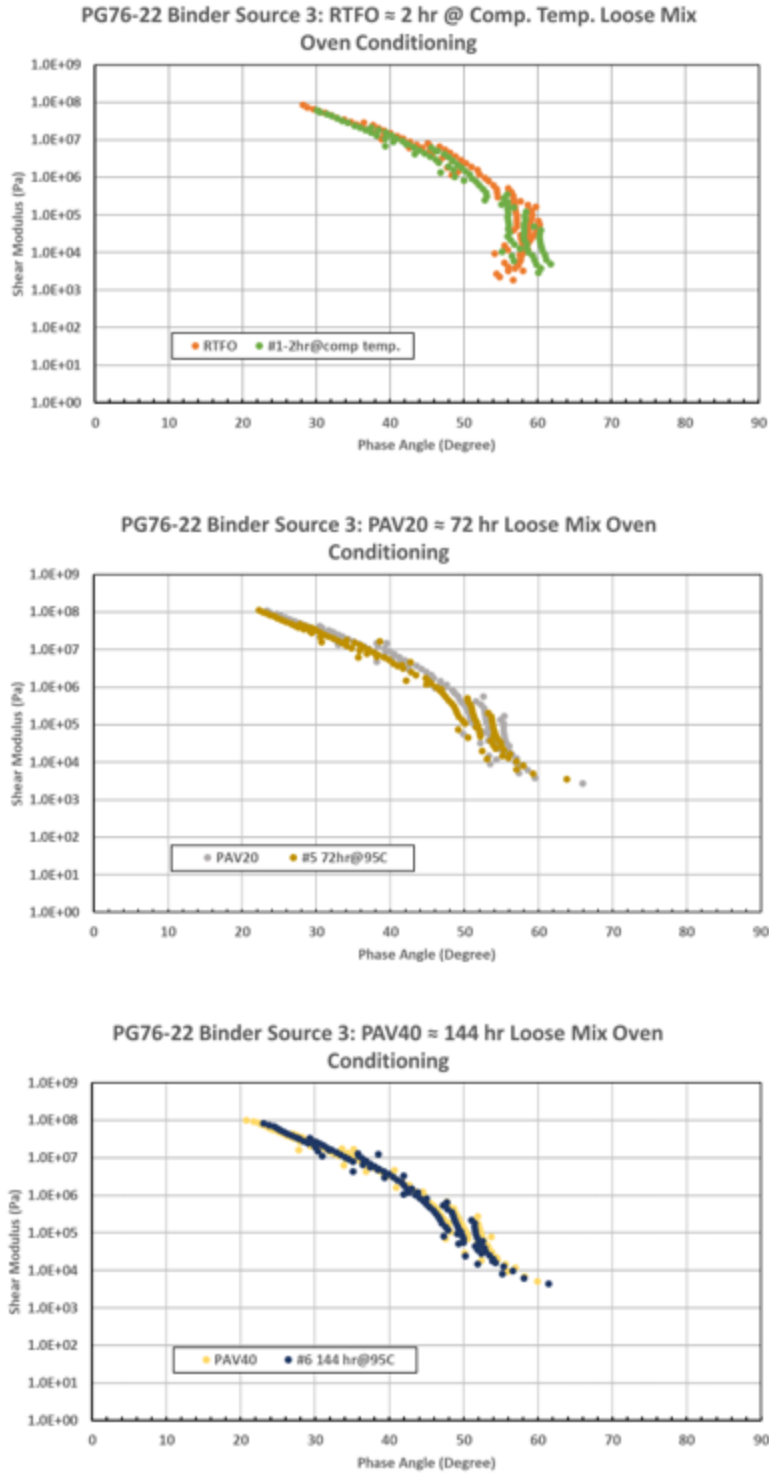


Figure 86. Comparison between Binder RTFO, PAV20, PAV40 Aging, and Loose Mix Oven Conditioning.

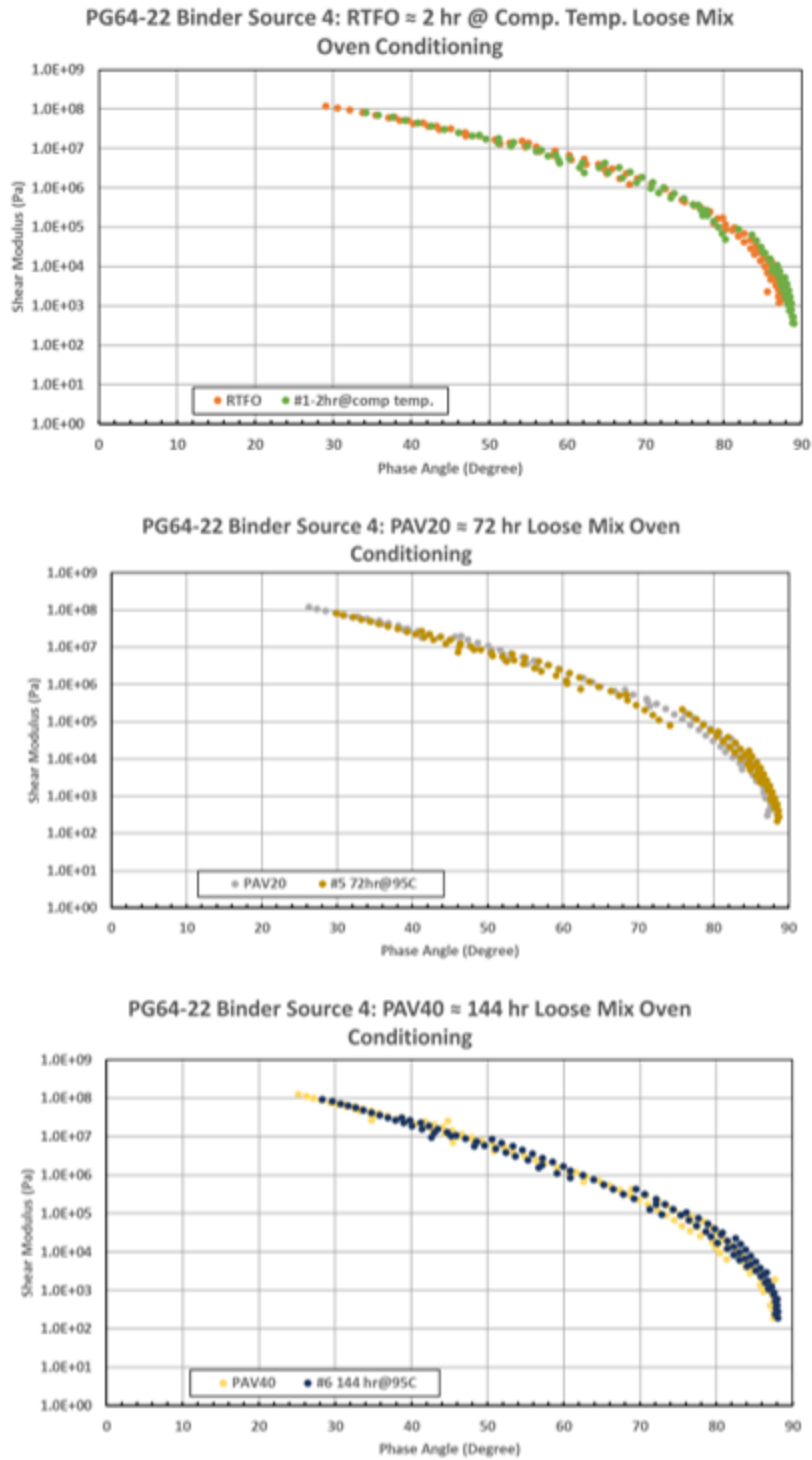


Figure 86. Comparison between Binder RTFO, PAV20, PAV40 Aging, and Loose Mix Oven Conditioning. Continued.

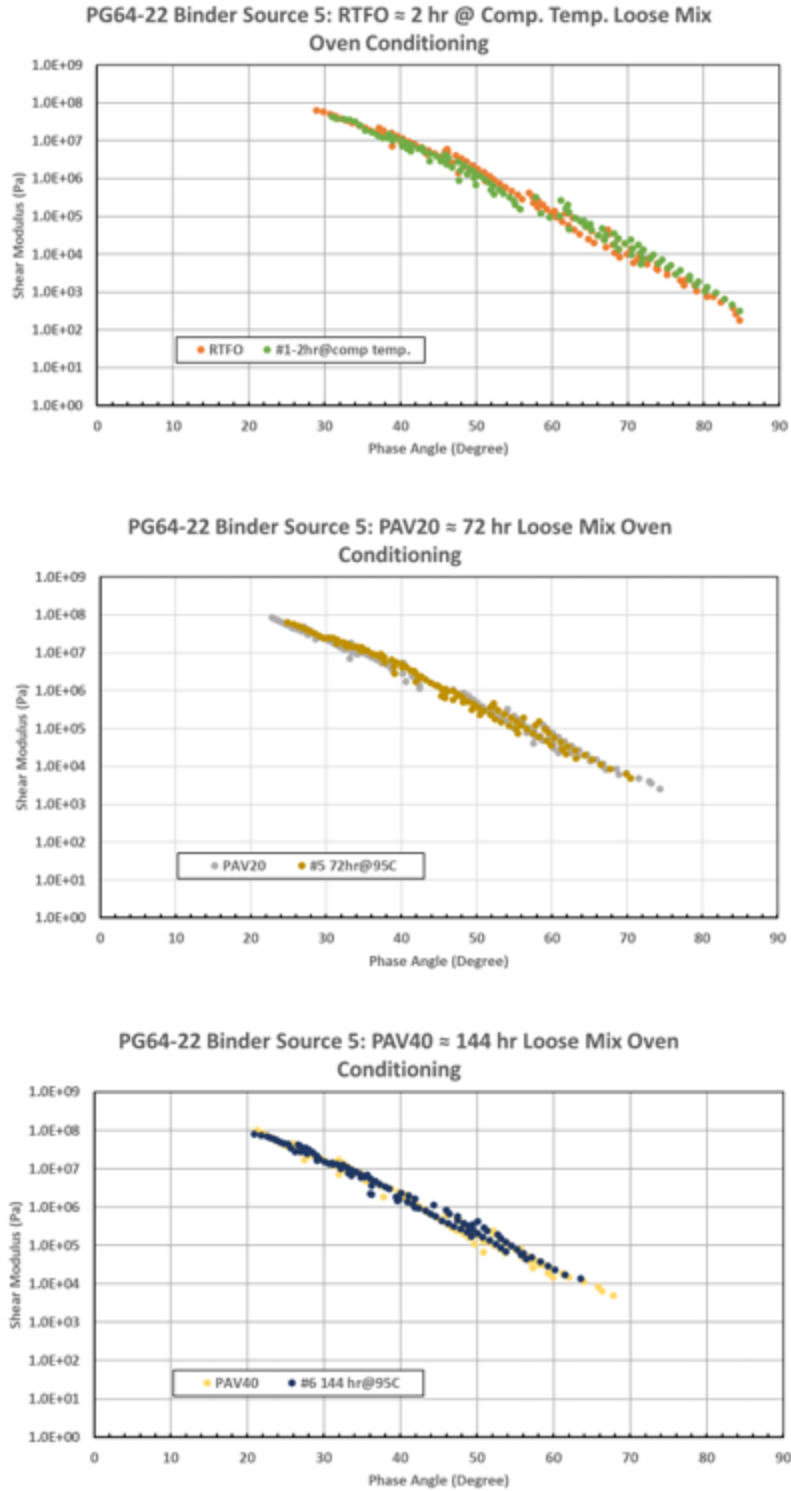


Figure 86. Comparison between Binder RTFO, PAV20, PAV40 Aging, and Loose Mix Oven Conditioning. Continued.

SUMMARY AND CONCLUSION

A series of IDEAL-CT tests for the 13 mixes were conducted, and the extracted binders were evaluated through frequency sweep testing in this study. Based on the test results presented in this paper, the following conclusions are offered:

- According to the IDEAL-CT test results, conditioning time significantly impacted cracking resistance of the mixes. The longer the conditioning time, the poorer the cracking resistance. When the loose mixes were conditioned too long (e.g., 144 h at 95°C), the normalized cracking resistance differences among various mixes diminished.
- For asphalt mix composition, binder source and asphalt absorption are two significant factors impacting the normalized cracking resistances of asphalt mixes. In contrast, mix type, asphalt binder content, and the use of rejuvenator had insignificant influence in distinguishing the cracking resistance evolution among the different mixtures.
- The 2 h loose mix conditioning at compaction temperature is equivalent to asphalt binder RTFO aging; the 72 h loose mix conditioning at 95°C is equivalent to asphalt binder PAV 20 h aging at 100°C, and the 144 h loose mix conditioning at 95°C is equivalent to asphalt binder PAV 40 h aging at 100°C.

CHAPTER 6. CONCLUSIONS AND RECOMMENDATION

Asphalt binder is one of the most expensive and critical materials used in the construction and maintenance of asphalt pavements. A key step toward a long-lasting asphalt pavement is selecting a proper binder grade. TxDOT's current binder PG selection method serves its purpose well for new pavement constructions. However, now TxDOT predominantly works with asphalt overlays. The most significant difference between new constructions and asphalt overlays is preexisting cracks underlying the asphalt overlays. The preexisting cracks significantly impact asphalt overlay performance in terms of early reflective cracking, which was not considered when developing current PG binder selection catalogs. Consequently, current PG asphalt binder selection catalogs (e.g., the one TxDOT uses) have severe limitations when applied to asphalt overlays.

This project evaluated many softer but polymer-modified asphalt binders (PGxx-28 and PGxx-34) in both laboratory and field performance. Based on the laboratory test results and field observations, a revised asphalt binder grade selection catalog was developed and validated. In addition, a series of laboratory experiments were performed to evaluate binder quality through aging and mix cracking resistance. Researchers confirmed that the same PG grade binders performed significantly differently in cracking resistance.

CONCLUSIONS

The conclusions according to the lab test and field survey results are as follows:

- The MSCR and PG grading tests were performed for nine asphalt binders ranging from the softest (PG58-34) to the hardest (PG76-22). The MSCR test and associated specification are proved to be better than the current $G^*/\sin \delta$ -based PG specification. HWTT was selected to assess the validity of the MSCR binder test.
- According to the HWTT results of 15 mixes (5 binders and 3 types of aggregates), the mixes with the PG64-34 binder have superior rutting performance to those with either PG64-22 or PG64-28 binder.
- Regarding the cracking resistance evaluation, the juxtaposition of the LAS and PLAS test reveals that PLAS is more effective than the LAS test in discriminating the effect of the sources and PG of asphalt binder sources, the conditions of chemical aging, and the source and dosage of engineering agents.
- Comparing the calculated PLAS results (FREI values) and those mixture cracking results (OT cycles or I-FIT flexibility indexes), it is clear that the rankings of cracking resistance between the PLAS test and mixture cracking tests are consistent.
- The PLAS test results match the overall trend of the FHWA-ALF fatigue data. The full-scale field fatigue data results indicated that the PLAS test effectively evaluated asphalt binder fatigue resistance.
- Multiple field test sections were constructed under this project. TTI researchers have been surveying the cracking and rutting distresses of these sections periodically since their initial construction. For the test sections constructed in 2020 and 2021, the corresponding plant mixes were collected at the asphalt plant. Their cracking and rutting resistance was evaluated using the IDEAL-CT, IDEAL-RT, and HWTT tests.
- The cracking and rutting surveys on field test sections in 10 districts (Amarillo, Childress, Fort Worth, Odessa, Laredo, Bryan, Lubbock, Dallas, San Angelo, and Austin)

show that soft, highly modified binders (PG_{xx}-28 or PG_{xx}-34) have better cracking resistance. Their benefits in the colder areas of Texas are confirmed.

- By simulating 2700 cases of overlays and comparing their cracking performances, the researchers have established a statewide binder selection method and catalog for overlays. The binder selection catalog for overlay was combined with the current Texas PG binder selection catalog.
- A series of IDEAL-CT tests for the 13 mixes were conducted, and the extracted binders were evaluated through frequency sweep testing in this study. According to the IDEAL-CT test results, conditioning time significantly impacted cracking resistance of the mixes. The longer the conditioning time, the poorer the cracking resistance. When the loose mixes were conditioned too long (e.g., 144 h at 95°C), the normalized cracking resistance differences among various mixes diminished.
- For asphalt mix composition, binder source and asphalt absorption are two significant factors impacting the normalized cracking resistances of asphalt mixes. In contrast, mix type, asphalt binder content, and the use of rejuvenator had insignificant influence in distinguishing the cracking resistance evolution among the different mixtures.

RECOMMENDATIONS

The recommendations according to the lab test and field survey results are as follows:

- The soft, highly modified binders (PG_{xx}-28 or PG_{xx}-34) have better cracking resistance, confirmed by both lab test and field survey results, and are recommended to be used in the colder areas of Texas.
- A new statewide asphalt binder selection catalog was proposed. The binder recommended by this new approach is usually softer than the binder recommended by TxDOT's current method. This difference highlights that binder recommendations for each county must be updated when an overlay construction is considered.
- The IDEAL-CT test can be used as a binder quality test to evaluate binders at different aging conditions and to differentiate binders with the same PG grade.
- The 2 h loose mix conditioning at compaction temperature is equivalent to asphalt binder RTFO aging; the 72 h loose mix conditioning at 95°C is equivalent to asphalt binder PAV 20 h aging at 100°C, and the 144 h loose mix conditioning at 95°C is equivalent to asphalt binder PAV 40 h aging at 100°C.

REFERENCES

- Al-Qadi, I. L., Ozer, H., Lambros, J., El Khatib, A., Singhvi, P., Khan, T., Rivera-Perez, J., and Doll, B. (2015). *Testing Protocols to Ensure Performance of High Asphalt Binder Replacement Mixes Using RAP and RAS*. Illinois Center for Transportation, Urbana, IL.
- Bazant, Z. P., and Prat, P. C. (1988). “Effect of Temperature and Humidity on Fracture Energy of Concrete.” *ACI Materials Journal*, 85(4), 262–271.
- Epps, J. A., Little, D. N., Holmgren, R. J., and Terrel, R. L. (1980). *Guidelines for Recycling Pavement Materials*. NCHRP Report No. 224, Transportation Research Board, Washington, DC.
- Gibson, N., Qi, X., Shenoy, A., Al-Khateeb, G., Kutay, M. E., Andriescu, A., Stuart, K., Youtcheff, J., and Harman, T. (2012). *Performance Testing for Superpave and Structural Validation*. Federal Highway Administration, McLean, VA.
- Glover, C., Davison, R., Domke, C., Ruan, Y., Juristyarini, P., Knorr, D., and Jung, S. (2005). *Development of a New Method for Assessing Asphalt Binder Durability with Field Validation*. Texas A&M Transportation Institute, College Station, TX.
- Hintz, C., and Bahia, H. U. (2013). “Understanding Mechanisms Leading to Asphalt Binder Fatigue in the Dynamic Shear Rheometer.” *Journal of the Association of Asphalt Paving Technologists*, 82, 465–501.
- Hu, S., Zhou, F., and Scullion, T. (2014). *Texas Cracking Performance Prediction, Simulation, and Binder Recommendation*. Texas A&M Transportation Institute, College Station, TX.
- Peterson, J. C. (2009). “A Review of the Fundamentals of Asphalt Oxidation: Chemical, Physicalchemical, Physical Properties, and Durability Relationships.” *TRB Transportation Research Circular*, E-C140.
- Schapery, R. A. (1984). “Correspondence Principles and a Generalized J Integral for Large Deformation and Fracture Analysis of Viscoelastic Media.” *International Journal of Fracture*, 25(3), 195–223.
- Vallerga, B. A. (1981). “Pavement Deficiencies Related to Asphalt Durability.” *Journal of the Association of Asphalt Paving Technologists*, 50, 481–491.
- Zhou, F., Im, S., Hu, S., Newcomb, D., and Scullion, T. (2016a). “Selection and Preliminary Evaluation of Laboratory Cracking Tests for Routine Asphalt Mix Designs.” *Journal of the Association of Asphalt Paving Technologists*, 85.
- Zhou, F., Newcomb, D., and Gurganus, C. (2016b). *Experimental Design for Field Validation of Laboratory Tests to Assess Cracking Resistance of Asphalt Mixtures*. Texas A&M Transportation Institute, College Station, TX.

